Neotropical Ichthyology

Original article

https://doi.org/10.1590/1982-0224-2025-0087

urn:lsid:zoobank.org:pub:81E36183-22FB-4BC8-A773-6C0225F1F940

Four new species of neotropical freshwater stingrays of the genus *Paratrygon* (Myliobatiformes: Potamotrygonidae) from clear water rivers of the Amazon basin

Correspondence:
Thiago Silva Loboda
lobodabio@usp.br

Thiago Silva Loboda

The second most diverse genus of the Potamotrygonidae, *Paratrygon*, with three previously recognized species, *P. aiereba*, *P. orinocensis* and *P. parvaspina*, is here expanded, with the description of four new species, each endemic to one of the four largest clear water rivers in the Amazon basin: Tapajós, Xingu, Araguaia and Tocantins. The new taxa occur in the middle and upper portions of their respective rivers, which originate and flow from the Brazilian Crystalline Shield. They are recognized by morphological characters such as coloration, dentition, morphometrics, morphology and distribution of dermal denticles and caudal spines, distribution of ventral canals of the lateral line system, and morphology and structure of major skeletal elements. Previously published molecular studies also confirm the validity of these species, and their data have been considered in the discussion. The description of these four new species and the reconfiguration of the distribution of *P. aiereba* in the Amazon basin led to a discussion of the possible influence of the water types of the Amazonian rivers on the diversity found in the genus. The hypothesis regarding this type of influence in potamotryginins was recently proposed by other authors. A key to identification of the species of *Paratrygon* is provided.

Keywords: Batoidea, Brazilian Shield, Elasmobranchii, Potamotrygoninae, Taxonomy.

Submitted May 13, 2025
Accepted November 1, 2025
Epub April 20, 2026

Associate Editor Shannon Corrigan
Section Editor William Crampton
Editor-in-chief José Birindelli

Online version ISSN 1982-0224
Print version ISSN 1679-6225

Neotrop. Ichthyol.
vol. 24, no. 1, 2026

1 Seção de Peixes, Museu de Zoologia da Universidade de São Paulo, Av. Nazaré, 481, Ipiranga, 04263-000, São Paulo, SP, Brazil. lobodabio@usp.br.

O segundo gênero mais diverso de Potamotrygonidae, *Paratrygon*, com três espécies previamente reconhecidas, *P. aiereba*, *P. orinocensis* e *P. parvaspina*, é aqui expandido, com a descrição de quatro novas espécies, cada uma endêmica de cada um dos quatro maiores rios de águas claras da bacia Amazônica: Tapajós, Xingu, Araguaia e Tocantins. Os novos táxons ocorrem nas partes médias e altas dos seus respectivos rios, que se originam e fluem do Escudo Cristalino Brasileiro. Elas são reconhecidas por caracteres morfológicos como coloração, dentição, morfometria, morfologia e a distribuição dos dentículos dérmicos e dos espinhos caudais, distribuição dos canais ventrais da linha lateral e morfologia e estrutura dos principais elementos do esqueleto. Estudos moleculares publicados anteriormente também confirmam a validade destas espécies, tendo seus respectivos dados considerados na discussão. A descrição destas quatro novas espécies e a reconfiguração da distribuição de *P. aiereba* na bacia amazônica permitem uma discussão sobre a possível influência dos tipos de água dos rios amazônicos na diversidade encontrada no gênero. A hipótese a respeito desse tipo de influência nos potamotrigonídeos foi proposta recentemente por outros autores. Uma chave para a identificação das espécies de *Paratrygon* é fornecida.

Palavras chave: Batoidea, Elasmobranchii, Escudo Brasileiro, Potamotrygoninae, Taxonomia.

INTRODUCTION

The family Potamotrygonidae is the second most diverse in the order Myliobatiformes, with a total of 40 species described to date, second only to Dasyatidae (which currently comprises 103 recognized species), and includes two subfamilies, Styracurinae, with the single marine/euryhaline genus *Styracura* Carvalho, Loboda & Silva, 2016 and its two species *S. schmardae* (Werner, 1904) and *S. pacifica* (Beebe & Tee-Van, 1941), and Potamotrygoninae, which includes the four genera that make up the Neotropical freshwater stingray clade: *Potamotrygon* Garman, 1877, *Paratrygon* Duméril, 1865, *Plesiotrygon* Rosa, Thorson & Castello, 1987, and *Heliotrygon* Carvalho & Lovejoy, 2011 (Thorson *et al*., 1983; Carvalho, Lovejoy, 2011; Carvalho *et al*., 2016; Silva, Loboda, 2019; Fontenelle *et al*., 2021a; Loboda *et al*., 2021; Fricke *et al*., 2025). *Plesiotrygon* and *Heliotrygon* have two species each, both genera are endemic to the Amazon basin and are the least speciose of the Potamotrygoninae (Carvalho, Lovejoy, 2011; Carvalho, Ragno, 2011; Lasso *et al*., 2013). *Potamotrygon* is the most abundant and widespread genus in the family, with 31 valid species distributed in all South American river basins where Potamotrygoninae occur (Carvalho *et al*., 2003; Lasso *et al*., 2013). *Paratrygon* is the second most diverse and widespread genus of Potamotrygoninae, with occurrences in the Amazon and Orinoco basins, and three described species to date: *P. aiereba* (Müller & Henle, 1841), endemic to the Amazon basin, and *P. orinocensis* Loboda, Lasso, Rosa & Carvalho, 2021 and *P. parvaspina* Loboda, Lasso, Rosa & Carvalho, 2021, both sympatric and restricted to the Orinoco basin (Loboda *et al*., 2021).

Potamotrygonidae is widely accepted as a monophyletic clade, and after the inclusion of Styracurinae, its recognized synapomorphies are: the presence of angular cartilages, dermal denticles with crowns that present dichotomous ridges, and the presence of a branch of the spiracularis muscle (which originates from the otic capsule), whose insertion extends beyond Meckel's cartilage and attaches to the ventral midline of the coracomandibularis (Lovejoy, 1996; Carvalho *et al*., 2016; Fontenelle *et al*., 2018). Neotropical freshwater stingrays, on the other hand, have the following known synapomorphies for their monophyletic clade (subfamily Potamotrygoninae): a very long pre-pelvic process on the anterior margin of the pelvic girdle, a reduced rectal gland, and a low concentration of urea in body fluids (Garman, 1913; Thorson *et al*., 1978; Rosa, 1985a; Carvalho *et al*., 2003). Potamotrygonids have recently experienced a significant increase in its diversity, with the number of species described in the last 10 years representing almost 1/3 of the total number of species in the family, mainly due to the recent taxonomic revisions of known species complexes and descriptions of new species (Fontenelle *et al*., 2014; Silva & Carvalho, 2015; Carvalho, 2016a,b; Fontenelle & Carvalho, 2017; Silva & Loboda, 2019; Loboda *et al*., 2021).

The taxonomic history of *Paratrygon* begins with Duméril (1865), who created the subgenus *Paratrygon* for *Trygon aiereba* Müller & Henle, 1841, and a few years later Günther (1870) raised *Paratrygon* to the level of a genus (Günther, 1870; Rosa, 1991). Garman (1877) described the genera *Disceus* and *Potamotrygon*, and until the revisions of Rosa (1985a,b, 1991) the taxonomic genera accepted for the family included these three plus *Elipesurus* Schomburgk, 1843 (Miranda Ribeiro, 1907; Garman, 1913; Fowler, 1948; Castex, 1964; Bailey, 1969). Rosa (1985b, 1991) based his taxonomic revision of *Paratrygon* on the recognition of *Disceus* as its junior synonym and *Elipesurus* as a *nomen dubium* (Rosa, 1985b, 1991; Carvalho *et al*., 2003; Loboda, 2016; Loboda *et al*., 2021).

Paratrygon aiereba (Müller & Henle, 1841), the type species of *Paratrygon*, was revised by Rosa (1985a,b, 1991), who examined the type specimens of *Trygon strogylopterus* Jardine, 1843 and *Disceus thayeri* Garman, 1913 and concluded that *P. aiereba* is the senior synonym of *T. strogylopterus* and *D. thayeri* (Loboda *et al*., 2021). Rosa (1991) stated that the type specimen of *P. aiereba* deposited in the Zoologische Staatssammlung München (ZSM) was lost, probably during the World War II. Due to the wide distribution of *Paratrygon* in the Amazon and Orinoco basins, Carvalho *et al*. (2003) and Rosa *et al*. (2010) suggested that *P. aiereba*, the only species of the genus until then, could possibly represent a species complex, mainly because populations show some morphological differences, such as coloration, throughout their distribution. Frederico *et al.* (2012) and Garcia *et al*. (2016) confirmed that through phylogenetic with the following molecular sequences: ATP synthase membrane subunit 6 (ATPase 6), cytochrome C oxidase I (COI) and cytochrome *b* (Cytb). The authors of the first study showed divergence of the first two genetic sequences between populations from the Xingu, Tapajós, Araguaia, Negro and Solimões-Amazonas rivers in the Amazon basin, and the authors of the second study showed divergence of the three sequences between populations from the Orinoco and Amazon basins.

Loboda (2016) reviewed *P. aiereba* using morphological characters and confirmed what had been suggested by Carvalho *et al*. (2003) and Rosa *et al*. (2010), as well as the results of molecular analyses by Frederico *et al*. (2012) and Garcia *et al*. (2016), that the species is indeed a complex. In addition, Loboda (2016) also confirmed two of

Rosa's (1991) taxonomic conclusions about the species: (1) that the original type was probably lost in a bombing raid in Munich at the end of World War II, and (2) that *Disceus thayeri* is a junior synonym of the species. Loboda *et al*. (2021) described two new species of *Paratrygon* for the Orinoco basin, *P. orinocensis* and *P. parvaspina*, and also redescribed *P. aiereba* for the Amazon basin, limiting the distribution of the species to this basin, more specifically to the main channel of the Solimões-Amazonas river, and also to the rivers of the upper part of the Amazon basin, such as the Purus, Juruá, and Madeira, among others. These authors also raised a neotype to *P. aiereba*, MZUSP 117155, specimen collected from the same locality where the original type specimen described by Müller, Henle (1841) was probably obtained by Spix and Martius journey (Loboda *et al*., 2021:72–74). The suspicion of the two new species for the Orinoco basin had already been raised by the morphological characters analyzed by Loboda (2016) and the molecular characters published by Garcia *et al*. (2016) and Rizo-Fuentes *et al*. (2021).

About the four species described here, which are all endemic to each of the four main clear-water tributaries on the right bank of the lower Solimões-Amazonas River, Tapajós, Xingu, Araguaia and Tocantins, the first authors to recognized a possible new taxon were Santos *et al.* (2004), who found morphologically distinct specimens of *Paratrygon* ("*Paratrygon* sp.") from *P. aiereba* in the Tucuruí power plant region, lower part of the Tocantins River. Although they did not specify the exact location where these specimens were collected, they provided a brief morphological description that distinguished them from *P. aiereba*. Frederico *et al*. (2012) found divergences between the Araguaia, Tapajós and Xingu taxa and the other populations of *P. aiereba* in their molecular phylogeny by analyzing COI and ATPase 6 sequences. In his taxonomic revision of *P. aiereba* based on morphological characters, Loboda (2016) also found a divergence of taxa from the Tapajós, Xingu, Araguaia and Tocantins rivers, confirming what was observed by Santos *et al*. (2004) in the Tocantins River, and also by Frederico *et al*. (2012) in the other three rivers. Loboda (2016) also concluded that these four different taxa of *Paratrygon*, endemic to each of these rivers, occur in their middle and upper portions, while in the lower portions, mainly at the confluence with the Solimões-Amazonas River, the occurrence of the genus is limited to *P. aiereba*. Sanches *et al.* (2021), using COI and Cytb data, also concluded in a phylogenetic analysis the presence of a possible new species of *Paratrygon* for the Xingu River in addition to *P. aiereba*, supporting Frederico *et al.* (2012) and Loboda (2016). Fontenelle *et al.* (2021a), through phylogenetic analyses of three mitochondrial genes (COI, ATPase 6 and Ctyb) and one nuclear gene (Nuclear ribosomal internal transcribed spacer 1 – its1), obtained the same results for possible new species of the genus *Paratrygon* as Loboda (2016) for Tapajós, Xingu, Araguaia and Tocantins.

MATERIAL AND METHODS

A total of 91 specimens of *Paratrygon* were measured, photographed, and analyzed for external morphological components (coloration, dermal denticles, and body proportions). Some specimens were selected for analysis of internal morphology by dissection, radiography and clear and stain methods, the latter following Dingerkus, Uhler (1977). Anatomical comparisons between the *Paratrygon* species described

here and the previously published species were made following Loboda (2016) and Loboda *et al*. (2021). The specimens examined were from the following collections: Instituto Nacional de Pesquisas da Amazônia (INPA), Manaus; Museu de Zoologia da Universidade de São Paulo (MZUSP), São Paulo; Universidade Federal do Pará (UFPA), Altamira; and Universidade Federal do Tocantins (UNT), Porto Nacional.

Twenty-eight measurements (in mm) were taken on all specimens following Rosa (1985), Taniuchi, Ishihara (1990), and Loboda, Carvalho (2013). Measurements were expressed as percentage of disc width (%DW) in the tables. Means and standard deviations (SD) were related to percentages of disc width, and ranges were expressed in milimeters and percentages (except for disc width). Means and SDs also include type and non-type specimens, and the number (N) of specimens analyzed was reported in a separate column. Specimens with deformities in the disc, tail, pelvic fins, and other parts of the body had measurements for these parts excluded.

The subsequent external morphological characters follow the description of Loboda *et al*. (2021): dorsal and ventral coloration of the disc, tail, pelvic fins, and clasper; morphology of the spiracular process and distribution and morphology of its dermal denticles; morphology and distribution of teeth in the dental plates; morphology and distribution of dermal denticles on the disc and tail; distribution and morphology of dorsal and lateral spine rows of the tail; morphology of the caudal sting; and arrangement of clasper grooves and pseudosiphons. Scanning electron microscopy (SEM) images were made at the Instituto de Biociências da Universidade de São Paulo (IBUSP), São Paulo. The following works were also used to analyze the external morphological characters: Deynat, Séret (1996) and Silva, Loboda (2019) for dermal denticles, Stehmann (1978) and Rosa (1985) for number of tooth rows, and Taniuchi, Ishihara (1990) and Moreira *et al*. (2018) for clasper structures.

Counts of vertebrae, fin radials and teeth were made from radiographs, either with a negatoscope or digitally with the program OsiriX, or on the specimens themselves, and in this case mainly for tooth counts with magnifying glasses or stereoscopic microscopes Leica EZ4 and M80. Radiographs were made at the Radiology Department of the Hospital Veterinário da Faculdade de Medicina Veterinária e Zootecnia (HOVET-USP), São Paulo. Vertebral and fin ray counts were performed according to Compagno (1999).

Analysis of internal morphological characters included the distribution and morphology of the ventral canals of the lateral line system and the following skeletal components: neurocranium, jaws and hyoid arches, synarcual cartilage, pectoral and pelvic girdle, and clasper. The nomenclature of the ventral canals of the lateral line follows Garman (1888), Lovejoy (1996), and Loboda *et al*. (2021). The nomenclature of skeletal components follows Garman (1913), Compagno (1977, 1999), Rosa (1985), Nishida (1990), Lovejoy (1996), Carvalho *et al*. (2004), Carvalho, Lovejoy (2011), Moreira *et al*. (2018), and Loboda *et al*. (2021). Abbreviations for internal morphological structures and their components follow Loboda *et al*. (2021), except for the frontoparietal component of the fontanelle of the neurocranium, which is abbreviated FCF here.

RESULTS

Paratrygon lucindai, new species

urn:lsid:zoobank.org:act:3E50DD7C-1F78-4468-A702-8295A3288834

(Figs. 1–15; Tabs. 1–2)

Paratrygon sp. —Santos *et al*., 2004:139, 184, 188, 214 (rio Tocantins species list, Tucuruí region, brief description of external morphology).

Paratrygon aiereba. —Carvalho, Lovejoy, 2011:16 (list of examined specimens). —Fontenelle *et al*., 2021a:6, 10, 12, fig. 2, suppl. 3–4, 10, 25, figs. S2–S3 (list of specimens with genetic material analyzed, molecular phylogenys).

Paratrygon sp. 7 —Loboda, 2016: vol. 1. vii, ix, 33, 60–61, 75, 87, 100, 113, 123, 126–127, 137–154, 156–157, 164–168, 190–192, 247–253, vol. 2. xix–xxi, 120–140, figs. 168–196 (morphological comparisons with another *Paratrygon* species, citation from rio Tocantins, synonymy, list of examined specimens, diagnosis, morphological description, distribution, endemicity for the rio Tocantins, morphometry, teeth count, meristics).

Holotype. UNT 7469, 505 mm DW, Brazil, Tocantins State, Municipality of Ipueiras, rio Tocantins, near the confluence with rio Manoel Alves, 11°19'S 48°28'W, 27 Jan 2004, NEAMB team.

Paratypes. All specimens from rio Tocantins, Brazil, Tocantins State: UNT 7454, 625 mm DW, Municipality of Peixe, Fazenda Água Branca, rio Santa Tereza, 11°48'07"S 48°38'21"W, 9 Jun 2003, NEAMB team (Former UNT 3861). UNT 7456, 602 mm DW, Municipality of Paranã, Fazenda Traadal, rio Tocantins, 12°29'S 48°12'W, 6 Jun 2000, NEAMB team (Former UNT 2413). UNT 7458, 701 mm DW, Municipality of Peixe, rio Tocantins, near the confluence with rio Santa Tereza, 11°47'27"S 48°37'02"W, 4 Feb 2002, NEAMB team (Former UNT 3538). UNT 7459, 436 mm DW, Municipality of Porto Nacional, rio Tocantins, 10°43'15"S 48°25'14"W, 15 Sep 1998, NEAMB team (Former UNT 2458). UNT 7460, 455 mm DW, same as anterior (Former UNT 2448). UNT 7461, 531 mm DW, Municipality of Lajeado, rio Tocantins, downstream of UHE Lajeado (Tocantins Funil), 09°45'2"S 48°21'56"W, 26 Jul 2000, NEAMB team (Former UNT 2652). UNT 7467, 380 mm DW, Municipality of Paranã, Fazenda Traadal, rio Paranã, 12°30'S 48°12'W, 28 Mar 1998 (Former UNT 2600). UNT 7475, 557 mm DW, Municipality of Miracema, rio Lajeadinho, near to UHE Lajeado, 09°46'32"S 48°24'15"W, 29 Oct 1999, NEAMB team (Former UNT 2615). UNT 7484, 645 mm DW, Municipality of Ipueiras, rio Tocantins near to the confluence with rio Manoel Alves, 11°19'S 48°28'W, 24 Feb 2001, NEAMB team (Former UNT 2661).

Non-type. All specimens from rio Tocantins, Brazil, Tocantins State: MZUSP 129965, 691 mm DW. MZUSP 129978, 560 mm DW. MZUSP 130341, 801 mm DW. MZUSP 104402, 284 mm DW, Municipality of Ipueiras, rio Tocantins in the confluence with rio Manuel Alves, 11°15'48.52"S 48°26'56.79"W, 18 Jun 2005, F. Marques, M. V. Domingues & G. Mattox. UNT 2459, 341 mm DW. UNT 2613. UNT

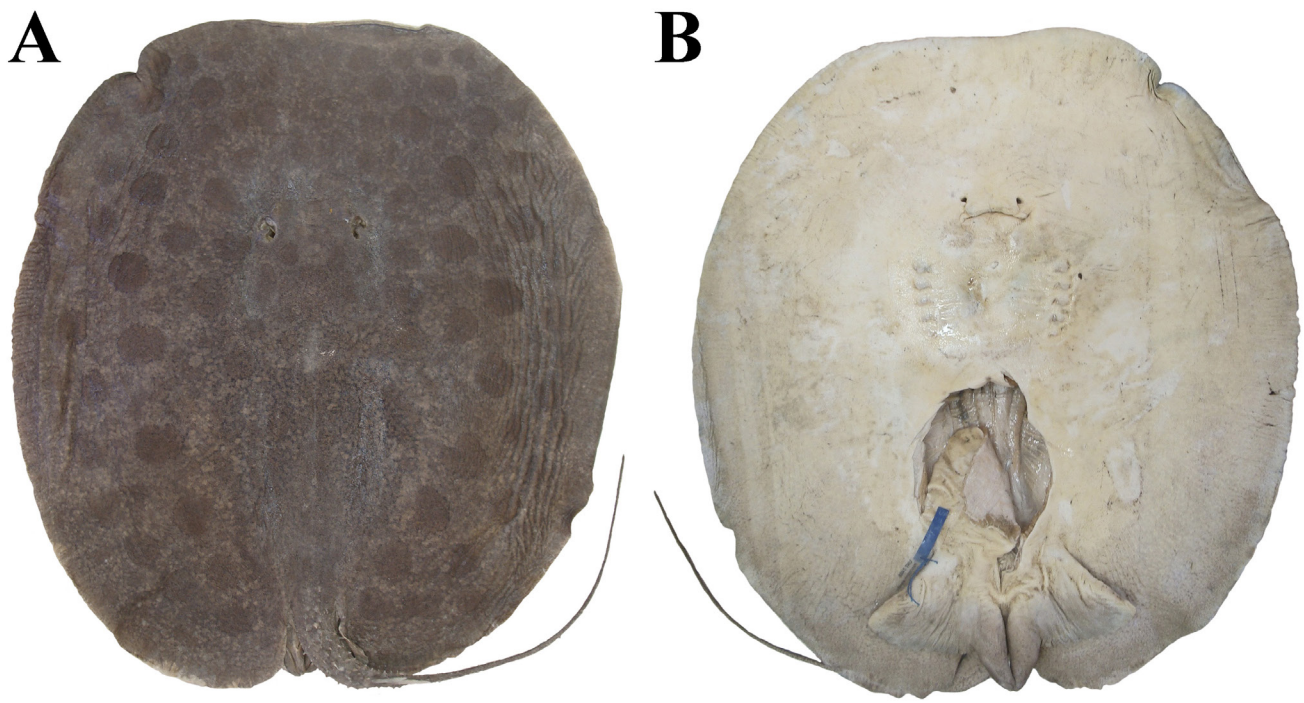

FIGURE 1 | Holotype of *Paratrygon lucindai*, UNT 7469, adult male, 505 mm DW, from Tocantins River. **A.** Dorsal; **B.** Ventral views.

2647, 214 mm DW. UNT 3711, 481 mm DW, Municipality of Peixe, rio Tocantins (fish rescue at UHE Peixe Angical), 12°15'S 48°23'W, 24 May 2005, A. B. Soares and team. UNT 7453, 637 mm DW, Municipality of Peixe, Fazenda Água Branca, rio Santa Tereza, 11°48'07"S 48°38'21"W, 16 May 2000, NEAMB team (Former UNT 2411). UNT 7455, 574 mm DW, Municipality of Lajeado, rio Tocantins downstream of UHE Lajeado (Tocantins Funil), 09°45'02"S 48°21'56"W, 12 Sep 2000, NEAMB team (Former UNT 2390). UNT 7457, 490 mm DW, municipality of Santa Rosa, rio Manoel Alves, near to the confluence with rio Tocantins, 11°19'S 48°27'W, 24 May 2000, NEAMB team (Former UNT 2399). UNT 7462, 512 mm DW, Municipality of Brejinho de Nazaré, rio Tocantins, 10°59'46"S 48°32'6"W, 18 Jul 2003, NEAMB team (Former UNT 3886). UNT 7463, 527 mm DW, Municipality of Porto Nacional, rio Tocantins, 10°43'15"S 48°25'14"W, 19 Jul 2000, NEAMB team (Former UNT 2394). UNT 7464, 444 mm DW, Municipality of Lajeado, rio Tocantins downstream of UHE Lajeado (Tocantins Funil), 09°45'02"S 48°21'56"W, 24 Mar 2003, NEAMB team (Former UNT 3857). UNT 7465, 500 mm DW, Municipality of Peixe, Fazenda Água Branca, rio Santa Tereza, 11°48'07"S 48°38'21"W, 29 Jul 2001, NEAMB team (Former UNT 3542). UNT 7466, 431 mm DW, Municipality of Miracema, rio Lajeadinho near to the UHE Lajeado, 09°46'32"S 48°24'15"W, 28 Jan 2000, NEAMB team (Former UNT 2614). UNT 7468, 520 mm DW, Municipality of Peixe, rio Tocantins, near to the confluence of rio Santa Tereza, 11°47'27"S 48°37'02"W, 23 Jan 2001, NEAMB team (Former UNT 2664). UNT 7470, 687 mm DW, Municipality of Peixe, Fazenda Água Branca, rio Santa Tereza, 11°48'07"S 48°38'21"W, 12 Sep 2000 (Former UNT

2438). UNT 7471, 440 mm DW, Municipality of Miracema, rio Lajeadinho, near to UHE Lajeado, 09°46'32"S 48°24'15"W, 21 Jun 2000, NEAMB team. UNT 7472, 388 mm DW, Municipality of Porto Nacional, rio Tocantins, 10°43'15"S 48°25'14"W, 10 Jun 1999 (Former UNT 2461). UNT 7473, 331 mm DW, Municipality of Porto Nacional, rio Mangues, 10°22'00"S 48°24'30"W, 23 Oct 2000, NEAMB team (Former UNT 2398). UNT 7474, 505 mm DW, Municipality of Paranã, Fazenda Traadal, rio Maranhão, 12°29'S 48°13'W, 5 Oct 2000, NEAMB team (Former UNT 2382). UNT 7476, 517 mm DW, Municipality of Paranã, Fazenda Traadal, rio Maranhão, 12°29'S 48°13'W, 24 Jun 1999, NEAMB team (Former UNT 2460). UNT 7477, 636 mm DW, Municipality of Miracema, rio Lajeadinho, near to UHE Lajeado, 09°46'32"S 48°24'15"W, 28 Jan 2000 (Former UNT 2604). UNT 7478, 322 mm DW, Municipality of Paranã, Fazenda Traadal, rio Paranã, 12°30'S 48°12'W, 29 Jul 1999, NEAMB team (Former UNT 2607). UNT 7479, 203 mm DW, Municipality of Lajeado, rio Tocantins downstream of UHE Lajeado (Tocantins Funil), 09°45'02"S 48°21'56"W, 17 Feb 2000, NEAMB team. UNT 7480, 271 mm DW, Municipality of Ipueiras, rio Tocantins, near to the confluence with rio Manoel Alves, 11°19'S 48°28'W, 27 May 2003, NEAMB team (Former UNT 3859). UNT 7481, 244 mm DW, Municipality of Paranã, Fazenda Traadal, rio Maranhão, 12°29'S 48°13'W, 9 Feb 2000, NEAMB team. UNT 7482, 487 mm DW, Municipality of Brejinho de Nazaré, rio Crixás, 11°03'S 48°38'W, 21 Nov 2002, NEAMB team (Former UNT 3826). UNT 7483, 218 mm DW, Municipality of Pedro Afonso, rio Tocantins, near to the confluence with rio Sono, 08°59'S 48°10'W, 14 Mar 2001, NEAMB team (Former UNT 3925). UNT 7485, 177 mm DW, Municipality of Ipueiras, rio Tocantins near to the confluence with rio Manoel Alves, 11°19'S 48°28'W, 24 Feb 2001, NEAMB team (Former UNT 3924). UNT 7492, Municipality of São Valério, rio São Valério, near to the confluence with rio Tocantins, 11°22'S 48°29'W, 22 Oct 1999 (Former UNT 2445). UNT 7493, 282 mm DW, Municipality of Ipueiras, rio Tocantins, near to the confluence with rio Manoel Alves, 11°19'S 48°28'W, 18 Oct 2001, NEAMB team (Former UNT 2991). UNT 7494, 536 mm DW, Municipality of Paranã, Fazenda Traadal, rio Paranã, 12°30'S 48°12'W, Jan 2000, NEAMB team (Former UNT 2464). UNT 7495, 438 mm DW, Municipality of Santa Rosa, rio Manoel Alves, in the confluence with rio Tocantins, 11°19'S 48°27'W, 16 May 2000, NEAMB team (Former UNT 2428). UNT 11786, 196 mm DW, rio Tocantins, Funil, 14 Aug 2002. INPA uncatalogued, 405 mm DW. UNT uncatalogued, 501 mm DW (Field number 270335). UNT uncatalogued, 235 mm DW, Arnos beach, 7 Mar 2007. UNT uncatalogued, 212 mm DW.

Diagnosis. *Paratrygon lucindai* is distinguished from congeners by the following combination of characters: dorsal disc coloration varying from gray and dark gray to brown, dark brown and reddish brown and characterized by the presence of largeround spots of beige, gray, brown, dark brown or reddish brown color throughout the disc, two to three times the diameter of the spiracle (*vs*. *P. aiereba*, *P. orinocensis*, *P. parvaspina* with gray or light brown dorsal coloration possessing detached small dark spots; *P. munduruku*, *P. raonii* with dark coloration having dark spots in vermicular or dendritic format; *P. araguaia* with brown dorsal coloration containing small brown, light brown or beige spots); spiracles small and rounded, mean spiracle length 4.4% DW [2.8–6.4% DW] with small and globular spiracular process (*vs*. *P. aiereba*, *P. parvaspina*, *P. munduruku*,

P. raonii with quadrangular spiracles; *P. orinocensis* with triangular spiracles; *P. araguaia*, which also has small and rounded spiracles, although with an average spiracle length in 5.3% DW [4.3–6.1% DW], and a reduced and straight spiracular process); dermal denticles on the central disc with small, narrow and slightly higher crowns with a well developed central coronal plate of quadrangular shape, surrounded by three to six smaller and conical lateral coronal ridges (*vs*. *P. aiereba*, *P. parvaspina*, *P. munduruku* with dermal denticles on the central disc with narrow and high crowns with a pointed central coronal plate surrounded by three to six smaller and pointed or rounded lateral coronal ridges;

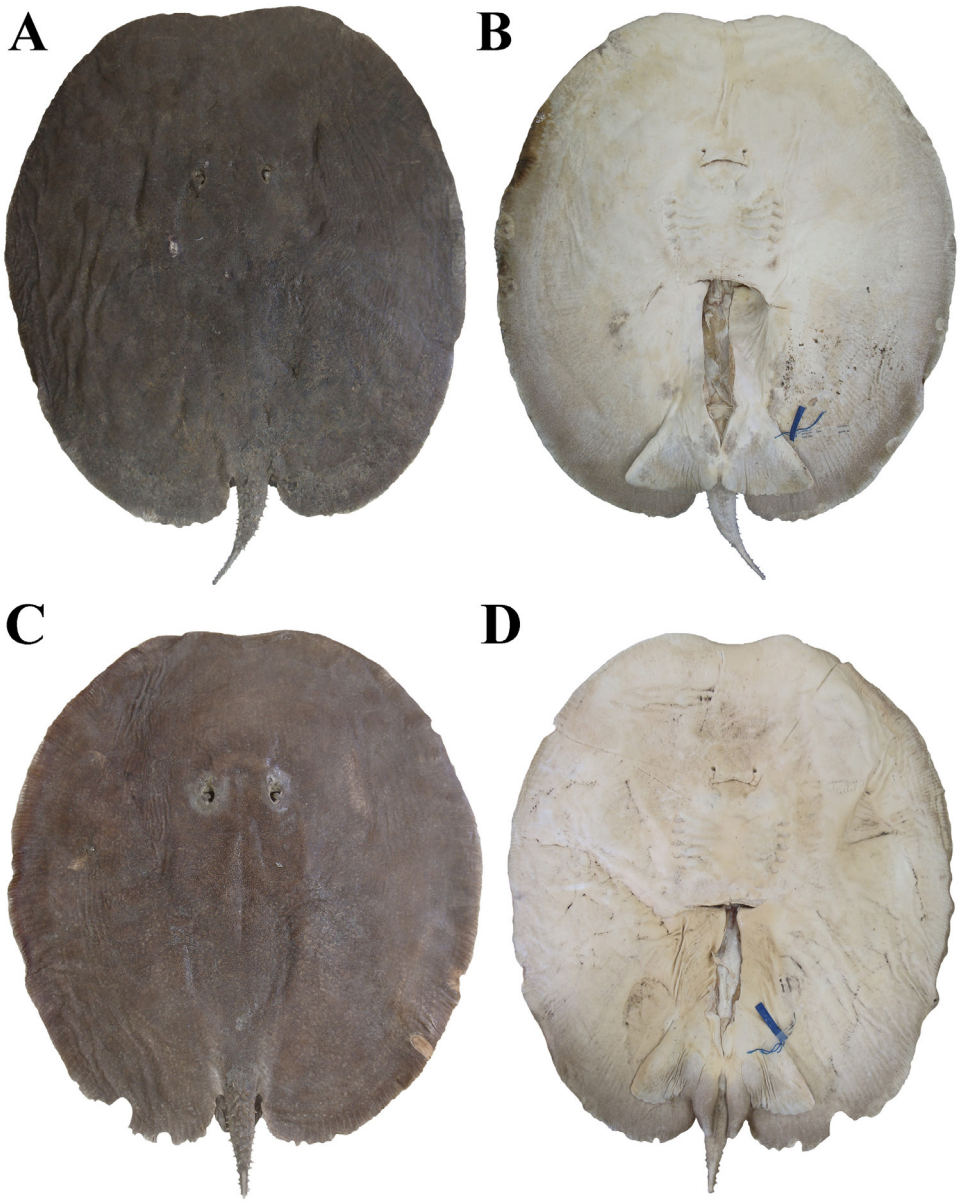

FIGURE 2 | Paratypes of *Paratrygon lucindai*, UNT 7454, adult female, 625 mm DW, from Santa Tereza River. **A.** Dorsal; **B.** Ventral views. UNT 7461, adult male, 531 mm DW, from Tocantins River. **C.** Dorsal; **D.** Ventral views.

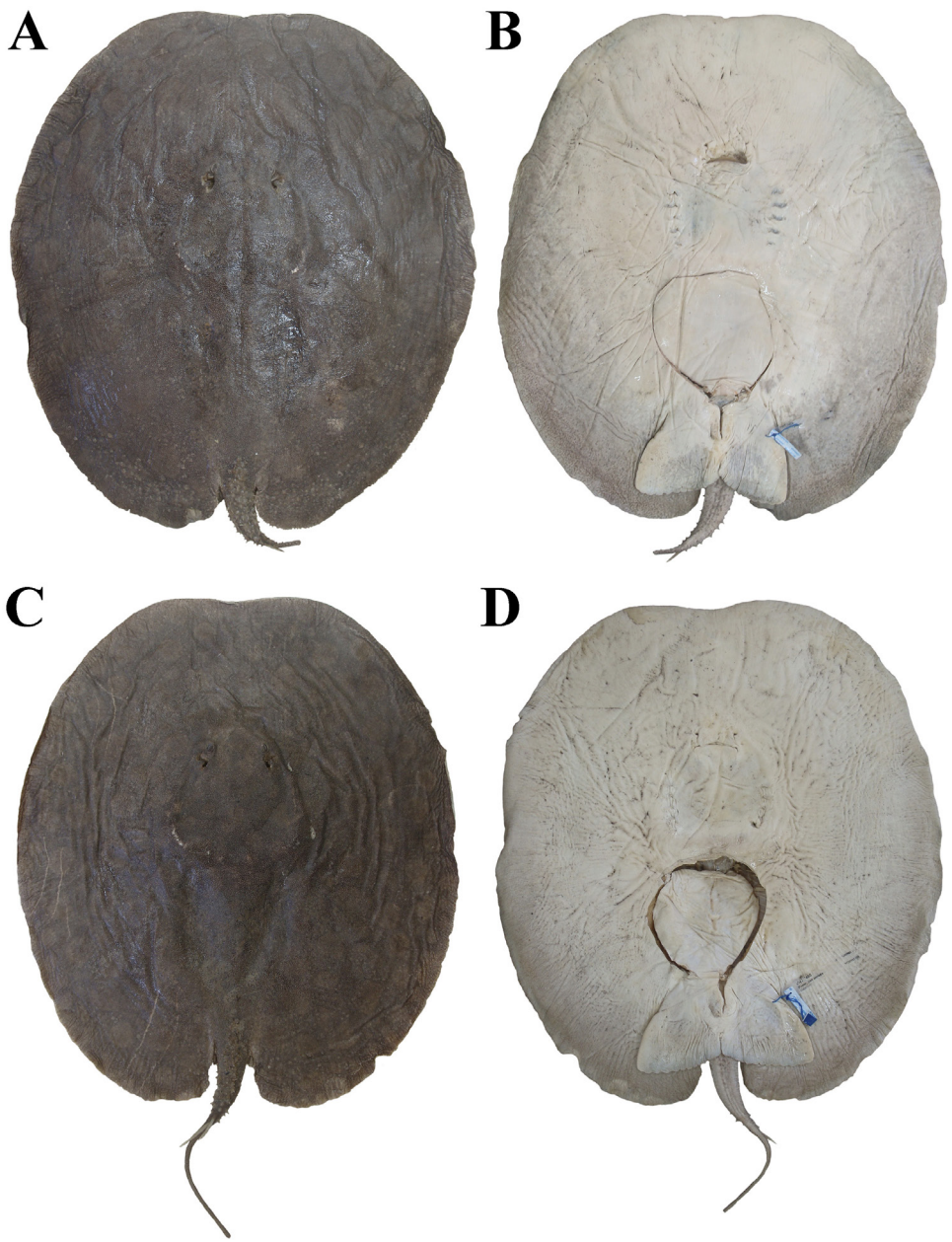

FIGURE 3 | Paratypes of *Paratrygon lucindai*, UNT 7475, adult female, 557 mm DW, from Lajeadinho River. **A.** Dorsal; **B.** Ventral views. UNT 7460, subadult female, 455 mm DW, from Tocantins River. **C.** Dorsal; **D.** Ventral views.

P. raonii with dermal denticles on central disc presenting narrow and high crowns with central coronal plate pointed surrounded by six or eight lateral coronal ridges smaller and similar in shape to the central coronal plate; *P. orinocensis* with dermal denticles on the central disc possessing wide and high crowns with a central coronal plate pointed surrounded by twelve or more lateral coronal ridges similar in size and shape to the central coronal plate; *P. araguaia* with dermal denticles on the central disc possessing narrow and not so high crowns with a very reduced and pointed central coronal plate

surrounded by three to five larger and rounded lateral coronal ridges); junction of four canals with the anterior end positioned more externally than the posterior end, with infraorbital and supraorbital canals connected at the anterior end, and hyomandibular and nasal canals connected at the posterior end (*vs*. all other *Paratrygon* species have the posterior end of the junction of the four canals positioned more externally than the anterior, with the anterior junction formed by the junction of the nasal and supraorbital canals, while the posterior junction is formed by the junction of the hyomandibular and infraorbital canals); posterior end of the frontoparietal component of the fontanelle straight to slightly oval (*vs*. *P. orinocensis* with posterior end of frontoparietal component of fontanelle oval; *P. munduruku* with posterior end of frontoparietal component of fontanelle oval to slightly rounded; *P. aiereba*, *P. parvaspina*, *P. araguaia* and *P. raonii* with posterior end of frontoparietal component of fontanelle rounded).

Description. Adult specimens of *P. lucindai* with average of 734.5 mm and maximum of 951 mm in total lenght. Disc length large with average of 624.6 mm and maximum of 845 mm, and disc width with average of 594.2 mm, and maximum of 801 mm. Measurements in Tabs. 1, **S1**.

Disc subcircular with mean disc lenght 109% DW [103.3–114% DW]. Anterior margin of disc with slight concavity in its medial portion (Figs. 1–3). Mean of distance between anterior margin of disc and cloaca 87.3% DW, slightly decreasing with maturity: adults mean 86.4% DW, subadults 85.8% DW, juveniles 88.4% DW, and neonate 92.1% DW (Tab. **S2**). Small head with mean interorbital distance 10.2% DW [8–11.9% DW] and mean interespiracular distance 14.3% DW [12.9–17.3% DW]. Eyes small, not pedunculated (Fig. 4) with mean eye length 1.3% DW [0.7–2.3% DW]; eye length decreasing with maturity: adults mean 1% DW [0.7–1.6% DW], subadults 1.1% DW [0.9–1.6% DW], juveniles 1.8% DW [1.2–2.3% DW], and neonate 2.3% DW (Tab. **S2**). Small and rounded spiracles (Fig. 5), with mean spiracle lenght 4.4% DW [2.8–6.4% DW]. Spiracular process short, globular and robust, with growth at maturity, covering much of posterior portion of spiracular opening. Spiracular process with numerous apparent dermal denticles. Adult specimens with pointed dermal denticles (Fig. 5). Preorbital, prenasal and preoral distances with means respectively 31% DW, 29.1% DW and 32% DW. Internasal distance mean 7.8% DW [7.0–8.7% DW], and mouth width mean 9.4% DW [8.2–10.7% DW]. Teeth triangular, arranged in quincunx in both jaws, without size difference between central and lateral rows. Adult and subadult specimens with more developed cusps, mainly in males; juveniles without cusps (Fig. 6). Tooth rows 16–19/13–15, subadults with higher number of rows than juveniles (Tab. 2).

Branchial basket with mean distance between first pair of gill slits 20.2% DW, mean distance between fifth pair of gill slits 17.9% DW, and mean distance between first and fifth gill slits pairs 10.2% DW. Pelvic fin triangular and dorsally covered by disc (Figs. 1–3, **S3**), with mean length of anterior margin 17.4% DW [14.0–21.4% DW]. Distances between distal portions of pelvic fins, and between axils of pectoral and pelvic fins, with means respectively 39.9% DW [32.5–51.0% DW] and 4.0% DW [2.2–6.0% DW] (Tab. 1). Short, robust and conical clasper, with distal end not round, but little more tapered (Fig. **S3**B). Means of external and internal lengths of clasper respectively 6.4% DW [2.6–9.8% DW] and 14% DW [6.8–17.5% DW], and means of pseudosiphon and

TABLE 1 | Measurements of specimens of *Paratrygon lucindai* including the holotype, UNT 7469. Mean, Standard Deviation (SD) and Ranges are expressed in millimeters (mm) and proportions of disc width (%DW); (N) corresponds to the number of specimens analyzed.

Paratrygon lucindai	Holotype		Mean		SD		Range				N
	mm	%DW	mm	%DW	mm	%DW	mm		%DW		
Total length	866	171.5	636.7	151.7	142.2	38.8	340	951	114.8	270.1	42
Disc length	546	108.1	491.9	109.0	166.9	2.6	195	845	103.3	114.0	48
Disc width	505	100.0	451.6	100.0	154.5	0.0	177	801	100.0	100.0	48
Interorbital distance	52	10.3	45.8	10.2	16.7	0.7	18	82	8.0	11.9	48
Interespiracular distance	70	13.9	63.4	14.3	21.3	1.0	28	110	12.9	17.3	48
Eye length	5	1.0	5.2	1.3	0.9	0.5	4	7	0.7	2.3	48
Spiracle length	20	4.0	19.1	4.4	6.5	0.7	8	32	2.8	6.4	48
Preorbital length	153	30.3	139.7	31.0	49.0	1.5	53	247	25.8	34.0	46
Prenasal length	136	26.9	130.3	29.1	44.3	1.0	53	220	26.9	31.6	46
Preoral length	153	30.3	143.2	32.0	48.3	1.1	58	248	30.2	34.8	46
Internasal length	38	7.5	34.9	7.8	12.2	0.4	14	62	7.0	8.7	48
Mouth width	48	9.5	41.6	9.4	14.2	0.5	19	77	8.2	10.7	48
Distance between first gill slits	95	18.8	90.3	20.2	32.0	1.1	37	171	18.7	22.6	46
Distance between fifth gill slits	87	17.2	81.8	17.9	28.8	0.9	31	150	16.3	20.2	45
Branchial basket length	54	10.7	45.6	10.2	15.8	0.6	20	75	9.2	11.6	48
Length of anterior margin of pelvic fin	80	15.8	77.1	17.4	26.6	1.5	35	130	14.0	21.4	48
Pelvic fins width	214	42.4	183.2	39.9	63.0	3.3	67	304	32.5	51.0	45
External length of clasper	42	8.3	30.2	6.4	15.6	2.4	5	50	2.6	9.8	20
Internal length of clasper	85	16.8	64.1	14.0	27.4	3.5	12	95	6.8	17.5	20
Distance between cloaca and tail tip	413	81.8	230.0	61.6	71.5	37.9	128	481	24.3	180.2	41
Tail width	35	6.9	29.4	6.6	10.5	0.5	12	48	5.4	7.7	46
Distance between snout tip and cloaca	–	–	363.7	87.3	146.1	3.2	163	690	81.2	92.3	26
Distance between pectoral axil and posterior margin of pelvic fin	15	3.0	18.2	4.0	8.9	0.9	6	40	2.2	6.0	48
Distance between cloaca and caudal sting	105	20.8	96.4	22.1	35.4	2.2	45	174	18.0	27.1	42
Caudal sting length	45	8.9	37.7	9.3	8.3	2.7	26	60	4.3	14.7	29
Caudal sting width	5	1.0	3.3	0.7	1.3	0.2	1	5	0.4	1.2	37
Pseudosiphon length	9	1.8	7.1	1.4	1.3	0.2	5	9	1.0	1.8	14
Ventral pseudosiphon length	36	7.1	31.4	6.3	6.2	1.3	13	36	3.0	8.4	14

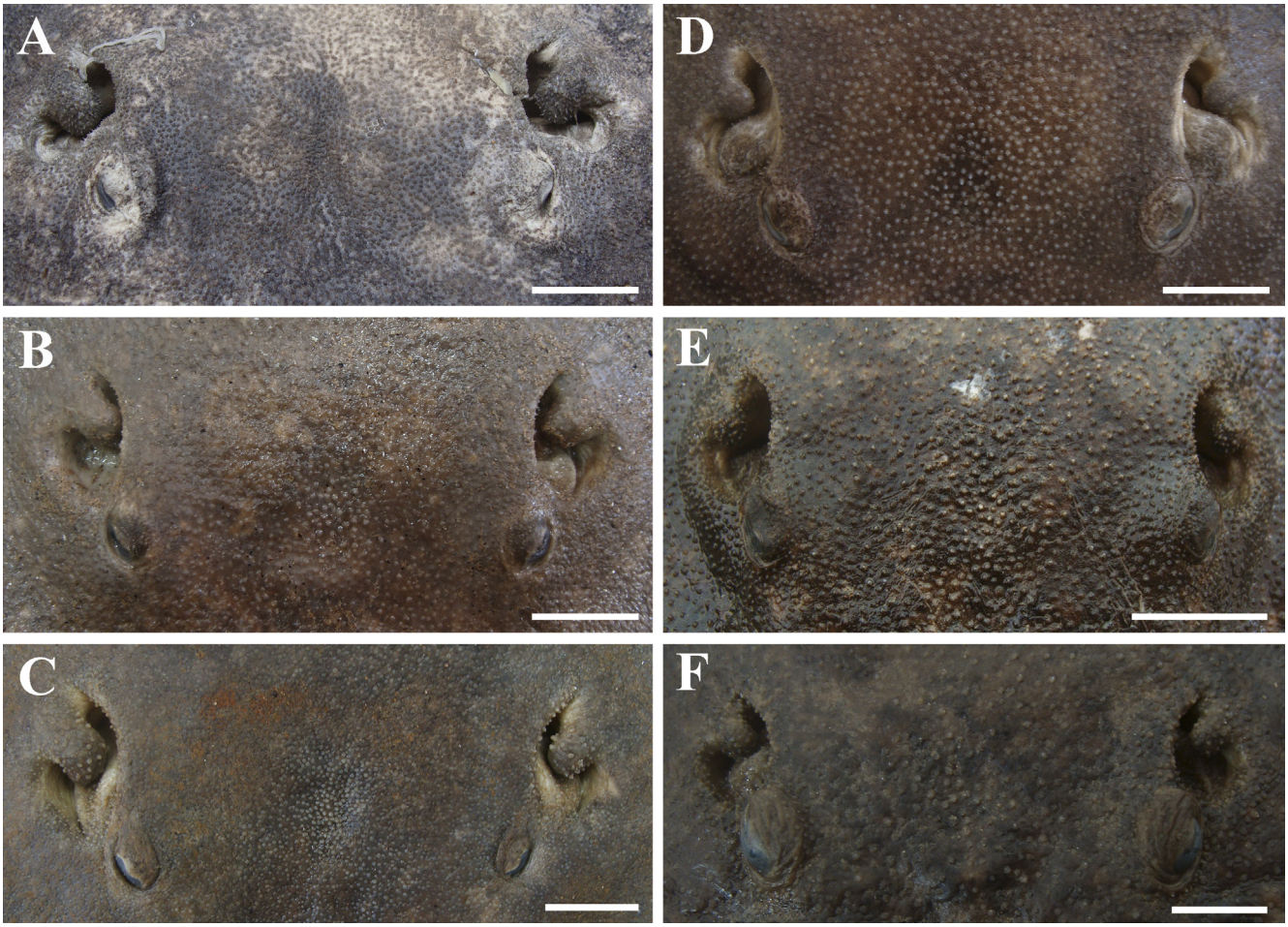

FIGURE 4 | Frontal view of eyes and spiracles of six specimens of *Paratrygon lucindai*. **A.** MZUSP 130341, adult female, 801 mm DW; **B.** UNT 3711, adult male, 481 mm DW; **C.** UNT 7484, paratype, adult female, 645 mm DW; **D.** UNT 7459, paratype, subadult male, 436 mm DW; **E.** UNT 2613, juvenile male; **F.** UNT 7481, juvenile female, 244 mm DW. Scale bars = **A.** 20 mm; **B–E.** 10 mm; **F.** 5 mm.

ventral pseudosiphon lengths respectively 1.4% DW [1.0–1.8% DW] and 6.3% DW [3.0–8.4% DW] (Tab. 1). Claspers with significant increase in size from neonate to adults male specimens: external and internal length means respectively 3.4% DW and 6.8% DW in neonate specimen, 3.0% DW [2.6–4.0% DW] and 9.8% DW [7.7–12.8% DW] in juveniles, 6.5% DW [5.5–7.4% DW] and 14.7% DW [12.2–17.2% DW] in subadults, and 8.1% DW [6.4–9.8% DW] and 17.2% DW [14.6–17.5% DW] in adult specimens. Pseudosiphon and ventral pseudosiphon of claspers with slightly increase in length between subadult and adult male specimens, means respectively 1.4% DW [1.1–1.6% DW] and 5.7% DW [3.0–8.4% DW] in subadults, and 1.4% DW [1.0–1.8% DW] and 6.4% DW [5.7–7.5% DW] in adults (Tab. **S2**).

Tail not long with short pre-caudal sting portion and long and filiform post-caudal sting portion (Figs. 1–3). Mean distance between cloaca and caudal sting (pre-caudal sting portion) 22.1% DW [18.0–27.1% DW], mean tail width 6.6% DW [5.4–7.7% DW], and mean distance between cloaca and tail tip 61.6% DW [24.3 to 180.2% DW]. Tail size decreases with maturity, especially in post-caudal sting portion, with means

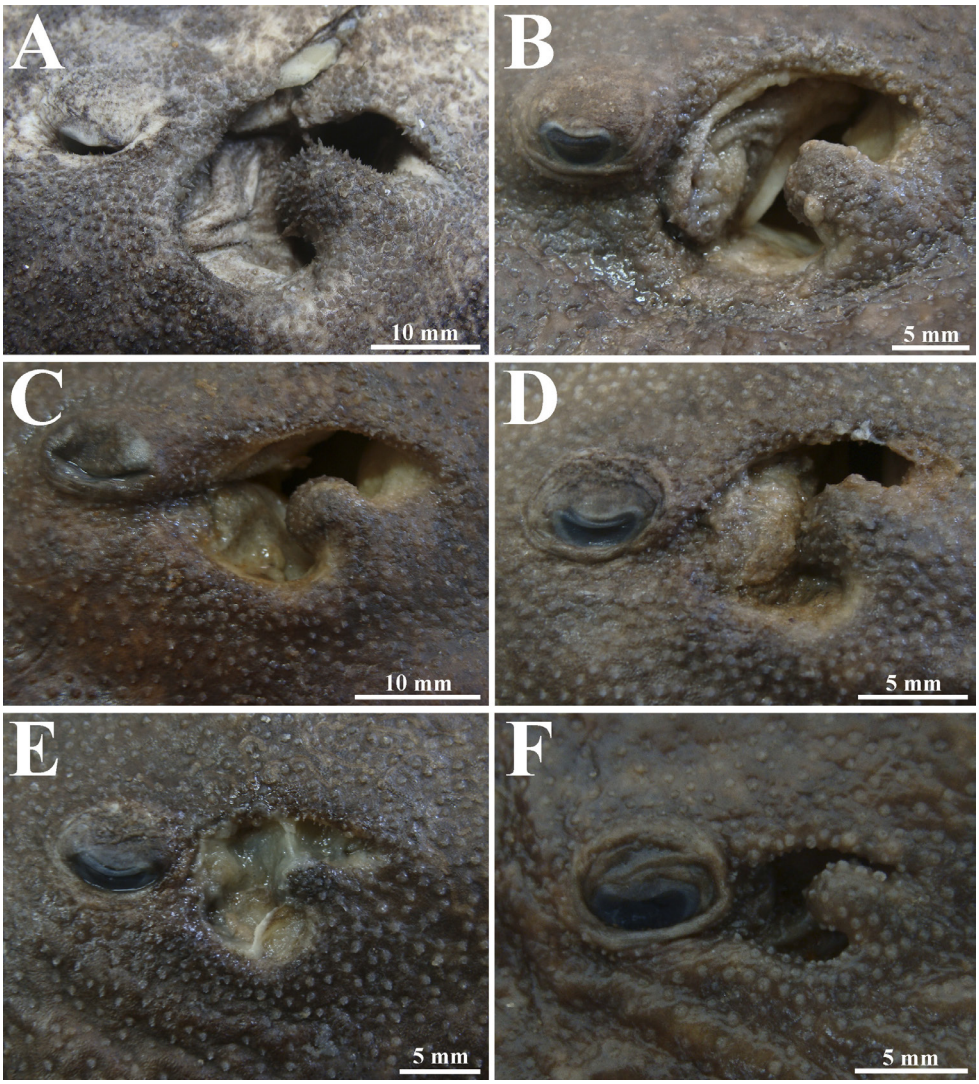

FIGURE 5 | Lateral view of spiracles and spiracles process of six specimens of *Paratrygon lucindai*. **A.** MZUSP 130341, adult female, 801 mm DW; **B.** UNT 7469, holotype, adult male, 505 mm DW; **C.** UNT 7471, adult male, 440 mm DW; **D.** UNT 7460, paratype, subadult female, 455 mm DW; **E.** UNT 7478, juvenile female, 322 mm DW; **F.** UNT 7483, 218 mm DW.

of distance between cloaca and tail tip 180.2% DW in neonate specimen, 88.9% DW [37.6–141.4% DW] in juveniles, 61.6% DW [38.7–108.3% DW] in subadults, and 37.8% DW [24.3–81.8% DW] in adults (Tab. **S2**). Lateral folds on tail from basis to insertion of caudal sting. Very discreet dorsal and ventral tail folds from insertion of caudal sting to tail tip.

Coloration in alcohol. Dorsal disc coloration gray, dark gray, brown, dark brown or reddish brown with large round spots scattered throughout disc. Marginal spots smaller than centrals (Figs. 1A, 2A, C, 3A, C). Large round spots beige, gray, brown, dark brown or reddish brown, more evident in middle region of pectoral fins. Large spots little camouflaged with main color of disc above head, synarcual cartilage and

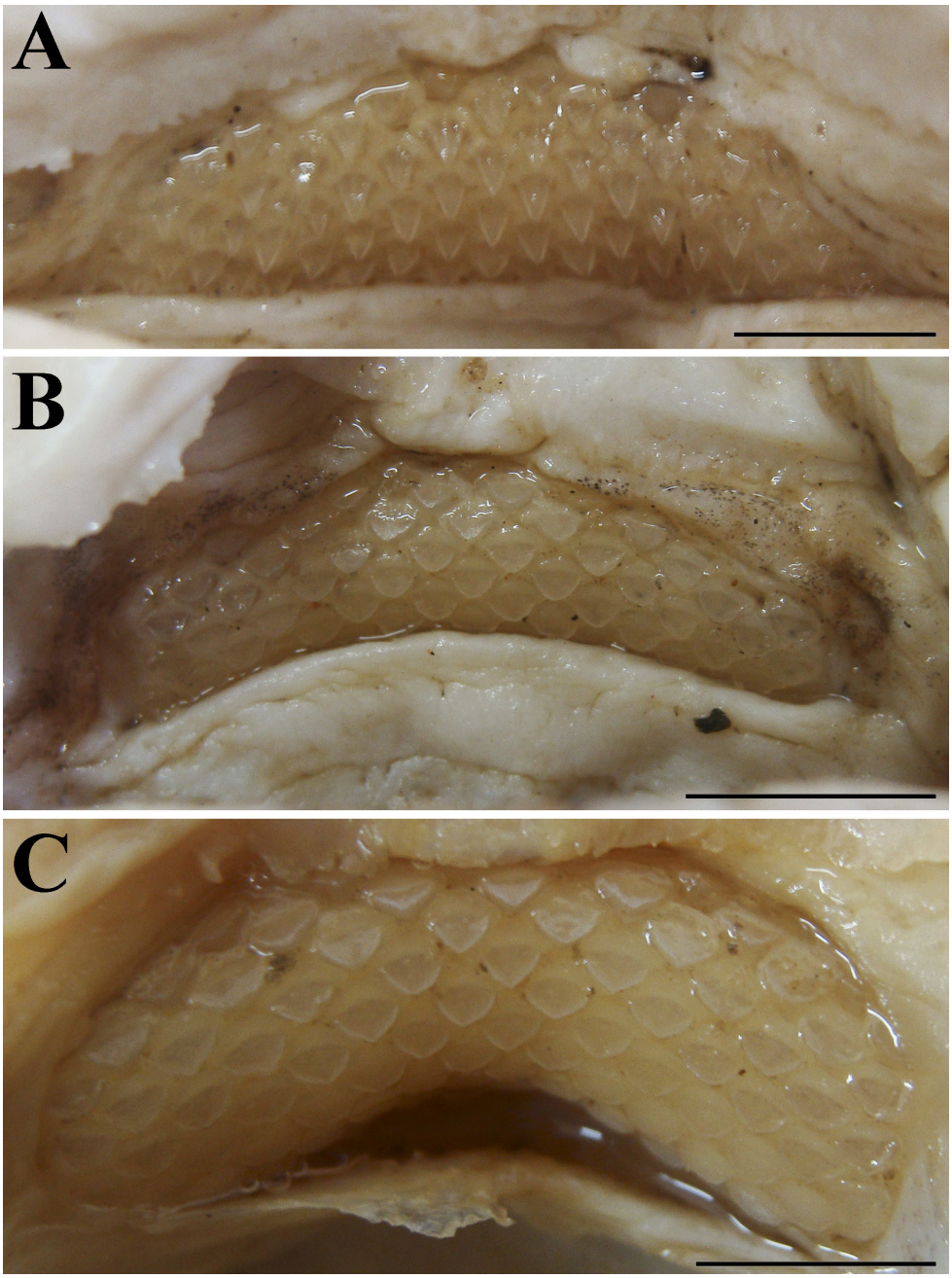

FIGURE 6 | Upper teeth of three specimens of *Paratrygon lucindai*. **A.** UNT 7466, subadult male, 431 mm DW; **B.** UNT 7478, juvenile female, 322 mm DW; **C.** UNT 2613, juvenile male. Scale bars = 5 mm.

scapular girdle in some specimens. Some large spots with thin black peripheral ring. Live specimens with orange or light beige spots. Large round spots two to three times spiracle's diameter, in some specimens five to six times. Numerous small rounded light spots (same size of eye length) in beige or light brown colors also on dorsal disc. Some specimens with small dark spots in vermiculated shape in brown dark or black colors. Both types of small spots generally camouflaged with main disc tonality, and in some specimens mixed with large spots. Some specimens with large number of these small

TABLE 2 | Meristic data taken from specimens of *Paratrygon lucindai* radiographed or dissected; "M" corresponds to mode, and "R" corresponds to range.

Paratrygon lucindai	UNT 7466	UNT 7495	UNT 2613	UNT 7472	UNT 7467	UNT 7473	UNT 7478	UNT 7480	UNT 7479	M	R
Precaudal vertebrae	–	–	–	42	41	41	42	40	39	42	39–42
Caudal vertebrae	–	–	–	–	–	84	78	–	82	–	78–82
Total vertebrae	–	–	–	–	–	125	120	–	121	–	120–121
Diplospoldylic vertebrae	–	–	–	–	–	89	75	–	85	–	75–89
Propterygial radials	–	–	–	48	48	49	49	47	48	48	47–49
Mesopterygial radials	–	–	–	24	26	23	25	25	25	25	23–26
Metapterygial radials	–	–	–	41	38	42	40	38	37	38	37–42
Total radials	–	–	–	113	112	114	114	110	110	114	110–114
Pelvic radials	–	–	–	22	21	17	22	17	22	22	17–22
Tooth rows of upper jaw	19	18	16	–	–	–	17	–	–	–	16–19
Tooth rows of lower jaw	–	–	–	14	15	14	14	13	15	14	13–15
Symphysis of upper jaw	4	3	3	–	–	–	3	–	–	3	3–4
Symphysis of lower jaw	–	–	–	–	–	–	–	–	–	–	–

spots, with large ones camouflaged. Tail dorsal coloration similar to dorsal disc; main tonality with large spots at tail base. Small rounded light and dark vermicular spots from base to tip tail.

Ventral disc coloration with two main tonalities, one light in central disc and anterior margin, and one dark in lateral and posterior margins (Figs. 1B, 2B, D, 3B, D). Light tonality whitish or light beige, and dark tonality gray, beige or light brown. Some specimens with small dark vermiculated spots closer to disc margins. Ventral pelvic fin coloration with same tonalities of ventral disc, and occurance of tonalities varies between specimens: some with light tonality in anterior fin portion and dark one in rest portion of fin; others with light tonality in central portion of fin and dark one in posterior margin. Claspers color pattern similar to pelvic fins: base in lighter tonality, rest with darker one; when dark tonality predominates in pelvic fins, entire clasper in dark color. Ventral tail coloration, from base to caudal sting level, similar to disc margins tonalities. Vermiculated dark spots occur in this portion of tail if margins possess these spots. Ventral coloration of tail after caudal sting level very dark until tail tip.

Squamation. Dermal denticles throughout dorsal regions of disc and tail, with denticles on central disc larger and more visible than denticles on disc margins (Fig. 7A). Posterior margins of disc in adult specimens with numerous thorns in well-developed basal plates (Fig. 7B). On tail, denticles from base to insertion of caudal sting larger than those from caudal sting to tail tip, and in some adult specimens, denticles in this terminal region of tail well developed (Figs. 7B–C).

Dermal denticles on disc with median size, in central disc with 0.5 mm in diameter, whereas in margins and head region smaller (Fig. 8). Denticles on central disc with higher crown not so narrow. Central coronal plate (ccp) well developed, tall, quadrangular in shape, and usually slightly offset from central axis of crown. Lateral coronal ridges (lcr)

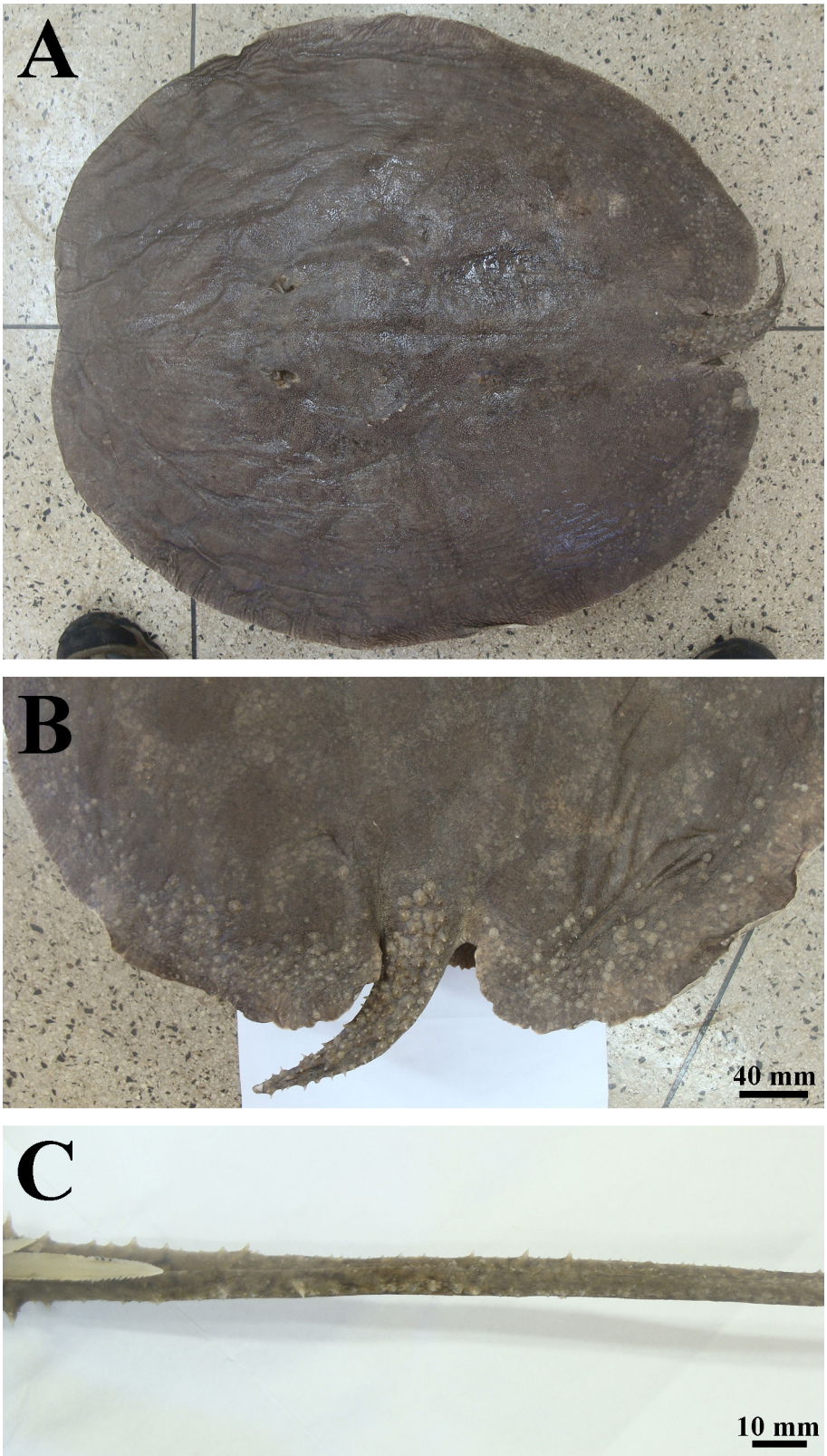

FIGURE 7 | Dermal denticles present on dorsal disc and tail in *Paratrygon lucindai*. **A.** distribution of dermal denticles in paratype UNT 7475, adult female; **B.** denticles present on posterior margins of disc and tail in paratype UNT 7484, adult female; **C.** dermal denticles and thorns present on the post-caudal spine portion in holotype UNT 7469, adult male.

surround central coronal plate, slightly smaller than ccp and conical; range from three to six (Figs. 8B, E–F). Head and marginal dermal denticles similar to centrals in shape, smaller, with fewer lcrs, and ccp sometimes slightly conical in shape (Figs. 8A, C, G). Denticles on posterior margins and at tail base with central coronal plate in conical shape, much more developed and higher than lcrs (when these occur); denticles in this region often in thorn shape. On posterior margins of disc numerous thorns with broad basal plates (bp) (generally larger than three millimeters in diameter and two in height), and tall pointed crowns (cr); small dermal denticles can occur over their basal plates (Figs. 8D, H).

Adult specimens of *P. lucindai* with rows of thorns on dorsal and laterals of tail (Figs. 9A–E). Rows of dorsal thorns from three to five, from before tail base to caudal sting insertion; dorsal thorns developed, not so high, broad-based, often tubercular, and covering practically all dorsal region of tail. Lateral rows in adults between one or two, usually one, from little after tail base to after caudal sting portion; lateral spines developed, similar to dorsals (Figs. 9A–E). Subadult specimens with dorsal and lateral rows very similar to adults, slightly smaller in distribution, with dorsal row from tail base, and laterals until caudal sting region (Figs. 9F–G). Larger juveniles with dorsal and lateral rows similar to adults, although with thorns not developed, and rows shorter than subadults (Fig. 9H). Most juveniles with only dorsal rows in initial development phase, with few, small and sparse spines; lateral rows poorly developed (Figs. 9I–J). Neonate with only initial development of dorsal rows on tail, with rows from base to caudal sting, and thorns with more developed shape.

Mean length and mean width of caudal sting respectively 9.3% DW [4.3–14.7% DW] and 0.7% DW [0.4–1.2% DW] (Tab. 1). Caudal sting length mean decreases with maturity: adults with 7.4% DW [4.3–10.8% DW], subadults 9% DW [7.4–10.3% DW], juveniles 11.9% DW [9.7–14.5% DW], and neonate 14.7% DW. Caudal sting width more stable with maturity: means range from 0.6 to 1% DW with overlap between ranges (Tab. **S2**). One or two well-developed caudal stings in adult and subadults specimens with lateral serrations throughout its extension, serrations larger close to apical portion. Medial dorsal groove in proximal two-thirds of sting (Figs. 10A–D). Larger juvenile specimens with caudal stings similar to adults and subadults, although without medial dorsal groove (Fig. 10E). Smaller caudal sting in most juveniles and neonate specimen with fewer serrations, just in final two-thirds or final half sting; serrations more developed closer to tip (Fig. 10F).

Ventral lateral line canals. Small junction of four canals (JFC), with anterior end positioned more externally than posterior. Anterior end of JFC formed by connection between infraorbital canal (IOC) and supraorbital canal (SPO), and posterior end formed by the connection between hyomandibular (HMD) and nasal (NAS) canals (Fig. 11).

From JFC, angular component of HMD (ang) with open curvature. At height of scapularcoracoid, jugular component of HMD (jug) in large curvature surrounding branchial basket externally. Subpleural loop (spl) with three posterior subpleural tubules (pst); most posterior bifurcated. From spl, subpleural component of HMD (spc) externally and parallel to jug. Slightly below scapulocoraicod bar level, spc at 45° angle to lateral margin of disc. Subpleural tubules (spt) in anterior portion of spc, at level of second pair of gill slits. Close to anterior margin of disc, HMD connects to prenasal component of nasal canal (pnc) (Fig. 11).

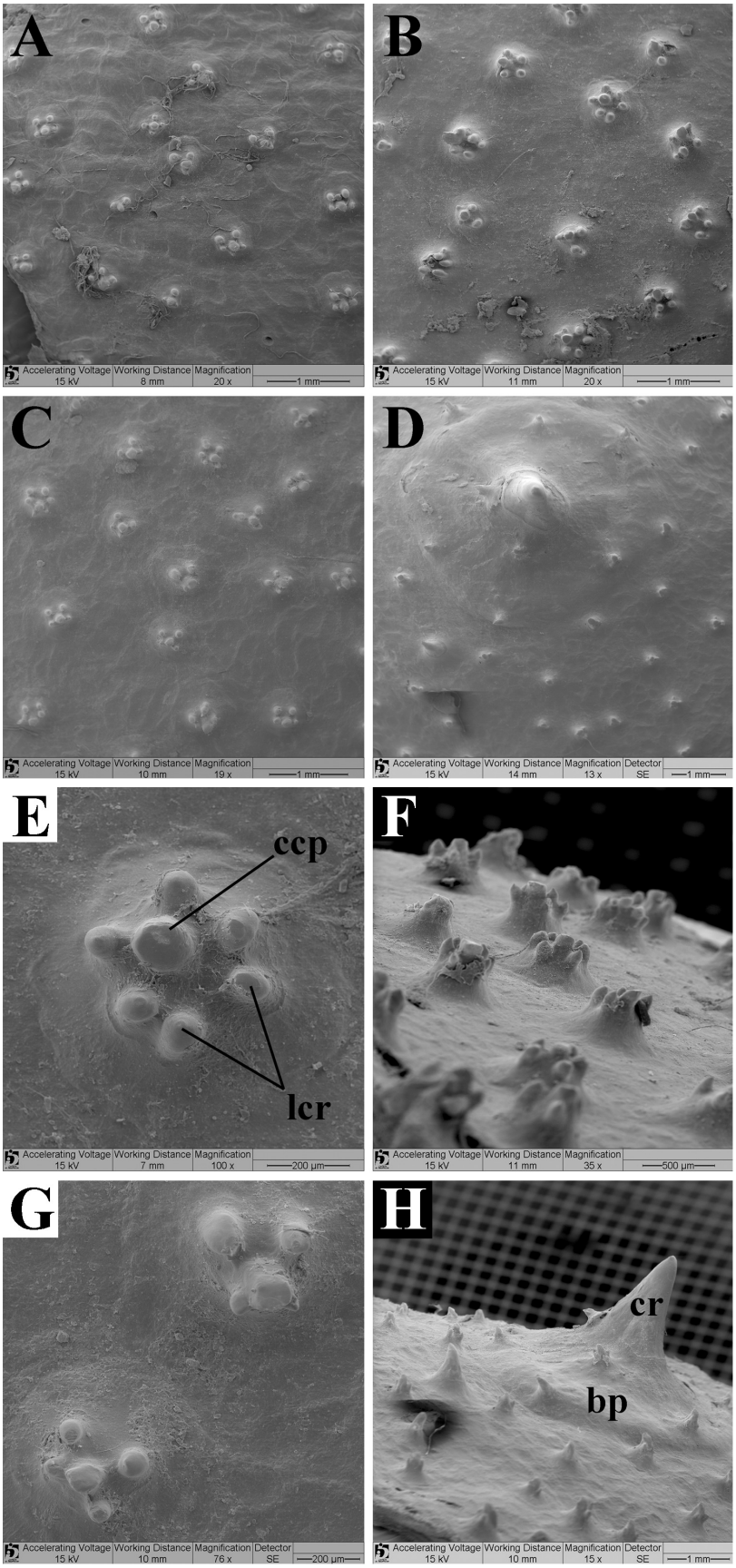

FIGURE 8 | Dorsal view of dermal denticles taken from SEM images of the following regions of the disc from *Paratrygon lucindai*, paratype UNT 7460, subadult female. **A.** Head; **B.** Central; **C.** Lateral; **D.** Posterior; **E.** Central; **F.** Lateral view of dermal denticles from central disc; **G.** Lateral; **H.** Posterior. Abbreviations: bp = basal plate, ccp = central coronal plate, cr = crown, lcr = lateral coronal ridge.

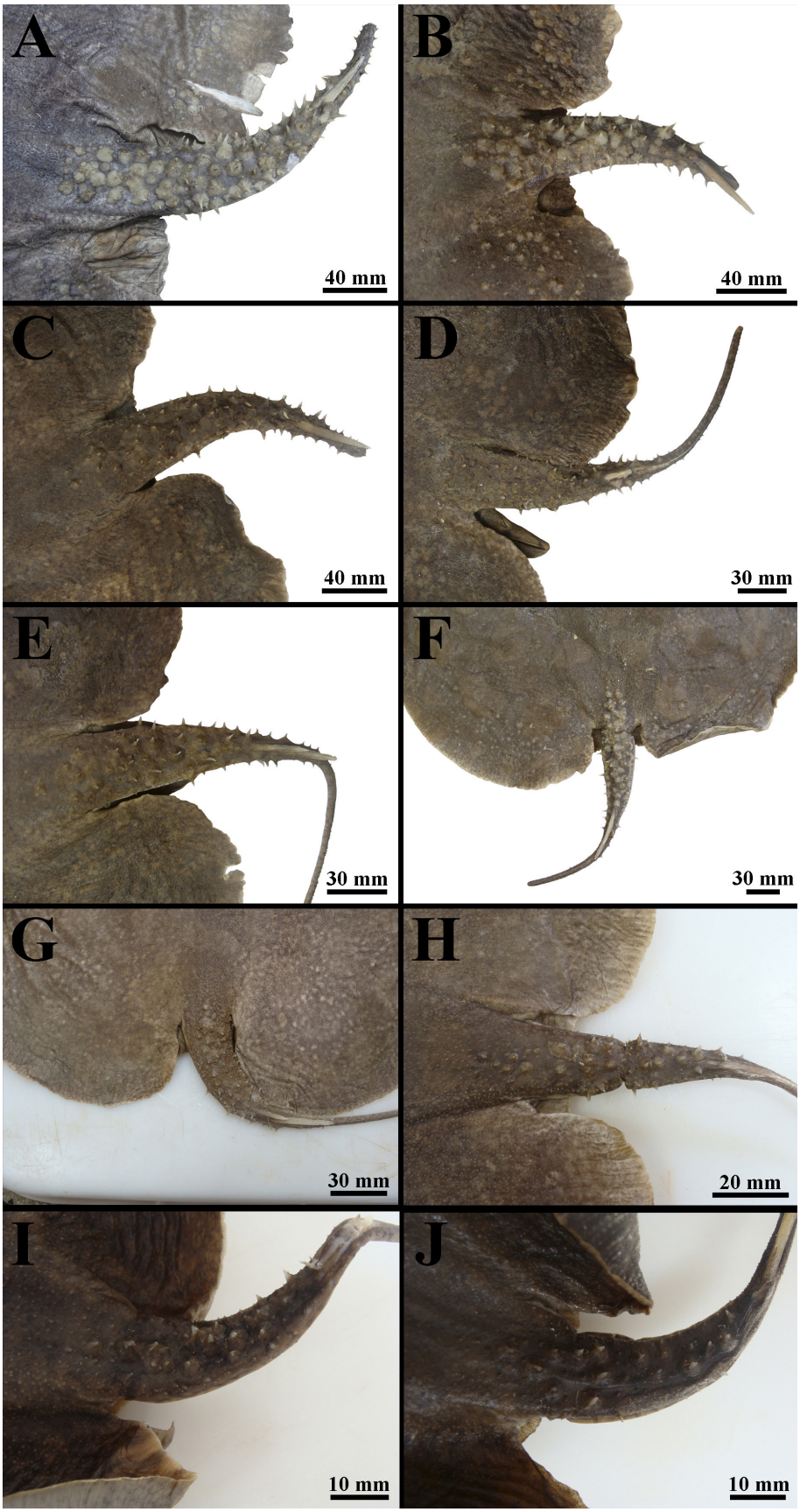

FIGURE 9 | Dorsal view of dorsal and lateral rows of thorns on tail of *Paratrygon lucindai*. **A.** MZUSP 130341, adult female; **B.** UNT 7453, adult female; **C.** UNT 7455, adult female; **D.** UNT 7457, adult male; **E.** UNT 7462, adult male; **F.** UNT 7465, subadult female; **G.** UNT 7495, subadult female; **H.** UNT 7478, juvenile female; **I.** UNT 7481, juvenile female; **J.** UNT 7492, juvenile female.

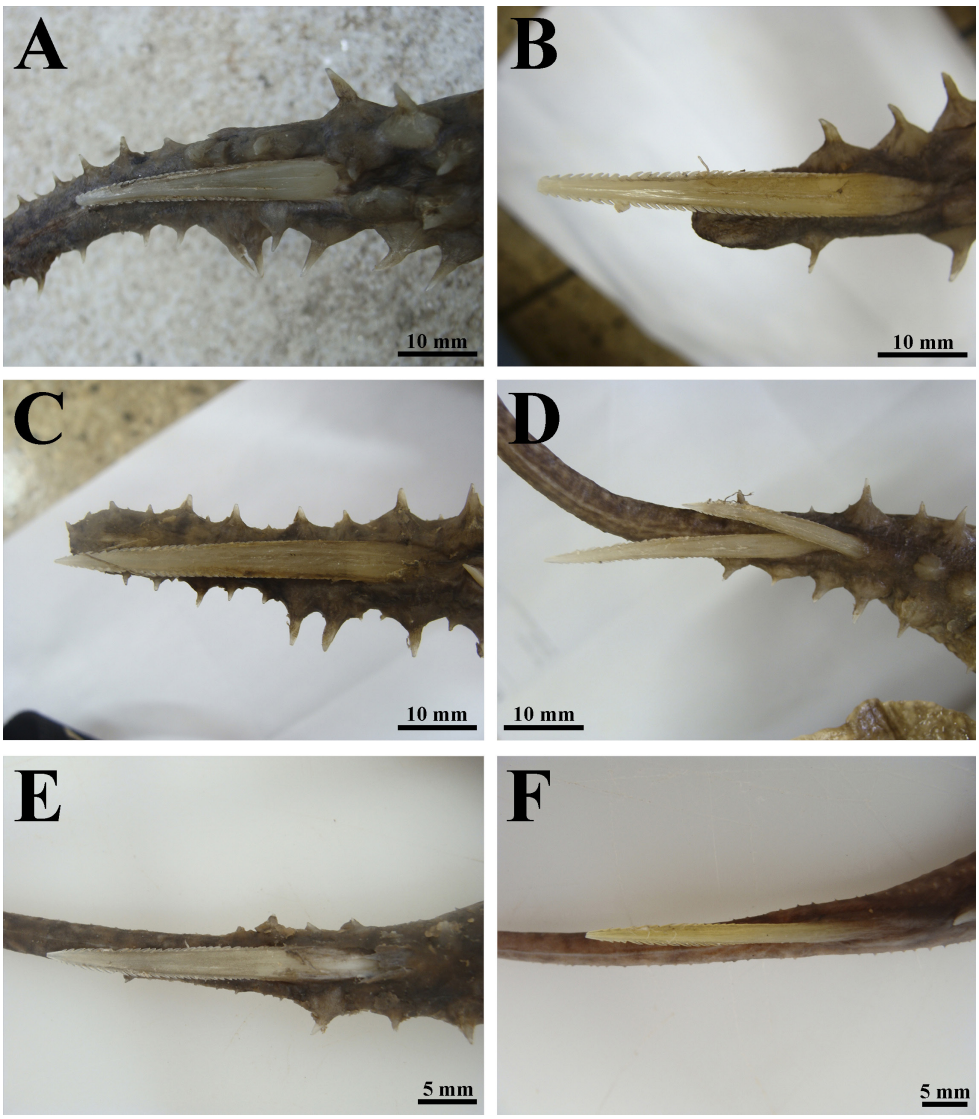

FIGURE 10 | Dorsal view of caudal stings of *Paratrygon lucindai*. **A.** MZUSP 130341, adult female; **B.** UNT 7453, adult female; **C.** UNT 7455, adult female; **D.** UNT 7460, paratype, subadult female; **E.** UNT 7473, juvenile male; **F.** UNT 2467, juvenile female.

IOC with infraorbital curvature (ic) between junction of four canals and suborbital component (sub). Suborbital component reduced, with its ramifications above mouth level in small number. Sub presents one single connection to pnc. SPO from JFC in open and pronounced curvature. Orbitonasal component (orb) with slight central curvature before prenasal loop (pnl). Wide nasointernal loop (nil). Subrostral component (sbr) almost to median portion of pnc, with five to six vesicles of Savi (vS) more concentrated close to nil. *NAS* with slight curvature before entering body close to nasal opening. Close to anterior margin of disc pnc with curvature towards hyomandibular and infraorbital canals. Mandibular canal (MAN) in small curvature posteriorly from Meckel's cartilage, surrounding *adductor mandibulae* muscle (Fig. 11).

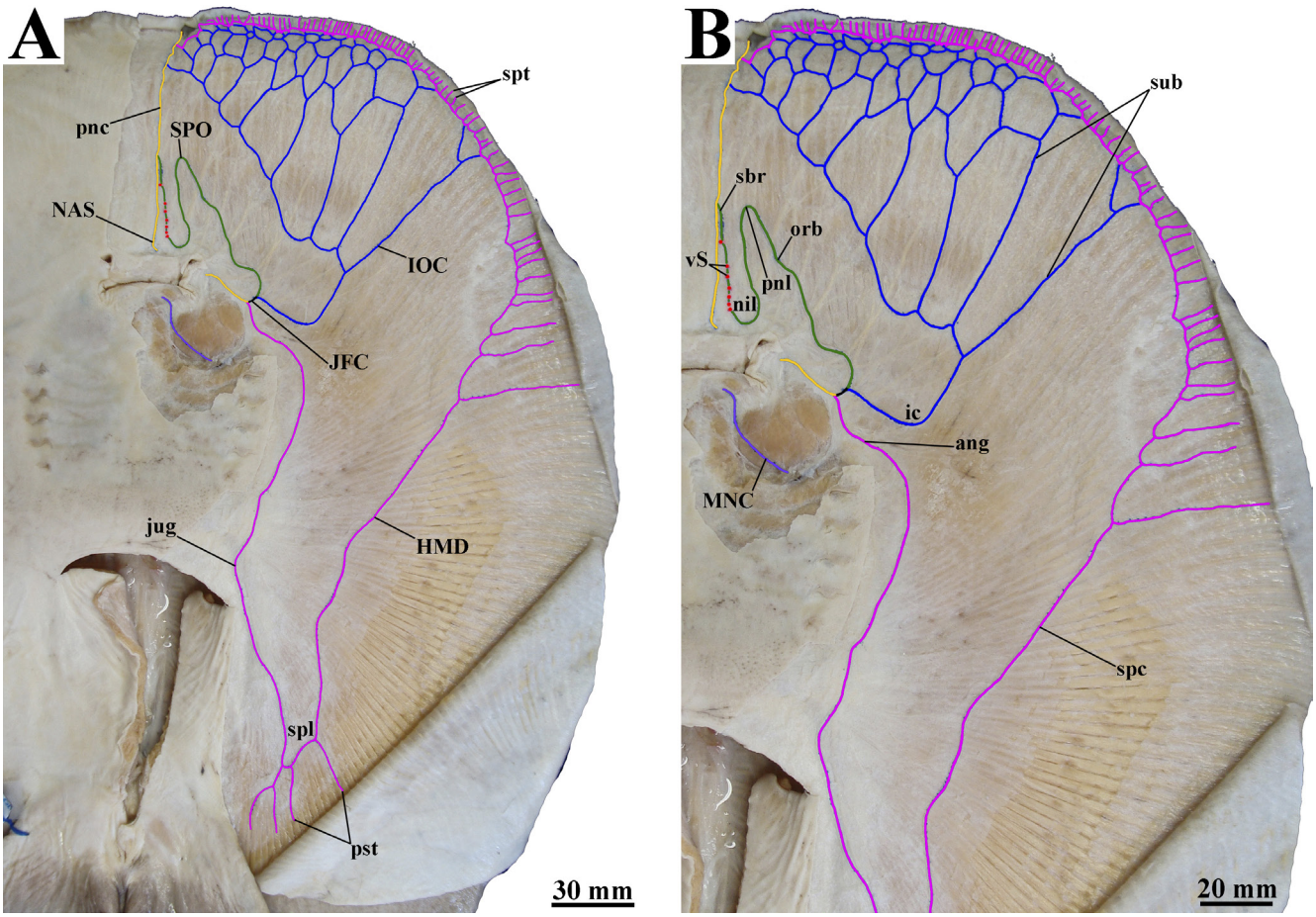

FIGURE 11 | Ventral canals of lateral line system in *Paratrygon lucindai*, specimen UNT 7473, juvenile male. **A.** Distribution of all ventral canals. **B.** Detail of the anterior central disc ventral canals. Abbreviations: ang = angular component of hyomandibular canal, HMD = hyomandibular canal, ic = infraorbital curvature, IOC = infraorbital canal, JFC = junction of the four canals, jug = jugular component of hyomandibular canal, MNC = mandibular canal, NAS = nasal canal, nil = nasointernal loop, orb = orbitonasal component of supraorbital canal, pnc = prenasal component of nasal canal, pnl = prenasal loop, pst = posterior subpleural tubules, sbr = subrostral component of supraorbital canal, spc = subpleural component of hyomandibular canal, spl = subpleural loop, SPO = supraorbital canal, spt = subpleural tubule, sub = suborbital component of supraorbital canal, vS = vesicles of Savi.

Skeleton. Meristic counts of vertebrae and pectoral and pelvic fins radials in Tab. 2. Neurocranium with very small rostral projection (RPJ), short internasal septum (IS) and nasal capsules (NC) very close to each other. Frontoparietal component of fontanelle (FCF) narrow and straight. Mandibular arch with robust, arched and short palatoquadrate (PQ) and Meckel's cartilage (MC), and thin and short hyomandibula (HYO) (Fig. 12). Synarcual cartilage not lateral expanded, with dorsal socket (DS) distal from antero-posterior axis. Lateral stay (LS) well developed and anterolaterally expanded (Fig. 13A). Scapulocoracoid with robust coracoid bar (CB). Both anterior and posterior faces of coracoid bar with curvatures, anterior more curved than posterior. Dorsolateral crest (DLC) of scapular process pronounced and without laterally extending beyond level of mesocondyle (MSC) (Fig. 14A). Propterygium (PPT) robust and arched with evident difference between its anterior and posterior portions. Small articulation surface (SAS)

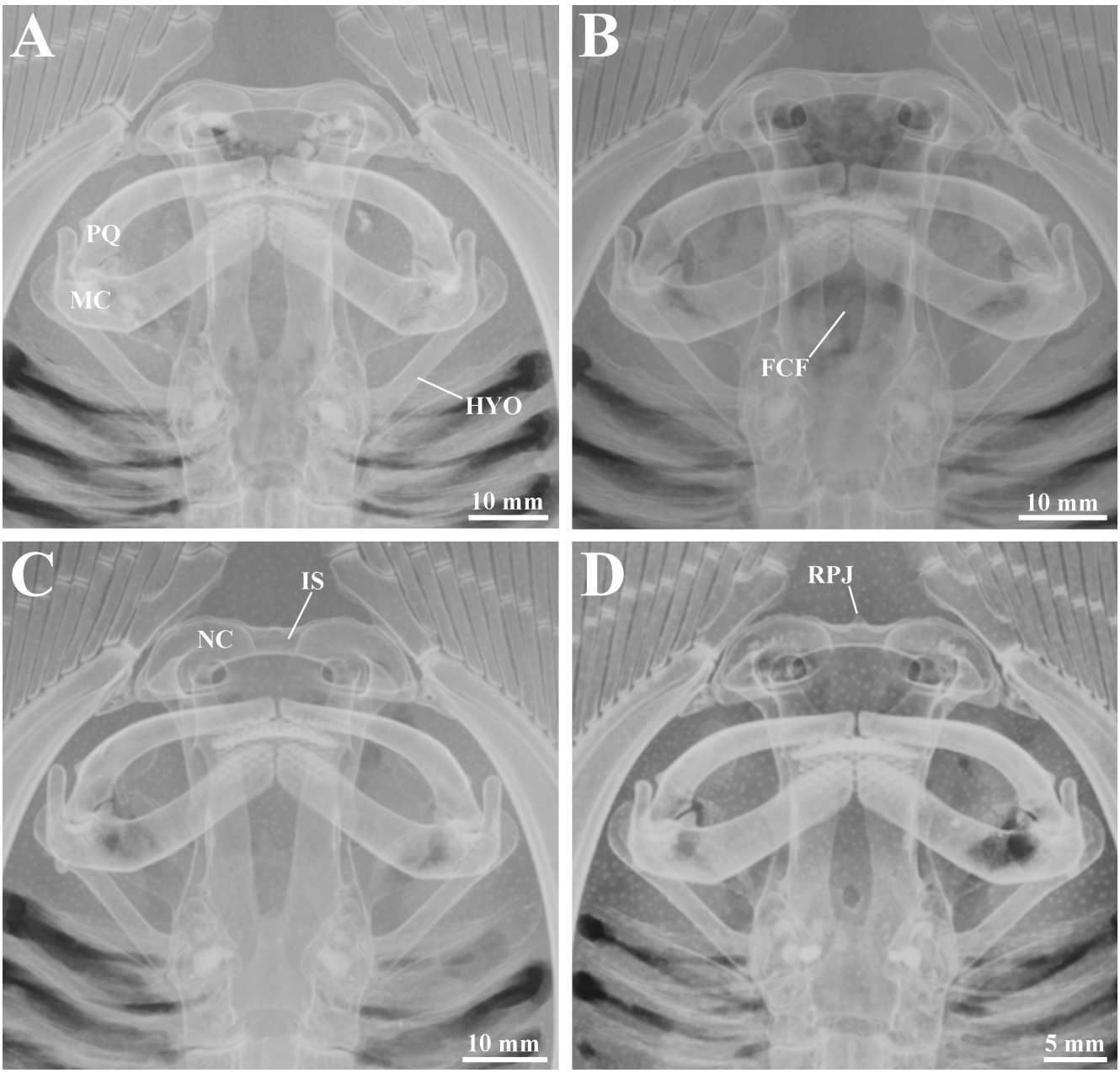

FIGURE 12 | Radiographys of neurocranium and mandibular arch of *Paratrygon lucindai*, upper views. **A.** UNT 7467, paratype, juvenile female; **B.** UNT 7472, juvenile female; **C.** UNT 7473, juvenile male; **D.** UNT 7480, juvenile male. Abbreviations: MC = Meckel's cartilage, FCF = frontoparietal component of fontanelle, HYO = hyomandibula, IS = internasal septum, NC = nasal capsule, PQ = palatoquadrate, RPJ = rostral projection.

of posterior portion of PPT with large area contacting mesopterygium. First segment of propterygium (FSP) one-fourth of PPT (Fig. 14A). Mesopterygium (MSP) with anterior portion width minor than posteriors and well projected anteriorly. Posterior end of MSP pronounced and large. Junctions of medial radials (JMR) occurring in anterior and posterior extremities of MSP (Fig. 14B). Metapterygium (MTP) arched and robust, with its posterior segments (PSM) at level of anterior portion of pelvic girdle (Fig. 14C). Pelvic girdle with arched puboischiadic bar (PB) in upsidedown letter "V"

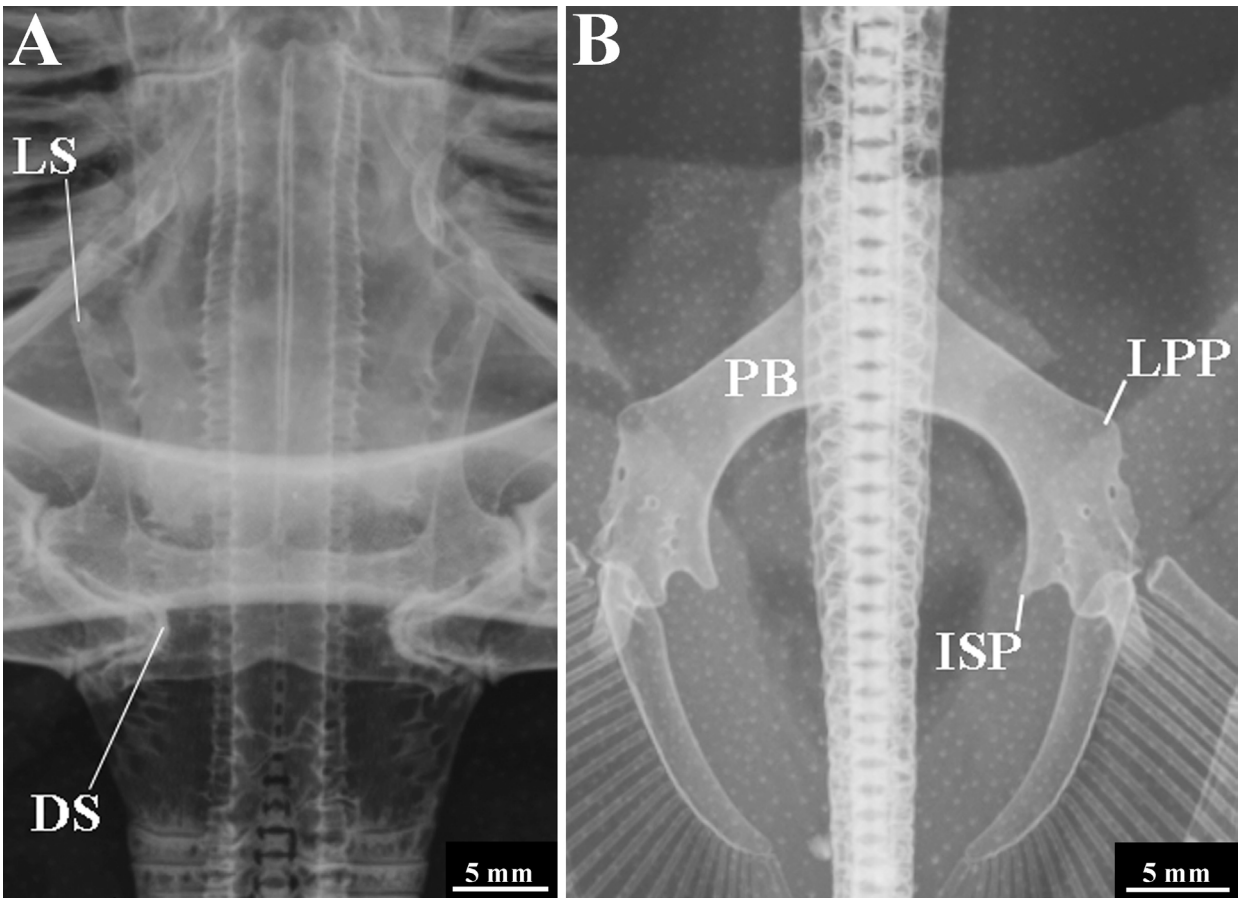

FIGURE 13 | Radiographys of **A.** Synarcual cartilage, UNT 7467, paratype, juvenile female, upper view, and **B.** Pelvic girdle, UNT 7478, juvenile female, upper view, of *Paratrygon lucindai*. Abbreviations: DS = dorsal socket, ISP = ischial process, LPP = lateral prepelvic process, LS = lateral stay, PB = puboischiadic bar.

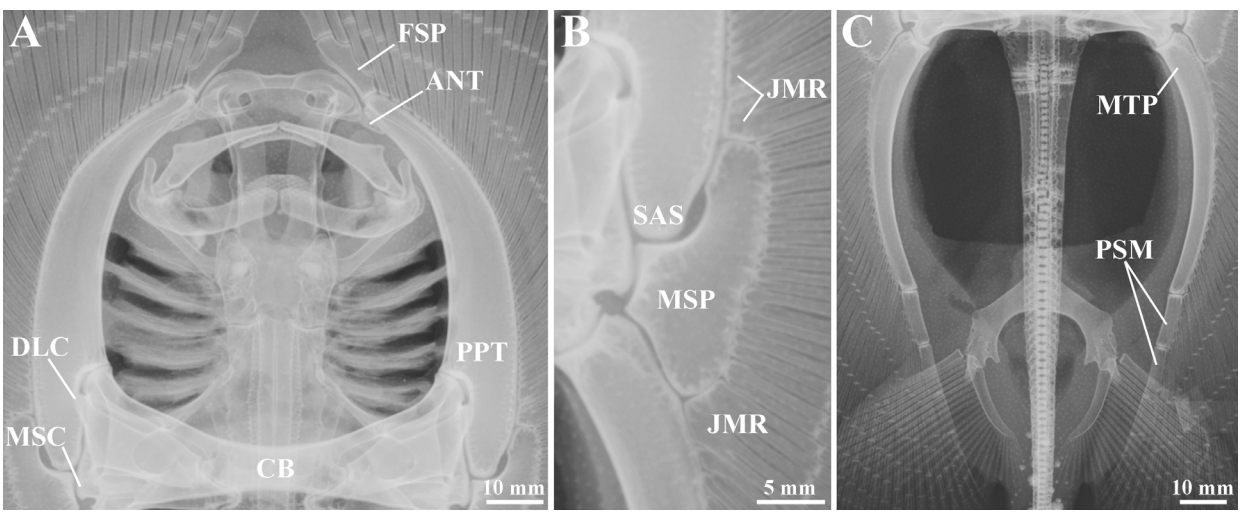

FIGURE 14 | Radiographys of scapulocoracoid and basal elements of pectoral fin of *Paratrygon lucindai*, UNT 7478, juvenile female, upper views. Abbreviations: ANT = antorbital cartilage, CB = coracoid bar, DLC = dorsolateral crest, FSP = first segment of propterygium, JMR = junction of medial radials, MSC = mesocondyle, MSP = mesopterygium, MTP = metapterygium, PPT = propterygium, PSM = posterior segments of metapterygium, SAS = small articulation surface.

format, with lateral extremities posteriorly projected and compressed (Fig. 13B). Ischial process (ISP) projected posteriorly, and lateral prepelvic process (LPP) small and not pronounced (Fig. 13B).

Geographical distribution. *Paratrygon lucindai* is an endemic species of the Tocantins River, occurring in its upper and middle portions, including its tributaries as the Paranã River (Fig. 15).

Etymology. The species epithet is dedicated to Dr. Paulo Lucinda, Professor of the Universidade Federal do Tocantins (UFT), who kindly received the author in his laboratory and also provided and loaned a considerable number of specimens of this endemic species of *Paratrygon* from the Tocantins River. A noun in a genitive case.

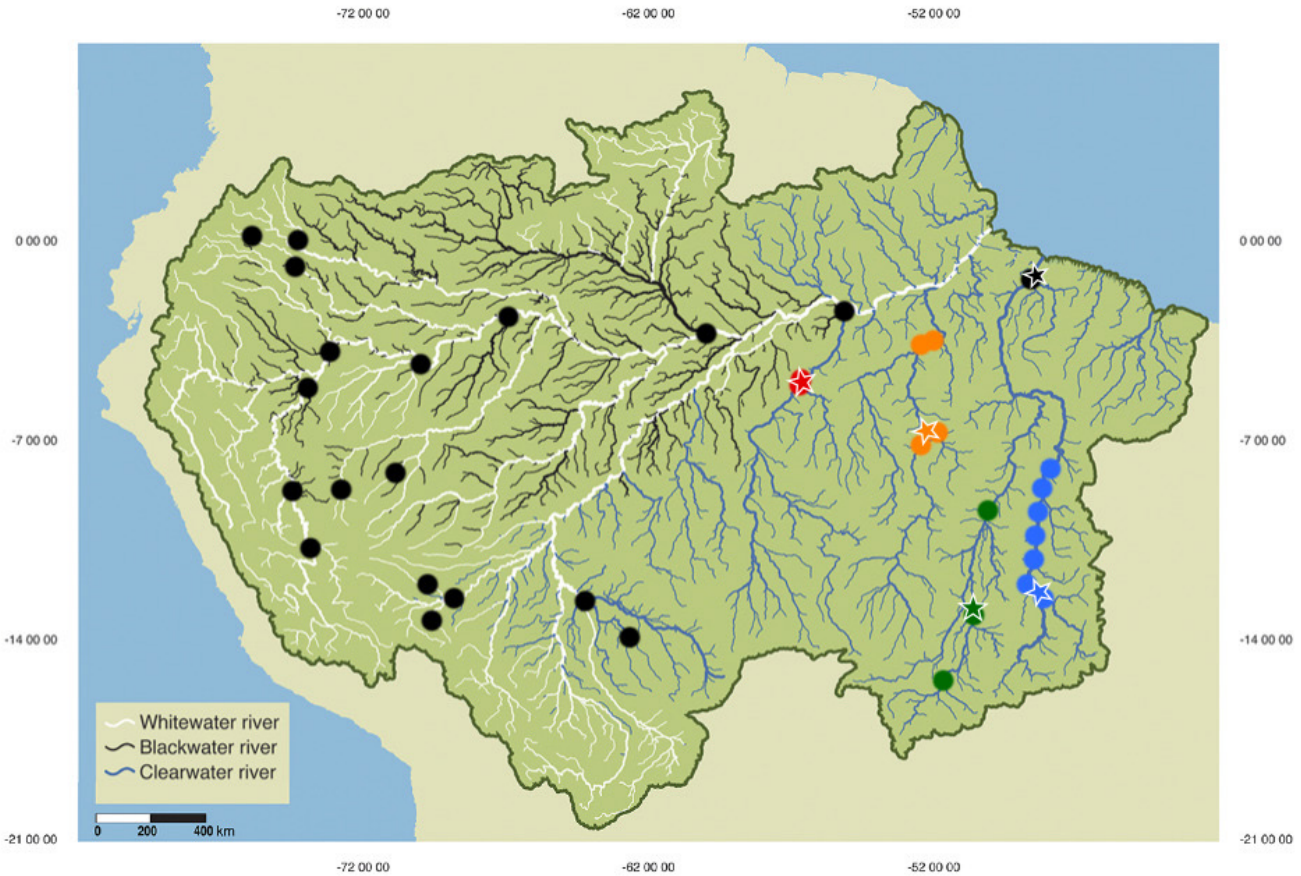

FIGURE 15 | Distribution map of the Amazon basin species of genus *Paratrygon* described in this work and based in Loboda *et al.* (2021) for *P. aiereba*. Black points correspond to *P. aiereba* and star to neotype MZUSP 117155, blue points to *P. lucindai* and star to holotype UNT 7469, green points to *P. araguaia* and star to holotype MZUSP 104390, red points to *P. munduruku* and star to holotype MZUSP 103916, and orange points to *P. raonii* and star to holotype MZUSP 104444. This map, created and modified from Venticinque *et al.* (2016, fig. 4) shows the distribution of Amazonian species of *Paratrygon* according to the type of river water present in the basin. Note that *P. aiereba* has a typical distribution in whitewater rivers, while the four new species occur in clearwater rivers.

Conservation status. *Paratrygon lucindai* is the most well-represented clear river species of *Paratrygon* in collections, particularly in the UFT collection in Porto Nacional, Tocantins. As it has been collected throughout the main stretches of the upper and middle parts of the Tocantins River and its tributaries, populations of this species currently do not face any imminent threats. This aligns with a Least Concern (LC) categorization according to the criteria established by the International Union for Conservation of Nature (IUCN, 2024).

Paratrygon araguaia, new species

urn:lsid:zoobank.org:act:FA450C66-9954-4B01-A103-BA51D07937FA

(Figs. 16–28; Tabs. 3–4)

Paratrygon aiereba. —Carvalho, Lovejoy, 2011:16–17 (list of examined specimens). —Frederico *et al*., 2012:73–79, figs. 1–3 (phylogeography, molecular analysis, conservation). —Fontenelle *et al*., 2021a:6, 10, 12, fig. 2, supplementary 3–4, 9–10, 24, figs. S2–S3 (list of specimens with genetic material analyzed, molecular phylogenys).

Paratrygon sp. 6. —Loboda, 2016: vol. 1. vii, ix, 3, 33, 60–61, 75–76, 87, 100, 113, 123–137, 142, 151–154, 156, 164–168, 190–192, 242–246, vol. 2. xvii–xix, 104–119, figures 146–167 [citation of Frederico *et al*. (2012), morphological comparisons with another *Paratrygon* species, citation from rio Araguaia, synonymy, list of examined specimens, diagnosis, morphological description, distribution, endemicity for rio Araguaia, morphometry, teeth count, meristics].

Holotype. MZUSP 104390, 287 mm DW, Brazil, Goiás State, Municipality of São Miguel do Araguaia, District of Luiz Alves, rio Araguaia, 13°13'3.04"S 50°35'07.86"W, 6 Jun 2005, F. Marques, M. V. Domingues & G. Mattox.

Paratypes. Specimens from rio Araguaia, Brazil. Goiás State: MZUSP 104397, 201 mm DW, Municipality of São Miguel do Araguaia, District of Luiz Alves, rio Araguaia, 13°13'3.04"S 50°35'7.86"W, 6 Jun 2005, F. Marques, M. V. Domingues & G. Mattox. MZUSP 104401, 303 mm DW, Municipality of São Miguel do Araguaia, District of Luiz Alves, rio Araguaia, 13°13'3.04"S 50°35'07.86"W, 7 Jun 2005, F. Marques, M. V. Domingues & G. Mattox. Tocantins State: MZUSP 104405, 285 mm DW, Municipality of Caseara, rio Araguaia, 09°16'11.66"S 49°58'18.70"W, 25 Jun 2005, F. Marques, M. V. Domingues & G. Mattox. MZUSP 104406, 244 mm DW, Municipality of Caseara, rio Araguaia, 09°16'11.66"S 49°58'18.70"W, 25 Jun 2005, F. Marques, M. V. Domingues & G. Mattox.

Non-type. All from Araguaia, Brazil, Goiás State: MZUSP 104366, 241 mm DW, Municipality of São Miguel do Araguaia, District of Luis Alves, rio Araguaia, 13°13'S 50°34'W, Mar 2000, R. A. S. Silvano. MZUSP 104391, 198 mm DW, Municipality of São Miguel do Araguaia, District of Luiz Alves, rio Araguaia, 13°13'3.04"S 50°35'07.86"W, 6 Jun 2005, F. Marques, M. V. Domingues & G. Mattox. MZUSP 104392, 247 mm DW, same data as previous. MZUSP 104393, 230 mm DW, same data as MZUSP 104391. MZUSP 104394, 224 mm DW, same data as MZUSP 104391. MZUSP 104395, 211 mm DW, same data as MZUSP 104391. MZUSP 104396, 223

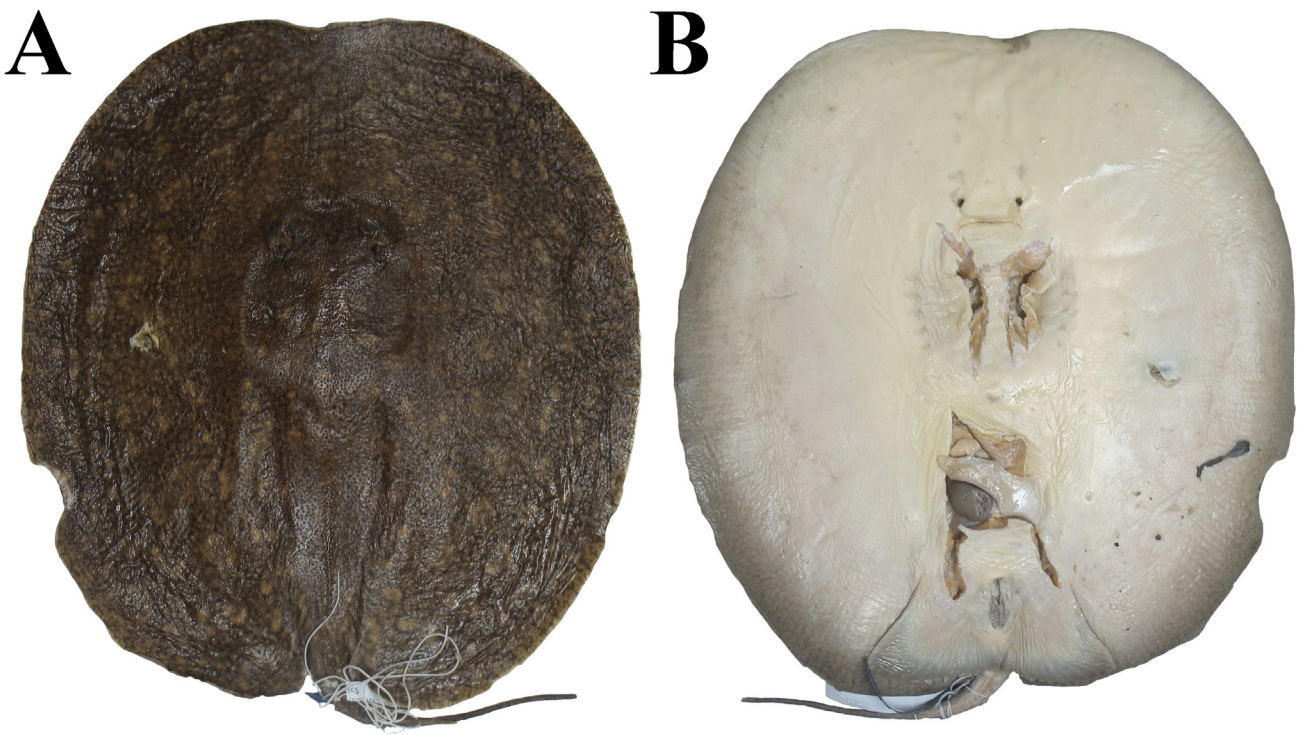

FIGURE 16 | Holotype of *Paratrygon araguaia*, MZUSP 104390, juvenile female, 287 mm DW, from Araguaia River. **A.** Dorsal; **B.** Ventral views.

mm DW, same data as MZUSP 104391. MZUSP 104398, 225 mm DW, same data as MZUSP 104391. MZUSP 104399, 236 mm DW, same data as MZUSP 104391. MZUSP 104000, 278 mm DW, same data as MZUSP 104391. MZUSP 130342, 288 mm DW, rio Araguaia. MZUSP 130343, 278 mm DW, rio Araguaia. MZUSP 130344, 235 mm DW, rio Araguaia. MZUSP 130345, 263 mm DW, rio Araguaia. MZUSP 130346, 236 mm DW, rio Araguaia. MZUSP 130347, 227 mm DW, rio Araguaia. MZUSP 130348, 213 mm DW, rio Araguaia. MZUSP 130349, 219 mm DW, rio Araguaia.

Diagnosis. *P. araguai*a differs from congeners by the following combination of characters: dorsal disc brown or dark brown with two types of spots scattered through the disc, one type light, larger and distinct in beige or light brown, rounded, with diameter similar to spiracles length, the other type being dark, small and vermicular in shape, occurring between the light ones (*vs*. *P. aiereba*, *P. orinocensis*, *P. parvaspina* with gray or light brown dorsal coloration with small dark spots; *P. munduruku* and *P. raonii* with very dark coloration possessing dark spots in vermicular or dendritic pattern; *P. lucindai* with grey, dark grey, brown, dark brown dorsal disc coloration with large round spots in beige, grey, brown, dark brown or reddish brown color); large and rounded spiracles, mean spiracle length 5.3% DW (4.3–6.1% DW), with reduced and straight spiracular process covering a small part of the posterior part of the spiracular aperture [*vs*. *P. aiereba*, *P. parvaspina*, *P. munduruku* and *P. raonii* with quadrangular spiracles; *P. orinocensis* with triangular spiracles; *P. lucindai* with rounded but small spiracles, mean spiracle length 4.4% DW (2.8–6.4% DW) with globular and larger spiracular process]; dermal denticles with central coronal plate acute and reduced, and lateral coronal ridges rounded and well developed (*vs*. *P. aiereba*, *P. parvaspina*, *P. munduruku*, *P. lucindai* with

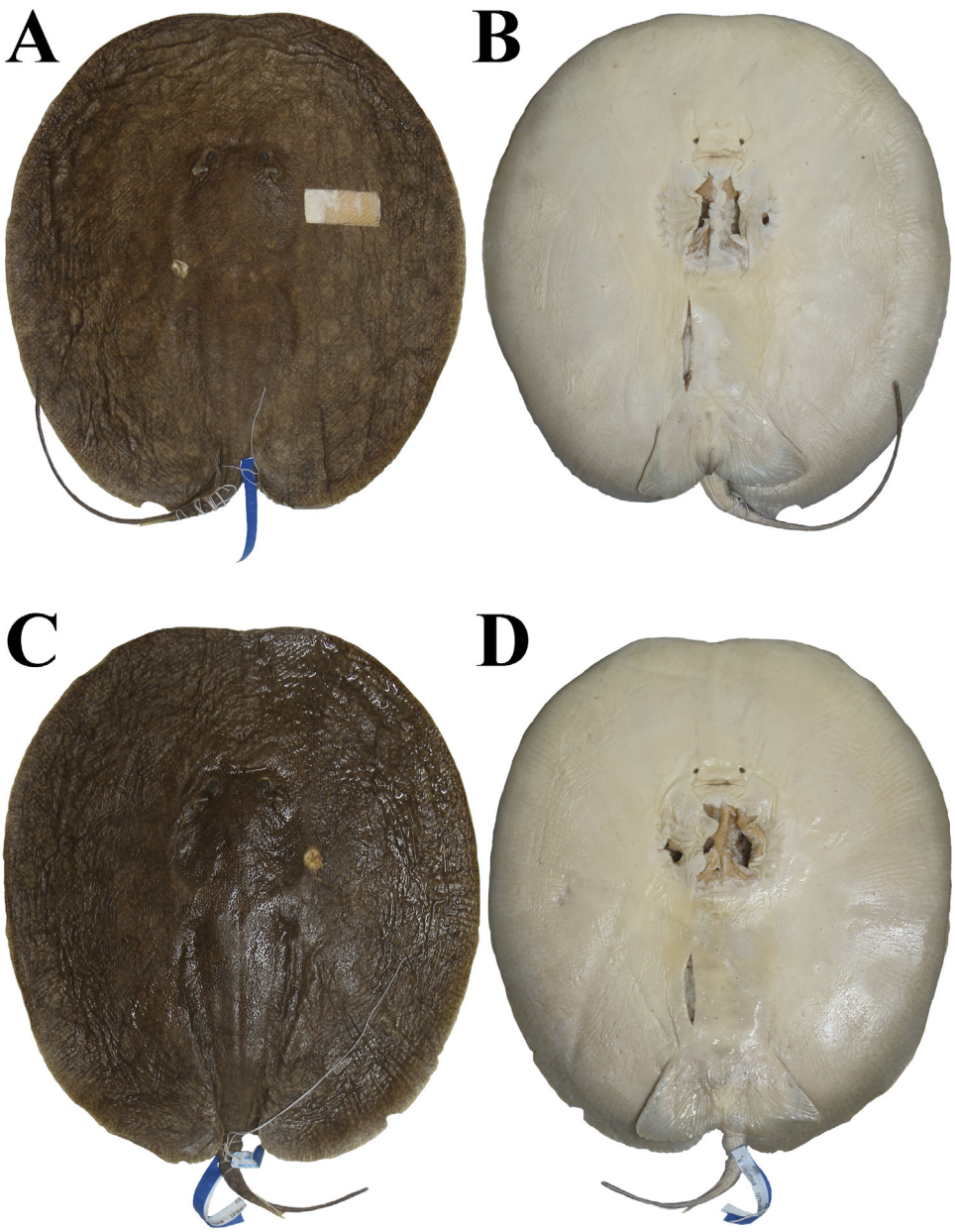

FIGURE 17 | Paratypes of *Paratrygon araguaia*, MZUSP 104401, juvenile male, 303 mm DW, from Araguaia River. **A.** Dorsal; **B.** Ventral views. MZUSP 104405, juvenile female, 285 mm DW, from Araguaia River. **C.** Dorsal; **D.** Ventral views.

dermal denticles possessing developed central coronal plate and reduced lateral coronal ridges; *P. orinocensis*, *P. raonii* also with developed central coronal plate, although with less developed lateral coronal ridges than *P. araguaia*); rostral projection well extended between the nasal capsules, with its extremity exceeding the anterior level of the nasal capsules (*vs*. *P. aiereba*, *P. orinocensis*, *P. lucindai*, *P. munduruku*, *P. raonii* with reduced projections; *P. parvaspina* with robust projection not reaching anterior level of nasal capsules); anterior part of mesopterygium with its length between half and slightly less than half of the posterior part (*vs*. other congeners with both parts similar in length or with the part anterior slightly larger than the posterior one).

Description. Measurements of *P. araguaia* in Tab. 3. Disc subcircular with mean disc lenght 107.9% DW (105–110.9% DW). Anterior margin of disc with slightly pronounced concavity (Figs. 16–18), and mean of distance between anterior margin of disc to cloaca 86.1% DW (82.6–89.8% DW). Small interorbital distance with 10% DW (8.4–11.2% DW), and great interspiracular distance mean: 15.9% DW (14.3–18.4% DW). Small pedunculated eyes (Fig. 19), with mean diameter 1.8% DW (1.4–2.3% DW). Great and rounded spiracles with wide opening and mean lenght in 5.3% DW (4.3–6.1% DW). Spiracular process with simple format, not long but slender, covering just part of posterior portion of spiracular aperture, with few dermal denticles very apparent (Fig. 20). Means of preorbital, prenasal and preoral distances respectively 30.1%, 28% and 31.4% DW, mean of internasal distance 8.2% DW (7.3–8.8% DW). Mouth width mean 9.9% DW (8.7–11.3% DW).

TABLE 3 | Measurements of specimens of *P. araguaia* including the holotype, MZUSP 104390. Mean, Standard Deviation (SD) and Ranges are expressed in millimeters (mm) and proportions of disc width (%DW); (N) corresponds to the number of specimens analyzed.

P. araguaia	MZUSP 104390		Average		SD		Range				N
	mm	%DW	mm	%DW	mm	%DW	mm		%DW		
Total length	412	143.6	450.6	184.4	63.4	34.1	368	624	130.2	237.0	17
Disc length	308	107.3	262.5	107.9	33.1	1.8	211	326	105.0	110.9	23
Disc width	287	100.0	243.1	100.0	29.6	0.0	198	303	100.0	100.0	23
Interorbital distance	27	9.4	24.2	10.0	2.8	0.7	21	32	8.4	11.2	23
Interespiracular distance	41	14.3	38.5	15.9	3.6	1.0	34	46	14.3	18.4	23
Eye length	5	1.7	4.3	1.8	0.5	0.2	4	5	1.4	2.3	23
Spiracle length	15	5.2	12.8	5.3	1.5	0.5	11	16	4.3	6.1	23
Preorbital length	89	31.0	73.2	30.1	9.7	0.9	59	90	27.7	31.7	23
Prenasal length	80	27.9	68.1	28.0	8.6	0.8	55	84	26.6	29.5	23
Preoral length	90	31.4	76.2	31.4	9.3	0.9	63	93	29.6	32.7	23
Internasal length	23	8.0	19.9	8.2	2.8	0.3	16	25	7.3	8.8	22
Mouth width	27	9.4	24.1	9.9	2.9	0.7	20	31	8.7	11.3	23
Distance between first gill slits	62	21.6	50.5	20.8	6.7	0.8	43	64	19.7	22.5	23
Distance between fifth gill slits	55	19.2	44.5	18.3	6.3	0.6	37	59	16.9	19.5	23
Branchial basket length	30	10.5	27.3	11.2	3.5	0.4	22	35	10.4	12.1	23
Length of anterior margin of pelvic fin	50	17.4	45.0	18.5	5.8	1.1	37	55	15.8	20.5	23
Pelvic fins width	109	38.0	89.4	36.7	12.7	2.8	73	110	31.4	41.3	22
External length of clasper	–	–	6.6	2.6	1.0	0.3	5	8	2.1	3.0	12
Internal length of clasper	–	–	18.8	7.5	2.7	0.6	15	24	6.1	8.3	12
Distance between cloaca and tail tip	144	50.2	215.4	89.2	67.3	31.4	108	370	37.5	138.9	17
Tail width	18	6.3	15.6	6.4	1.7	0.5	12	18	5.4	7.5	23
Distance between snout tip and cloaca	249	86.8	209.3	86.1	26.3	1.8	173	256	82.6	89.8	23
Distance between pectoral axil and posterior margin of pelvic fin	11	3.8	9.8	4.1	2.3	1.0	6	15	2.1	6.1	23
Distance between cloaca and caudal sting	58	20.2	49.9	20.4	9.5	2.2	31	73	15.4	24.1	21
Caudal sting length	30	10.5	26.2	10.7	1.5	1.3	23	30	8.6	12.8	15
Caudal sting width	2	0.7	2.1	0.8	0.2	0.2	2	3	0.7	1.3	16
Pseudosiphon length	–	–	–	–	–	–	–	–	–	–	–
Ventral pseudosiphon length	–	–	–	–	–	–	–	–	–	–	–

Branchial basket wide with mean of distance between first gill slits 20.8% DW (19.7–22.5% DW), mean of distance between fifth gill slits 18.3% DW (16.9–19.5% DW), and mean of distance bewteen first and fifth pairs of gill slits 11.2% DW (10.4–12.1% DW). Triangular pelvic fins dorsally covered by disc (Figs. 16B, 17B, D, 18B, D, **S4**), mean of anterior margin 18.5% DW (15.8–20.5% DW), and mean of distance between distal extremities of pelvic fins 36.7% DW (31.4–41.3% DW). Mean of distance between axils of pectoral and pelvic fins 4.1% DW (2.1–6.1% DW). Means of external and internal lenghts of clasper from male juveniles respectively 2.6% DW (2.1–3% DW) and 7.5% DW (6.1–8.3% DW).

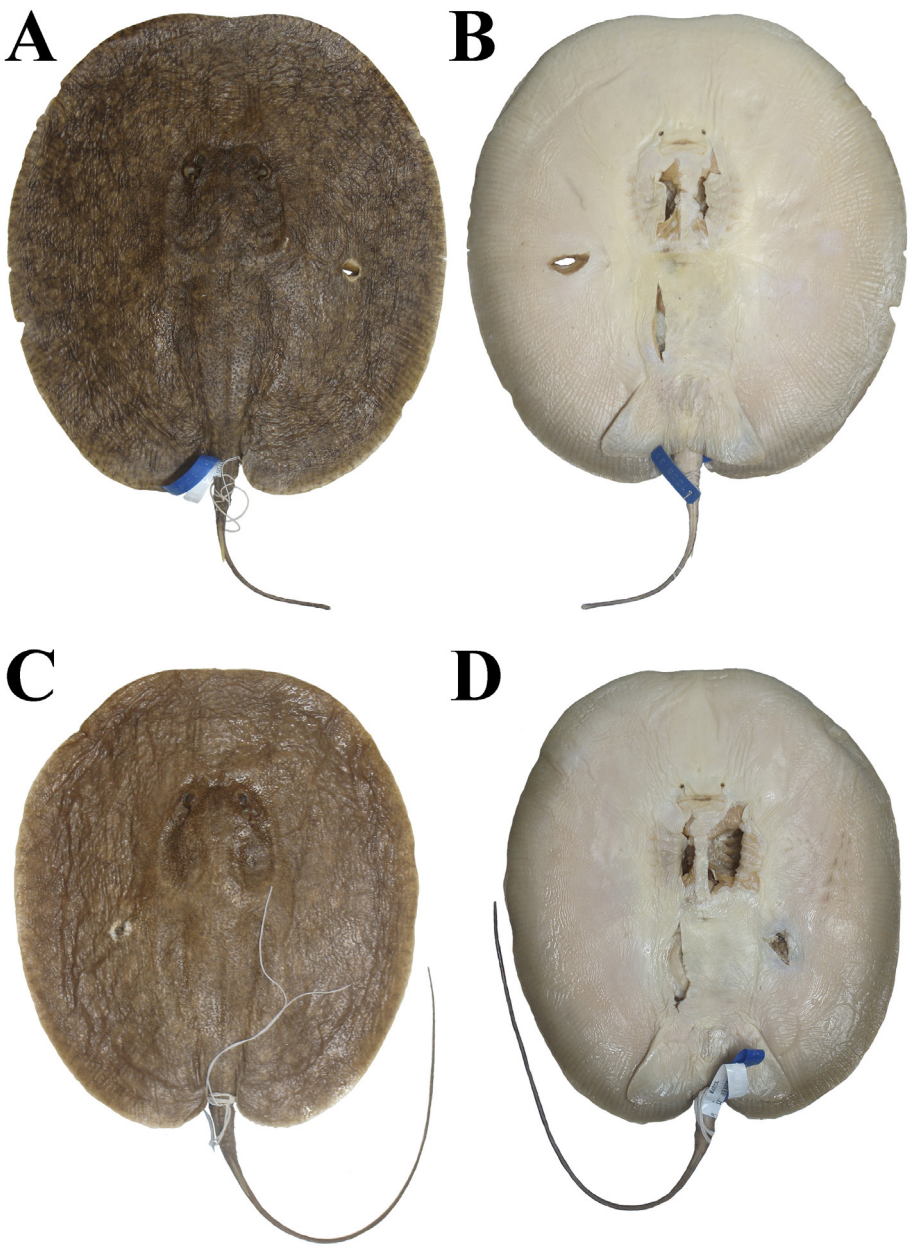

FIGURE 18 | Paratypes of *Paratrygon araguaia*, MZUSP 104406, juvenile female, 244 mm DW, from Araguaia River. **A.** Dorsal; **B.** Ventral views. MZUSP 104397, juvenile female, 201 mm DW, from Araguaia River. **C.** Dorsal; **D.** Ventral views.

Tail long, with pre-caudal sting portion thicker than post-caudal sting. Post-caudal sting of tail long and filiform. Mean of distance between cloaca and caudal sting insertion (pre-caudal sting portion) 20.4% DW (15.4–24.1% DW) and mean tail width (tail basis) 6.4% DW (5.4–7.5% DW). Lateral folds in all extention of pre-caudal sting portion. Dorsal and ventral folds very slim and just in post-caudal sting portion.

Coloration in alcohol. Dorsal coloration of disc brown or dark brown with two types of spots throughout disc, one light more evident and bigger, and other dark, small in size; dark spots generally between light ones (Figs. 16A, 17A, C, 18A, C). Light spots in beige or light brown colors, rounded, with diameter in same size or bigger than spiracle. Some of light spots with tiny dark brown dots in their central portions. Dark spots in brown or dark brown colors, in vermiculated format, with some as ramificated vermiculations. In some specimens these vermiculated dark spots with considerable size. Dorsal coloration of tail very similar with disc, with tail basis also with light spots that occur in disc, however in minor size.

Ventral coloration of disc with two tonalities, one light in central part and anterior margin of disc, and other dark in lateral and posterior margins (Figs. 16B, 17B, D, 18B, D). Light tonality in white and light beige colors, and dark tonality in light grey, grey and brown colors; some specimens with small rounded spots more darker in this tonality. Pelvic fin with same tonalities as disc: posterior margin with same dark tonality as posterior margin of disc, and rest of pelvic fin with same tonality of central disc. Clasper with its basis in light tonality colors, and rest of organ in dark tonality colors; clasper with same colors of pelvic fins. Tail with pre-caudal sting portion in light colors as white, light beige, or in little dark colors than these, as light grey or grey. Post-caudal sting portion in dark colors as dark grey in sting region and black near tip.

Squamation. Dermal denticles throughout dorsal disc and tail. Central disc denticles bigger and more visible than denticles on margins, and on tail, denticles bigger in basis and only in pre-caudal sting region. In central disc dermal denticles with diameter between 0.5 to 1 mm, and in head and tail base regions between 0.2 to 0.6 mm (Figs. 21–22). In central disc denticles with major crown with ccp small in diameter and in conical shape, generally high, and with lcr well developed, wide, and generally rounded in shape, with one of lcrs always higher than others (Figs. 21C–D, 22C–F). Some denticles with more developed lcrs and with dichotomous pattern (Figs. 21C–E). Lcrs range from one to five, and generally well developed (Figs. 21C–D, 22C–F). Dermal denticles on head similar to ones in central disc, with less lcrs, and on head with one to three lcrs (Figs. 21A–B, 22A–B). On tail base denticles in minor size, with small ccps and lcrs, and lcrs more pointed and with dichotomous pattern. On this region denticles with just pointed ccp (Figs. 21E–F, 22G–H).

Largest juvenile specimens with one to two dorsal rows of thorns not developed, however in tail base, spines higher, more developed, with broad basis, and some tubercular. Dorsal rows from tail base until insertion of caudal sting (just in pre-caudal sting portion). Lateral rows with just one small row, and in some specimens just near caudal sting. Thorns of lateral rows developed, in some specimens more developed than dorsal ones, with laterals higher, with broad basis, some tuberculars (Figs. 23A–B). Majority of juvenile specimens with just two dorsal rows not developed in almost

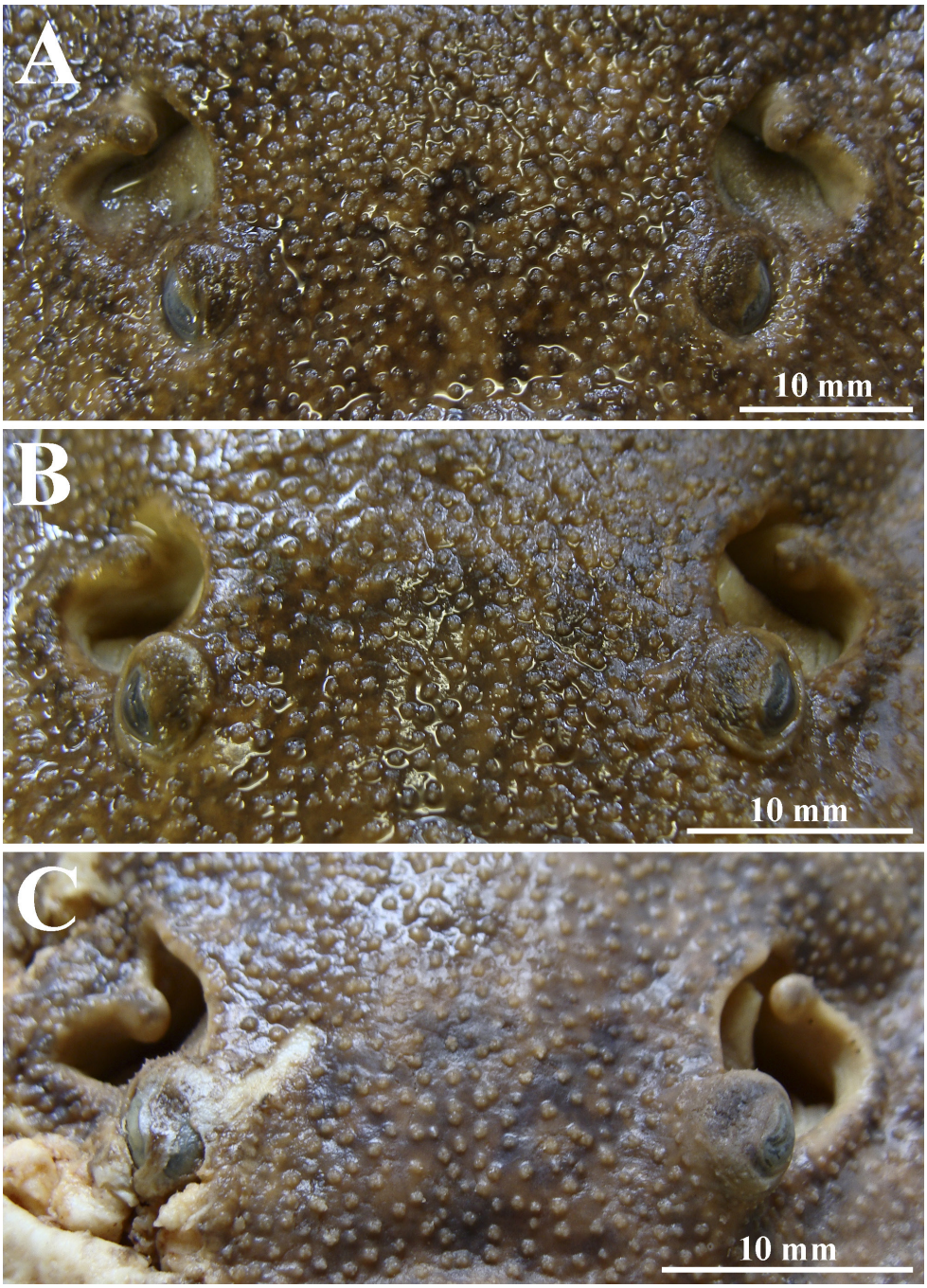

FIGURE 19 | Frontal view of eyes and spiracles of three specimens of *Paratrygon araguaia*. **A.** MZUSP 130342, juvenile male, 288 mm DW. **B.** MZUSP 130343, juvenile male, 278 mm DW. **C.** MZUSP 104366, juvenile male, 241 mm DW.

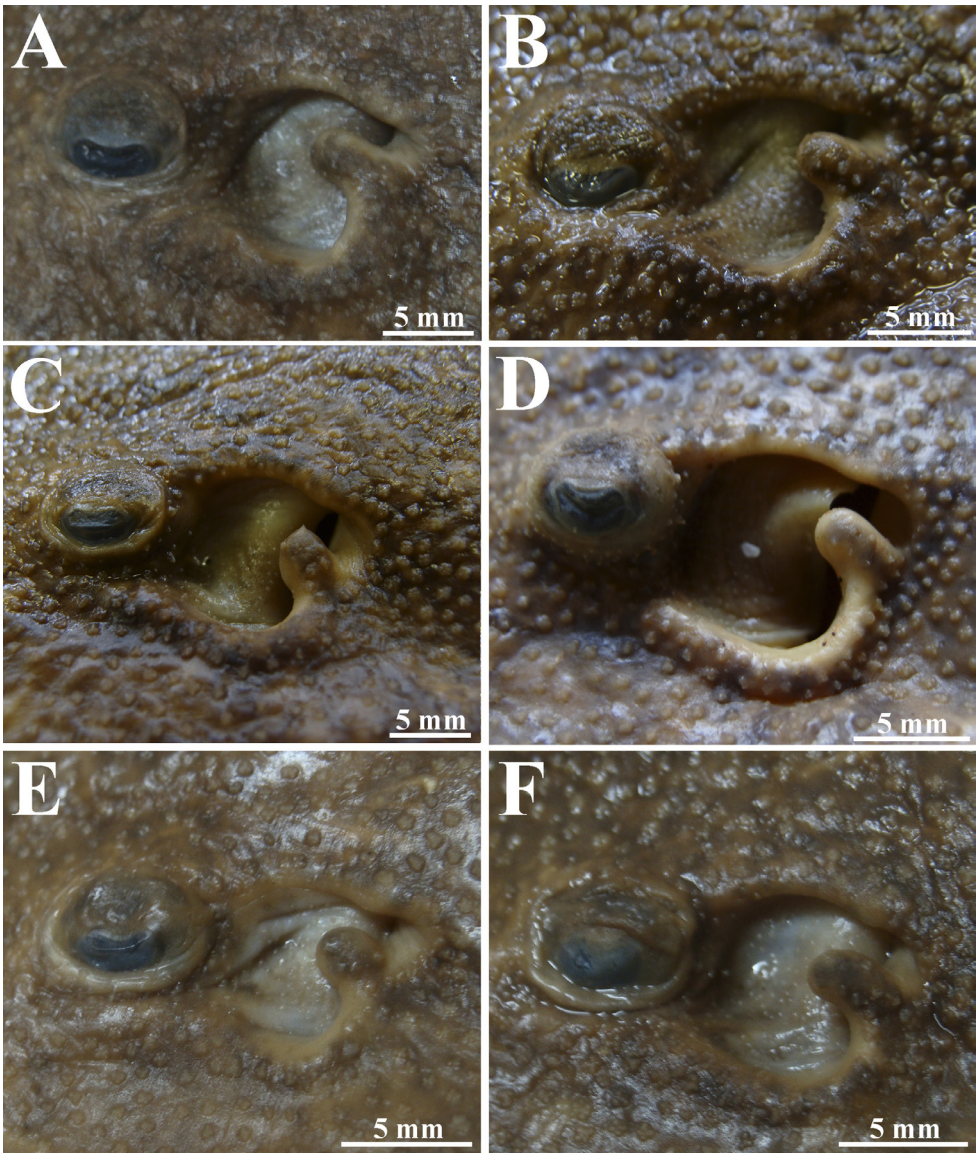

FIGURE 20 | Lateral view of spiracles and spiracles process of six specimens of *Paratrygon araguaia*. **A.** MZUSP 104401, paratype, juvenile male, 303 mm DW; **B.** MZUSP 130342, juvenile male, 288 mm DW; **C.** MZUSP 130343, juvenile male, 278 mm DW; **D.** MZUSP 104366, juvenile male, 241 mm DW; **E.** MZUSP uncatalogued, juvenile male, 235 mm DW. **F.** MZUSP 130346, juvenile male, 236 mm DW.

entire pre-caudal sting portion of tail. Thorns mostly small, with just ones next to tail base more developed (Figs. 23C–D). Younger juveniles and neonates with only more anterior part of dorsal rows, some specimens with thorns already developed.

Caudal sting long, with mean length 10.7% DW (8.6–12.8% DW), and mean width 0.8% DW (0.7–1.3% DW). Caudal sting in juveniles with lateral serrations in all length of sting, or serrations just in half distal length (majority). Lateral serrations well developed (Fig. 24).

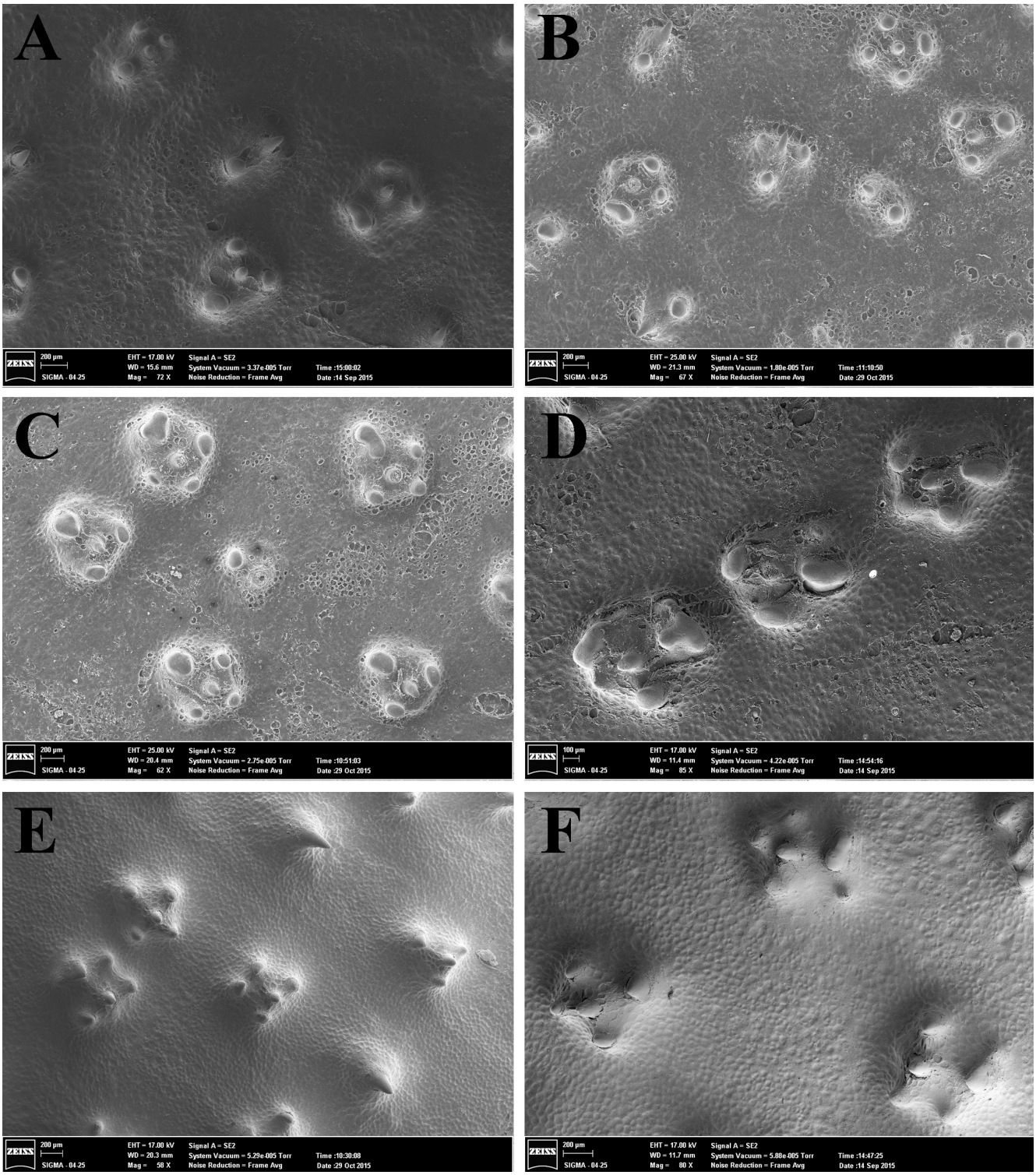

FIGURE 21 | Dorsal view of dermal denticles taken from SEM images of the following regions of the disc from *Paratrygon araguaia*, specimen MZUSP 130342, juvenile male. **A.** and **B.** Head; **C.** and **D.** Central; **E.** and **F.** Tail base.

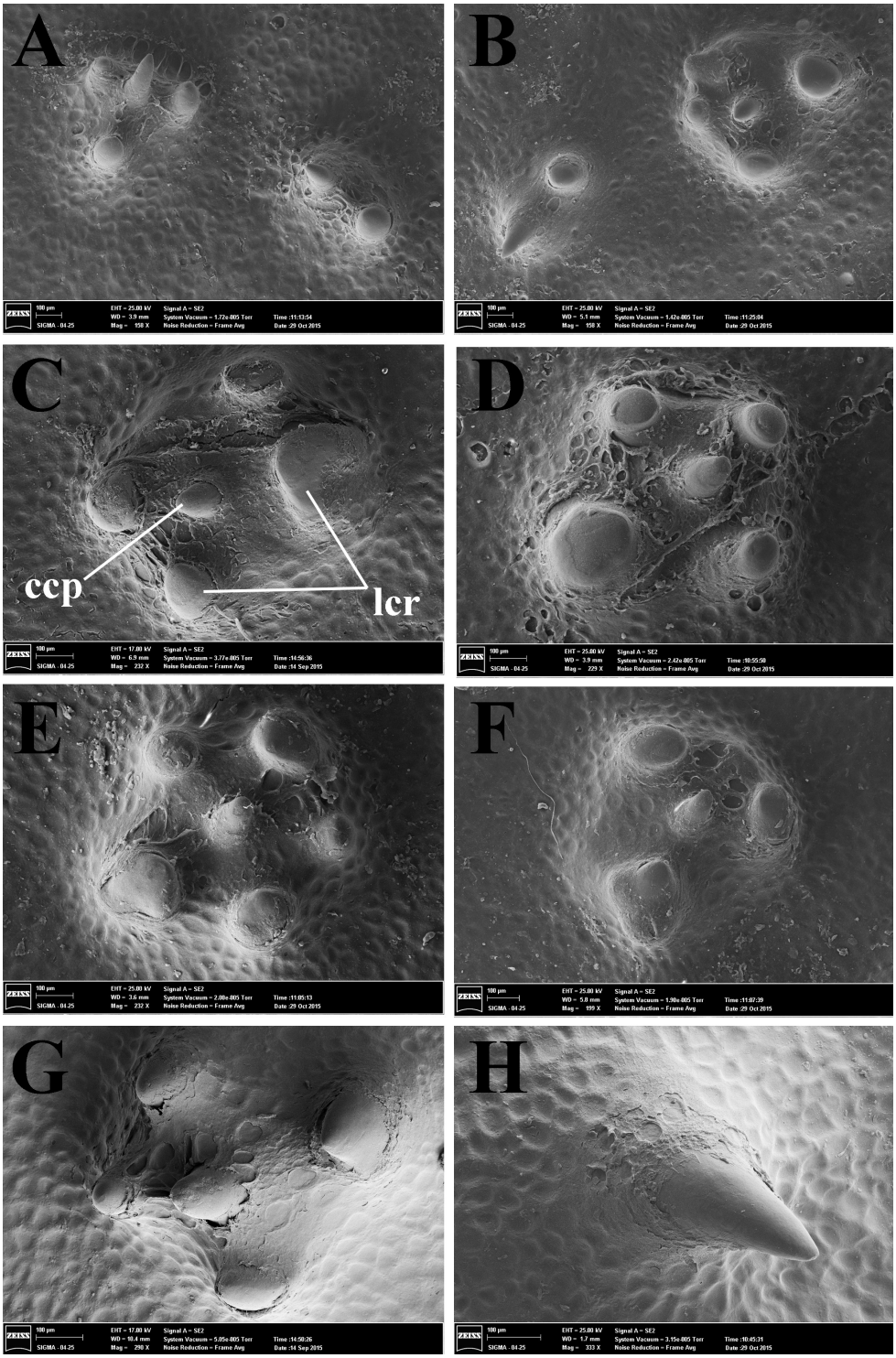

FIGURE 22 | Morphological details of dermal denticles taken from SEM images of the following regions of the disc from *Paratrygon araguaia*, specimen MZUSP 130342, juvenile male. **A.** and **B.** Head; **C–F.** Central; **G.** and **H.** Tail base. Notice the beginning of the dichotomous pattern in the more developed lateral coronal rigdes of the denticles in the images **C–E**. Abbreviations see Fig. 8.

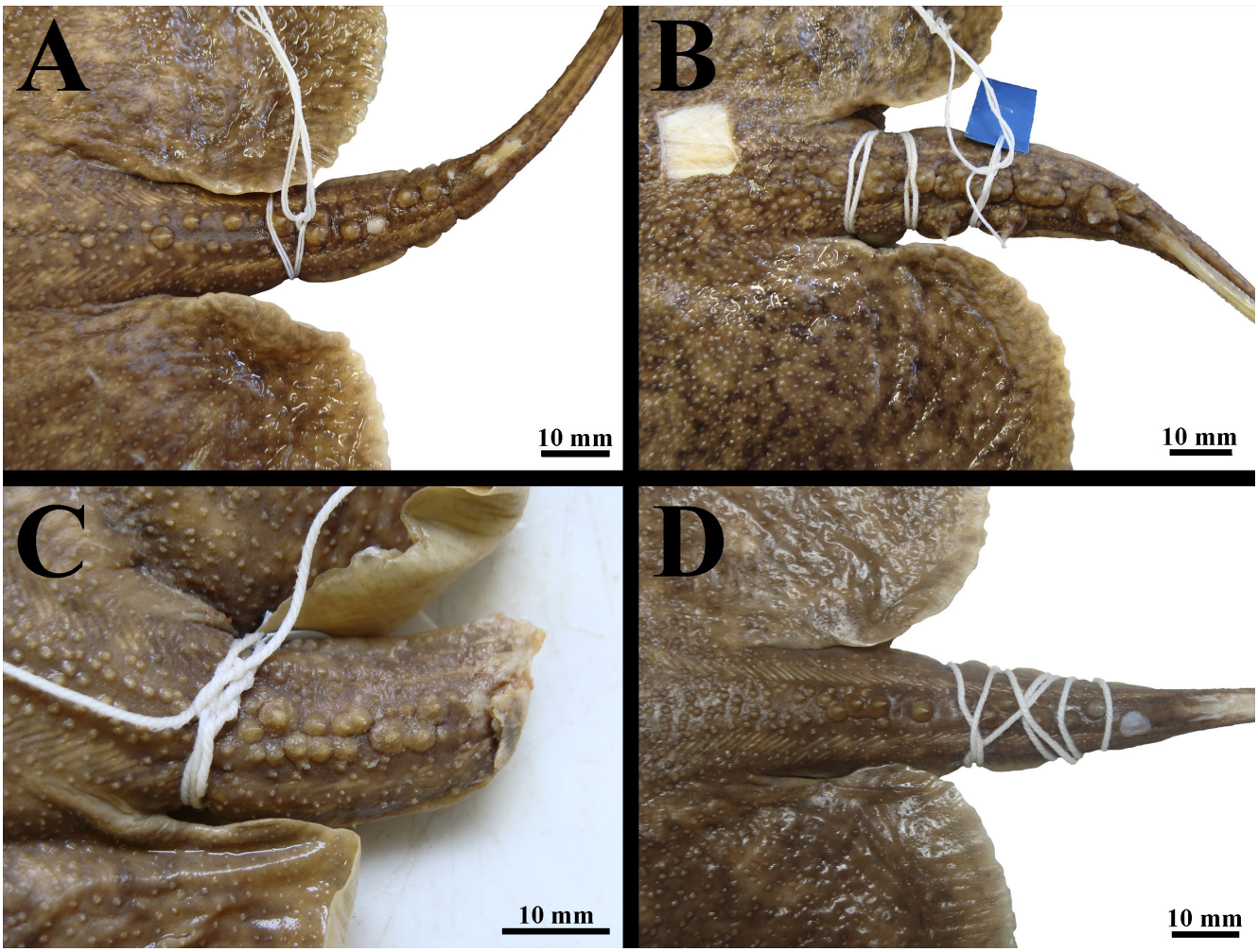

FIGURE 23 | Dorsal view of dorsal rows of thorns on tail of *Paratrygon araguaia*. **A.** MZUSP 130342, juvenile male; **B.** MZUSP 130343, juvenile male; **C.** MZUSP 104366, juvenile male; **D.** MZUSP 130347, juvenile male.

Ventral lateral line canals. Posterior extremity of JFC formed by connection of HMD and IOC canals, and anterior extremity by junction of SPO and NAS canals (Fig. 25). Ang of HMD with open and wide curvature. Jug of HMD slightly ondulated in its external contour at branchial basket region. Below of branchial basket, Jug with small and sharper curvature, and just posteriorly, with small tubule toward central disc region. Spl wide, with three pst, and most posterior ramified. Spc of HMD parallel to jug, and at level of fourth pair of gill slits more distant from margins of disc. Spt in HMD at level of mouth. Subpleural component end directed to posterior disc just after last spt (Fig. 25).

Sub of IOC without connections with pnc, connecting just spc. SPO after JFC in small open curvature format. Orb of SPO in antero-central direction with some discrete undulations. Nil wide, with six to seven vS in its central portion. Sbr of SPO small. NAS and MNC canals similar to *P. aiereba* ones (Fig. 25).

FIGURE 24 | Dorsal view of caudal stings of *Paratrygon araguaia*. **A.** MZUSP 104401, paratype, juvenile male; **B.** MZUSP 130343, juvenile male; **C.** MZUSP 104000, juvenile male; **D.** MZUSP 130346, juvenile male.

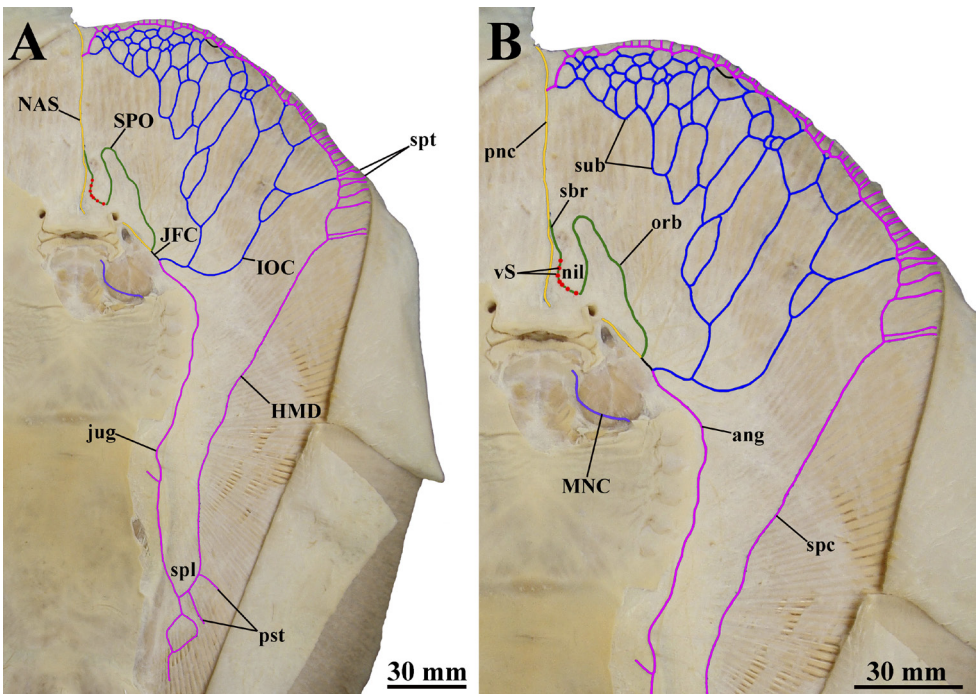

FIGURE 25 | Ventral canals of lateral line system in *Paratrygon araguaia*, specimen MZUSP 130343, juvenile male. **A.** Distribution of all ventral canals; **B.** Detail of the anterior central disc ventral canals. Abbreviations see Fig. 11.

Skeleton. Meristic counts of vertebrae, and pectoral and pelvic fins radials in Tab. 4. Neurocranium with expanded RPJ between NC, with RPJ's tip above anterior limit of NCs (Figs. 26A–B). FCF in "8" format, with its posterior portion major than anterior (Figs. 26A–B). Mandibular arch with PQ and MC slender and slightly straight. HYO thin with slight curvature in its medial portion (Figs. 26A–B). Synarcual cartilage narrow; articulation region of synarcual with pectoral girdle not laterally expanded. LS not expanded, and DS closer to synarcual center (Fig. 27A). Scapulocoracoid with CB slender; anterior face of CB discreetly curved, and with small convexity between central and lateral portions. Posterior face of CB straight. DLC pronounced, with its point just little beyond final third of MSC. Final third of MSC not so projected (Fig. 26C). PPT slender and straight, with curvature in anterior portion not so pronounced. Anterior and posterior portions of PPT with noticeable difference in width. FSP quarter to fifth of PPT length (Fig. 28A). Anterior portion of MSP short with its length between half and little less than half of MSP's posterior portion (Fig. 28B). MTP slender and arched. PSM of MTP at level of anterior margin of pelvic girdle (Fig. 28C). Pelvic girdle with PB in inverted "V" format slender with small distance between anterior and posterior faces. Extremities of PB long, compressed and posteriorly pronounced. ISP developed with LPP reduced (Fig. 27B).

Geographical distribution. *P. araguaia* is an endemic species from medium and upper portions of rio Araguaia and its main tributaries (Fig. 15).

TABLE 4 | Meristic data taken from two specimens of *P. araguaia* radiographed or dissected; "M" corresponds to mode, and "R" corresponds to range.

P. araguaia	MZUSP 130342	MZUSP 130343	M	R
Precaudal vertebrae	42	41	–	41–42
Caudal vertebrae	70	81	–	70–81
Total vertebrae	112	122	–	112–122
Diplospoldylic vertebrae	77	86	–	77–86
Propterygial radials	49	45	–	45–49
Mesopterygial radials	20	26	–	20–26
Metapterygial radials	41	39	–	39–41
Total radials	110	110	110	–
Pelvic radials	16	18	–	16–18
Tooth rows of upper jaw	–	–	–	–
Tooth rows of lower jaw	–	–	–	–
Symphysis of upper jaw	–	–	–	–
Symphysis of lower jaw	–	–	–	–

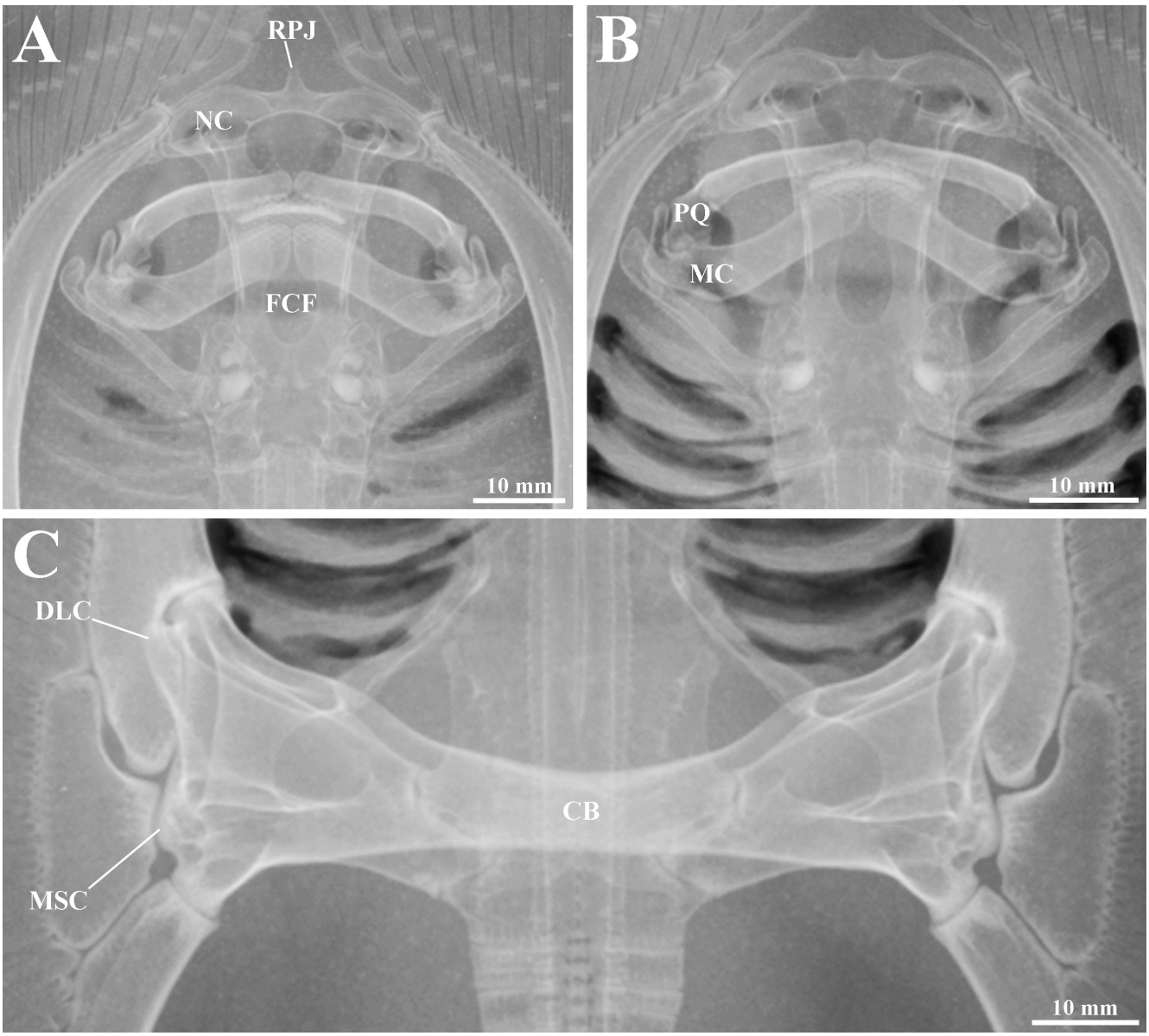

FIGURE 26 | Radiographys of neurocranium, mandibular arch **A.** and **B.** and scapulocoracoid **C.** of *Paratrygon araguaia*, upper views; **A.** MZUSP 130342, juvenile male; **B.** and **C.** MZUSP 130343, juvenile male. Abbreviations see Figs. 12 and 14A.

Etymology. Species epithet *araguaiaensis* is due to the endemicity of this species to rio Araguaia. A noun in apposition.

Conservation status. *P. araguaia* inhabits the upper and middle parts of the Araguaia River and its tributaries. Further research on the status of its populations is needed as the total extent of occurrence of this species is unknown. Therefore, based on the IUCN categories and criteria, the species could be classified as Data Deficient (DD) (IUCN, 2022).

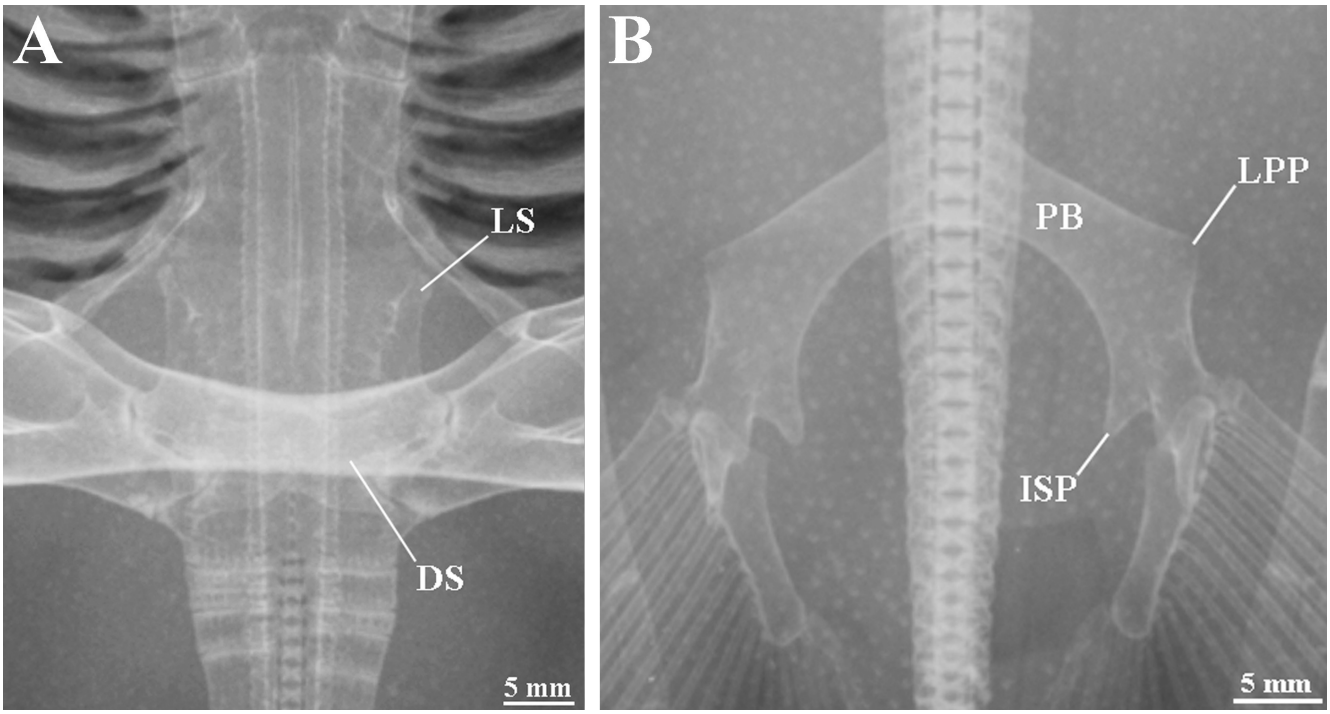

FIGURE 27 | Radiographys of **A.** Synarcual cartilage and **B.** Pelvic girdle of *Paratrygon araguaia*. **A.** MZUSP 130343, juvenile male, upper view; **B.** MZUSP 130342, juvenile male, upper view. Abbreviations see Fig. 13.

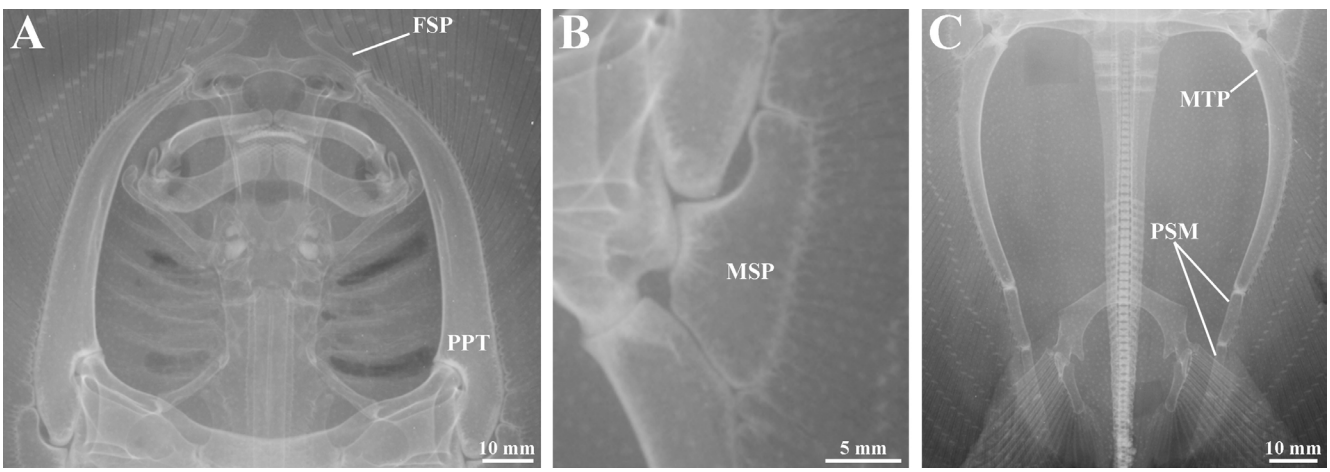

FIGURE 28 | Radiographys of basal elements of pectoral fin of *Paratrygon araguaia*, MZUSP 130342, juvenile male, upper view. Abbreviations see Fig. 14.

Paratrygon munduruku, new species

urn:lsid:zoobank.org:act:6378BA72-2317-487A-A410-E349846F8FC

(Figs. 29–40; Tabs. 5–6)

Paratrygon aiereba. —Rosa, 1985:487 (list of examined specimens). —Carvalho, Lovejoy, 2011:16 (list of examined specimens). —Frederico *et al*., 2012:73–74, 78, figs. 1, 3 (phylogeography, molecular analysis, conservation). —Carvalho, 2016:58 (brief description in rio Tapajós). —Fontenelle *et al*., 2021:6, 10, fig. 2, supplementary 3–4, 9, 25, figs. S2–S3 (list of specimens with genetic material analyzed, molecular phylogenys).

Paratrygon cf. *aiereba*. —Carvalho, 2016:58 (brief description in rio Tapajós).

Paratrygon sp. 5. —Loboda, 2016: vol. 1. vii–viii, 33, 58, 60–61, 75, 86–97, 100, 113, 126–127, 142, 156, 190–192, 225–228, vol. 2. xiii–xv, 63–75, figs. 85–104 [citation of Frederico *et al*. (2012), morphological comparisons with another *Paratrygon* species, citation from rio Tapajós, synonymy, list of examined specimens, diagnosis, morphological description, distribution, endemicity for rio Tapajós, morphometry, teeth count, meristics].

Holotype. MZUSP 103916, 315 mm DW, Brazil, Pará State, Municipality of Itaituba, District of Pimental, rio Tapajós, 04°36'29"S 56°16'22"W, 9 Oct 2005, M. Carvalho, M. Cardoso, M. L. G. Araújo & S. Mello.

Paratypes. All specimens from rio Tapajós, Brazil, Pará State: INPA 6884, 366 mm DW, Municipality of Itaituba, District of Pimental, rio Tapajós, 23 Oct 1991, L. Rapp Py Daniel & J. Zuanon. MZUSP 10288, 190 mm DW, Municipality of São Luis, rio Tapajós, 04°27'S 56°15'W, 5 Nov 1970, Expedição Permanente à Amazônia (EPA). MZUSP 103917, 251 mm DW, same data as holotype.

Diagnosis. *Paratrygon munduruku* is diagnosed by the following combination of characters: the dorsal coloration of the disc is brown with numerous small, dark brown spots in axon or vermiculated formats spread throughout the disc, not very conspicous and lacking withish withish spots (*vs*. *P. aiereba*, *P. orinocensis*, *P. parvaspina* which have gray or light brown coloration with apparent dark spots; *P. lucindai*, which has dorsal coloration in gray, dark gray, brown and dark brown with large, rounded dark spots throughout throughout the disc; *P. araguaia* with a brown or dark brown dorsal disc presenting two types of spots scattered throughout the disc, with one type light, big, rounded and evident in beige or light brown, and the other type dark, small, and vermiculated, occurring between light spots; *P. raonii* with a very dark coloration in dark brown and black tonalities and possessing very dark, evident, black spots in vermicular or dendritic format); small and quadrangular spiracle with a mean spiracle length of 4.6% DW (3.6–5.8% DW), with a reduced, rounded spiracular process that covers only a small part of the posterior portion of the spiracular aperture [*vs*. *P. orinocensis* with triangular spiracles; *P. lucindai*, *P. araguaia* with rounded spiracles; *P. aiereba* with quadrangular and large spiracles, and mean spiracle lenght of 6% DW (4.4–11.6% DW); *P. parvaspina* with quadrangular and small spiracle and an extremely reduced spiracular process; *P. raonii* with quadrangular and small spiracle and a developed, globular spiracular process];

dermal denticles on the central disc with a crown that possesses a central coronal plate and lateral coronal ridges in a leaf shape, with the lateral coronal ridges smaller and ranging from two (*vs*. *P. aiereba* which has a crown of central dermal denticles with pointed central coronal plates and pointed to slightly rounded lateral coronal ridges ranging from three to six; *P. parvaspina* with a crown of central dermal denticles with central coronal plates and pointed lateral coronal ridges, with a few ridges, between two and four; *P. lucindai* with a crown of central dermal denticles that possess a quadrangular central coronal plate and slightly round lateral coronal ridges, with three to six ridges; *P. orinocensis* and *P. raonii*, which have well developed, pointed lateral coronal ridges, more than twelve in *P. orinocensis*, and six to eight in *P. raonii*; *P. araguaia*, which has central dermal denticles that present a pointed and reduced central coronal plate and rounded, well developed lateral coronal ridges); the propterygium is arched and stout, with the posterior portion thicker than the anterior (*vs*. *P. aiereba*, *P. araguaia*, and *P. raonii*, which have a straight and slender propterygium; *P. orinocensis* has an arched propterygium, but its is thinner; *P. parvaspina* which has an arched and thicker propterygium with a thicker anterior portion than *P. munduruku*; *P. lucindai*, which has an arched and stout propterygium that is more arched than that of *P. munduruku*).

Description. Measurements of *Paratrygon munduruku* in Tab. 5. Disc subcircular with mean disc length 110.5% DW (108.9–112.1% DW). Anterior margin of disc with concavity few pronounced in its medial portion (Figs. 29A, 30A, 30C), and distance from anterior margin of disc to cloaca with mean 85.4% DW (78.7–89.5% DW). Head small, with means of interorbital and interespiracular distances respectively 10.6% DW (10.2–11.2% DW), and 14.2% DW (11.2–17.4% DW). Small and not pedunculated eyes with mean length 2% DW (1.6–2.5% DW) (Fig. 31). Spiracles in quandrangular format, slightly larger than eyes, with mean length 4.6% DW (3.6–5.8% DW) (Figs. 31–32). Spiracular process small, simple and rounded, covering only part of posterior portion of spiracular opening (Fig. 32), and with many and apparent dermal denticles. Preorbital, prenasal and preoral distances with means respectively 32.1% DW (30–33.5% DW), 30.3% DW (27.6–33.7% DW), and 33.7% DW (30.9–36.5% DW). Mean of internasal distance 7.9% DW (7.1–8.9% DW). Wide mouth, with mean 10.3% DW (10.1–10.5% DW). Larger teeth, in quincunx in both jaws and without size difference between teeth from central to lateral rows (Fig. 33). Number of teeth in both jaws 17/15 of paratype MZUSP 10288 (Tab. 6). Teeth from central rows more triangular in shape, and with more prominent cusps.

Branchial basket with means of distance between first pair, fifth pair and distance between first to fifth pair of branchial slits respectively 19.9% DW (19.1–21.6% DW), 17.4% DW (16.4–18.9% DW), and 10% DW (9–11.1% DW). Pelvic fins triangular and dorsally covered by disc (Fig. **S5**). Means of anterior margin length and distance between extremities of pelvic fins respectively 15.9% DW (13.4–18.3% DW), and 38.2% DW (36.3–41.1% DW). Mean of distance between pelvic and pectoral fins axils 3.9% DW (3.2–5.5% DW). Means of external and internal clasper lengths from male juvenile specimens respectively 2.8% DW (2.4–3.2% DW) and 8.4% DW.

TABLE 5 | Measurements of specimens of *Paratrygon munduruku* including the holotype, MZUSP 103916. Mean, Standard Deviation (SD) and Ranges are expressed in millimeters (mm) and proportions of disc width (%DW); (N) corresponds to the number of specimens analyzed.

Paratrygon munduruku	Holotype		Average		SD		Range				N
	mm	%DW	mm	%DW	mm	%DW	mm		%DW		
Total length	443	140.6	427.0	160.7	35.7	40.7	367	461	126.0	230.0	4
Disc length	343	108.9	309.0	110.5	69.8	1.4	213	400	108.9	112.1	4
Disc width	315	100.0	280.5	100.0	66.3	0.0	190	366	–	–	4
Interorbital distance	32	10.2	29.8	10.6	7.8	0.4	20	41	10.2	11.2	4
Interespiracular distance	44	14.0	39.5	14.2	9.7	2.2	28	53	11.2	17.4	4
Eye length	8	2.5	5.8	2.0	1.8	0.3	4	8	1.6	2.5	4
Spiracle length	12	3.8	12.3	4.6	0.8	0.9	11	13	3.6	5.8	4
Preorbital length	105	33.3	90.3	32.1	22.2	1.4	57	115	30.0	33.5	4
Prenasal length	106	33.7	85,0	30.3	20.0	2.2	56	106	27.6	33.7	4
Preoral length	115	36.5	94.3	33.7	21.6	2.1	62	115	30.9	36.5	4
Internasal length	23	7.3	21.8	7.9	3.3	0.8	17	26	7.1	8.9	4
Mouth width	32	10.2	28.8	10.3	6.4	0.2	20	37	10.1	10.5	4
Distance between first gill slits	–	–	53.0	19.9	12.4	1.2	41	70	19.1	21.6	3
Distance between fifth gill slits	–	–	46.0	17.4	10.2	1.1	36	60	16.4	18.9	3
Branchial basket length	31	9.8	27.5	10.0	4.8	0.7	21	33	9.0	11.1	4
Length of anterior margin of pelvic fin	51	16.2	44.0	15.9	8.3	1.8	30	51	13.4	18.3	4
Pelvic fins width	115	36.5	106.0	38.2	20.4	1.9	78	133	36.3	41.1	4
External length of clasper	–	–	6.0	2.8	0.0	0.4	6	6	2.4	3.2	2
Internal length of clasper	–	–	18.5	8.4	2.5	0.0	16	21	8.4	8.4	2
Distance between cloaca and tail tip	154	48.9	171.0	69.3	53.2	40.2	130	262	35.5	137.9	4
Tail width	19	6.0	15.3	5.8	2.6	1.5	12	19	3.3	7.4	4
Distance between snout tip and cloaca	273	86.7	237.3	85.4	46.8	4.0	170	288	78.7	89.5	4
Distance between pectoral axil and posterior margin of pelvic fin	12	3.8	11.5	3.9	5.4	0.9	6	20	3.2	5.5	4
Distance between cloaca and caudal sting	69	21.9	61.3	22.4	9.0	2.5	50	71	19.4	26.3	4
Caudal sting length	22	7.0	23.0	8.2	3.7	1.3	19	28	7.0	10.0	3
Caudal sting width	3	1.0	2.7	0.9	0.5	0.1	2	3	0.8	1.1	3
Pseudosiphon length	–	–	–	–	–	–	–	–	–	–	0
Ventral pseudosiphon length	–	–	–	–	–	–	–	–	–	–	0

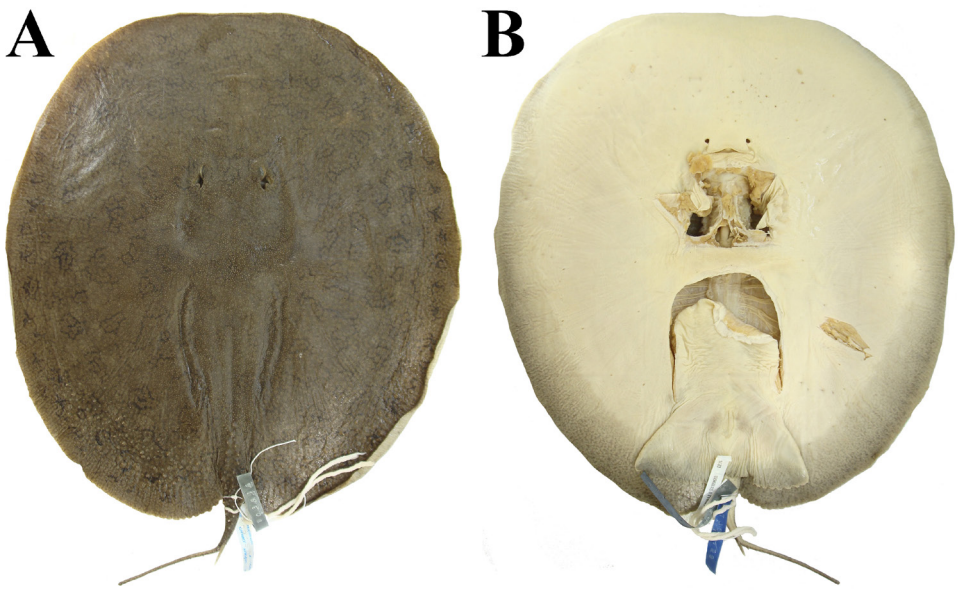

FIGURE 29 | Holotype of *Paratrygon munduruku*, MZUSP 103916, juvenile female, 315 mm DW, from Tapajós River. **A.** Dorsal; **B.** Ventral views.

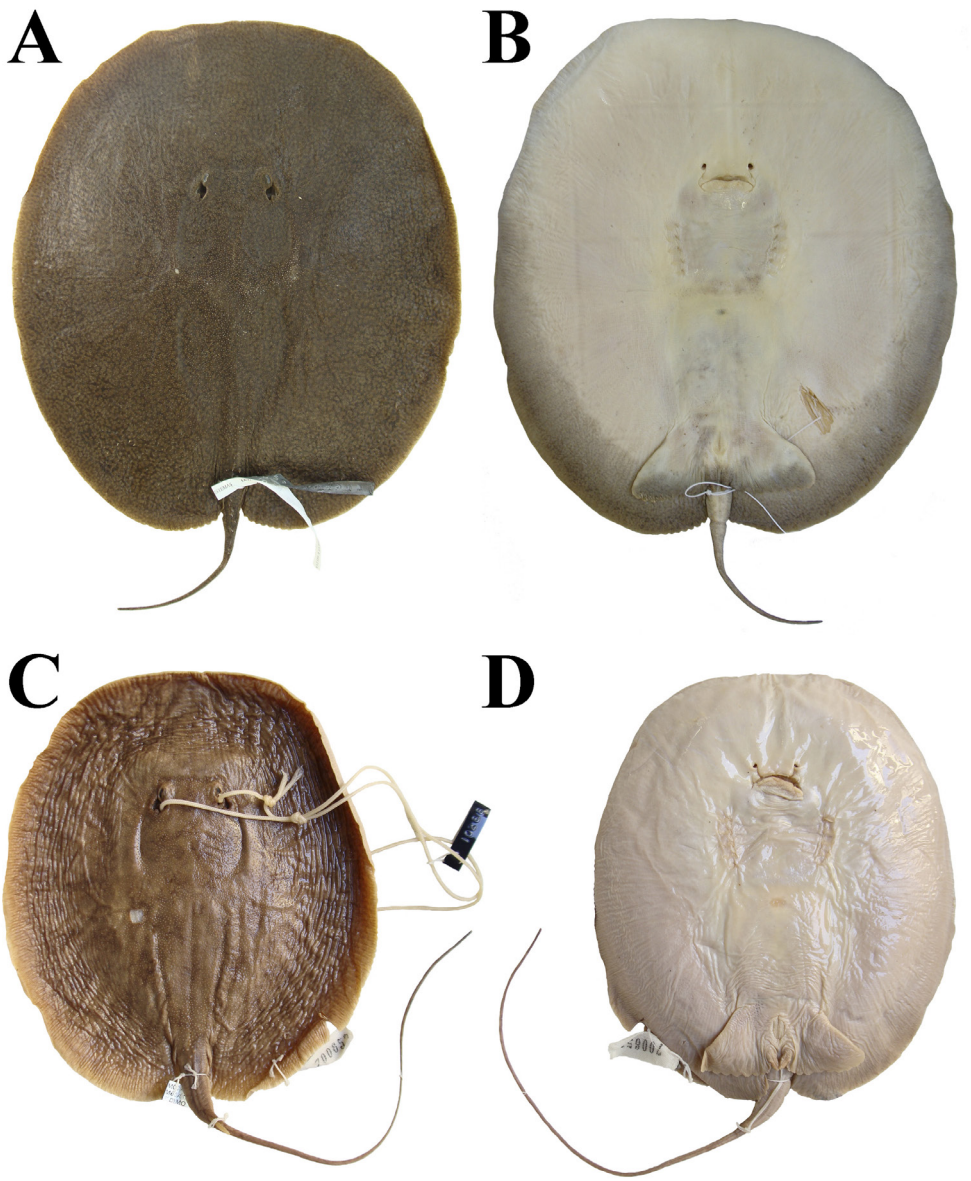

FIGURE 30 | Paratypes of *Paratrygon munduruku*, MZUSP 103917, juvenile male, 251 mm DW, from Tapajós River. **A.** Dorsal; **B.** Ventral views. MZUSP 10288, juvenile male, 190 mm DW, from Tapajós River. **C.** Dorsal; **D.** Ventral views.

Tail with pre-caudal sting portion small and slender at base, and post-caudal sting portion long and filiform. Mean of distance between cloaca and caudal sting (pre-caudal sting portion) 22.4% DW (19.4–26.3% DW), and mean of tail width at base 5.8% DW (3.3–7.4% DW). Lateral folds of tail slightly developed in all pre-caudal sting portion, and dorsal and ventral folds very small, just in post-caudal sting portion.

Coloration in alcohol. Dorsal disc coloration brown or dark brown with numerous small dark spots throughout disc (Figs. 29A, 30A, C). Dark spots in brown or black color, in axon or vermculated format, with vermiculated predominant. In some specimens

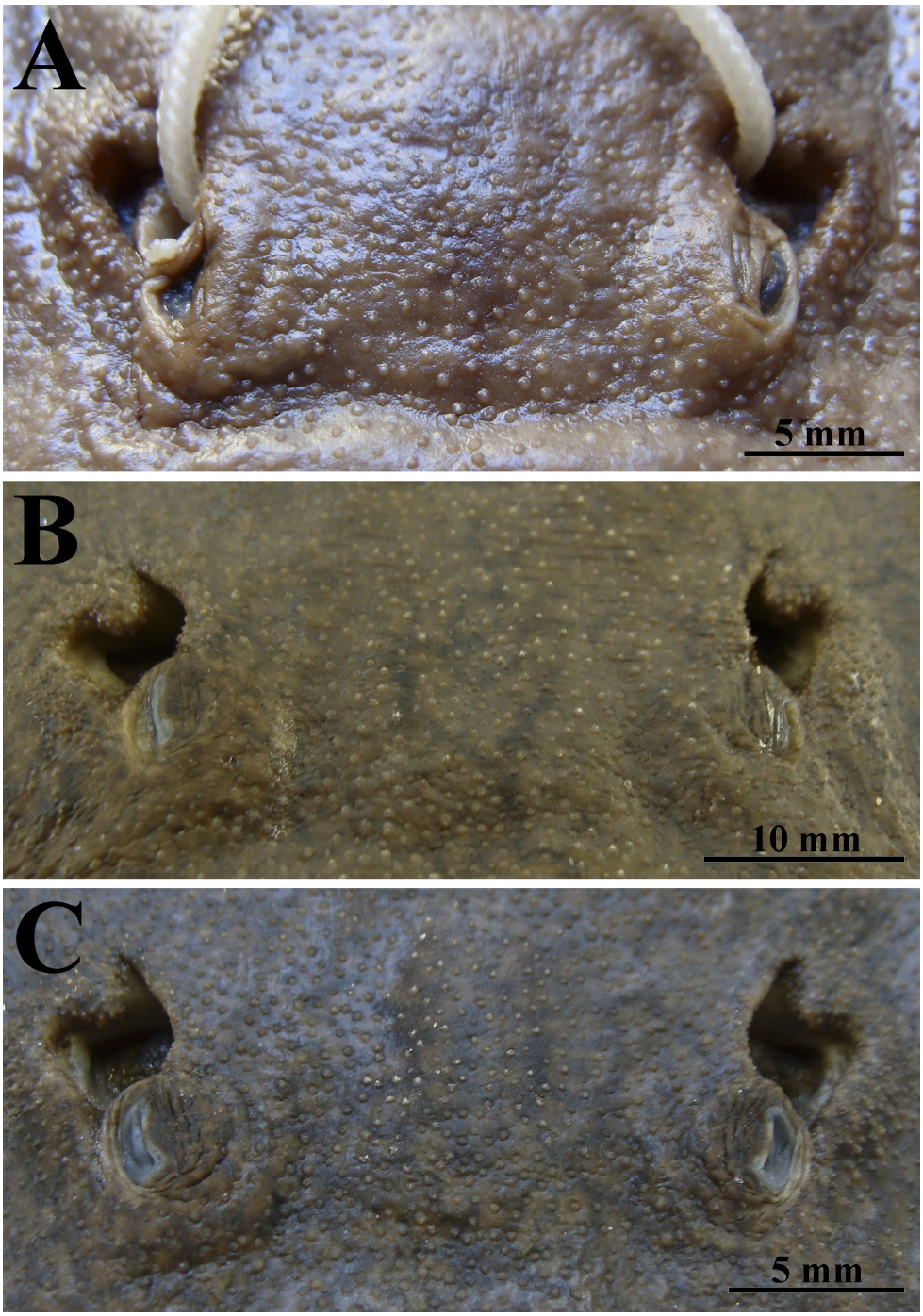

FIGURE 31 | Frontal view of eyes and spiracles of three specimens of *Paratrygon munduruku*. **A.** MZUSP 10288, paratype, juvenile male, 190 mm DW; **B.** MZUSP 103916, holotype, juvenile female, 315 mm DW; **C.** MZUSP 103917, paratype, juvenile male, 251 mm DW.

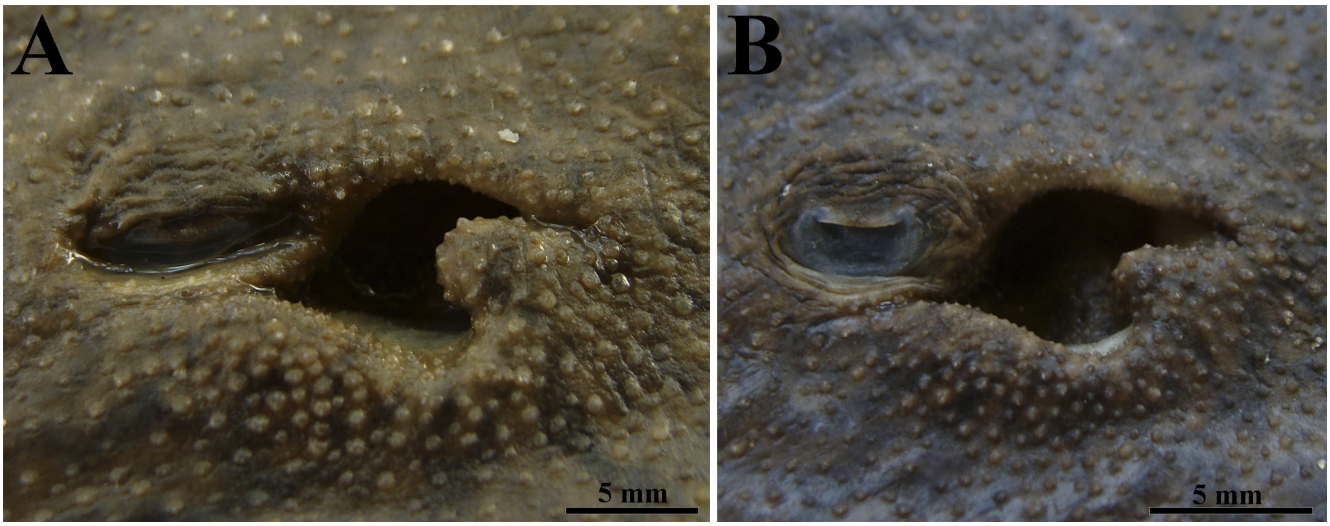

FIGURE 32 | Lateral view of spiracles and spiracles process of two specimens of *Paratrygon munduruku*. **A.** MZUSP 103916, holotype, juvenile female, 315 mm DW; **B.** MZUSP 103917, paratype, juvenile male, 251 mm DW.

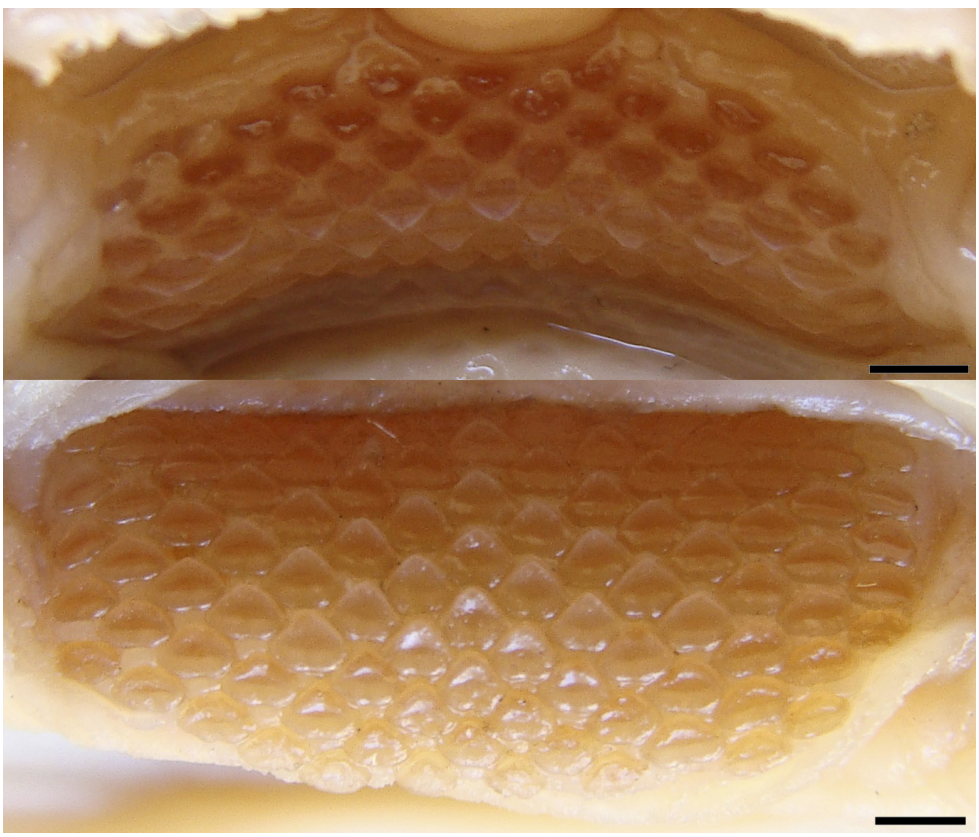

FIGURE 33 | Upper (above) and lower (below) teeth of *Paratrygon munduruku*, MZUSP 10288, paratype, juvenile male, 190 mm DW. Scale bars = 1 mm.

TABLE 6 | Meristic data taken from holotype, MZUSP 103916 and a paratype, MZUSP 10288 of *Paratrygon munduruku*.

Paratrygon munduruku	MZUSP 103916	MZUSP 10288
Precaudal vertebrae	41	–
Caudal vertebrae	66	–
Total vertebrae	107	–
Diplospoldylic vertebrae	72	–
Propterygial radials	48	–
Mesopterygial radials	22	–
Metapterygial radials	39	–
Total radials	109	–
Pelvic radials	23	–
Tooth rows of upper jaw	–	17
Tooth rows of lower jaw	–	15
Symphysis of upper jaw	–	4
Symphysis of lower jaw	–	5

vermiculated spots in all dorsal disc (Fig. 30A). Dorsal tail coloration similar to disc in all extension, with vermiculated spots in reduced size. Dark tonality in post caudal sting portions. Ventral coloration of disc with two tonalities: one clear in center and anterior margin of disc, and one dark in lateral and posterior margins (Figs. 29B, 30B, D). Clear tonality whitish or light beige, and dark tonality gray and in posterior margins with numerous small dark gray spots in polygonal shape. Pelvic fins with same tonalities as disc, with center region and anterior margins in clear tonality, and posterior margins with dark tonality. Dark tonality in some specimens with small darker spots. In claspers, clear tonality at base, with dark tonality in rest, and specimens with dark spots in dark tonality of posterior margin of pelvic fins, also with darker spots in dark portion of clasper. Ventral coloration of pre caudal sting portion of tail in light beige or whitish color, and dark in post caudal sting portion, mainly near tip.

Squamation. Dermal denticles throughout dorsal disc and tail (Fig. 34). On central portion of disc, denticles large than marginals. Posterior margins with concentration of developed pointed spines, some as tubercles (Fig. 34B). On tail, denticles large in pre caudal sting portion, and in post caudal sting portion small, mainly in tip region.

Dermal denticles small on central, lateral and frontal portions of disc, generally with 0.2 mm in diameter, and in region near tail basis, denticles with large size, 0.5 mm (Figs. 35–36). On central disc, denticles with high and narrow crown. Ccp developed, high, conical and larger than lcrs. Lcrs generally small, rounded, and from two to five (Figs. 35C–D, 36C–D). Denticles of frontal disc small, with developed ccp and small lcrs; lcrs generally in three (Figs. 35A–B, 36A–B). Denticles on lateral disc similar to central ones, however with small crowns and one or two lcrs (Figs. 35E–F, 36E–F). Denticles

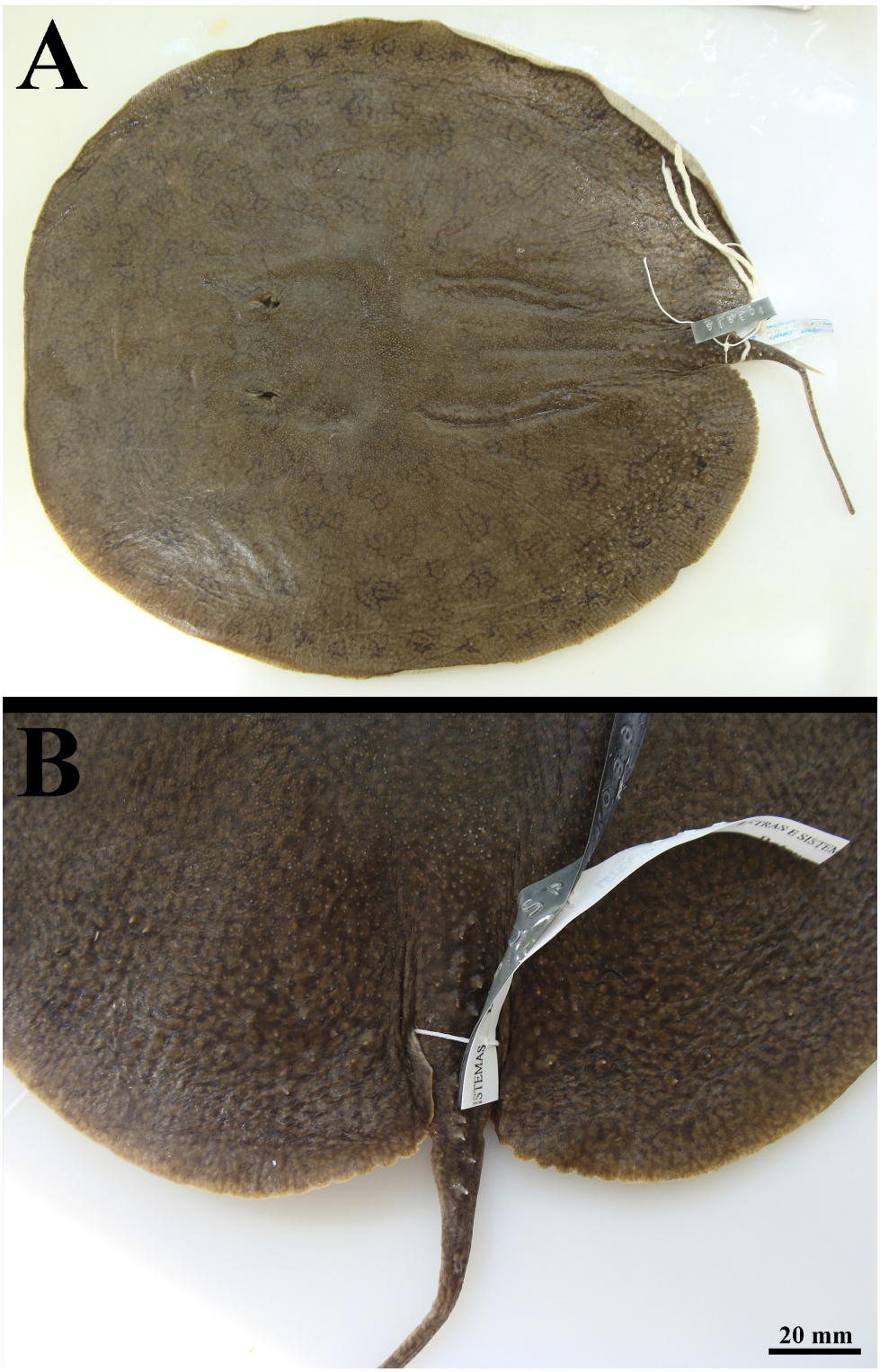

FIGURE 34 | Dermal denticles present on dorsal disc and tail in *Paratrygon munduruku*. **A.** Distribution of dermal denticles in holotype MZUSP 103916, juvenile female; **B.** Denticles present on posterior margins of disc and tail in paratype MZUSP 103917, juvenile male.

on tail basis large, with ccp conical, well developed and spine shaped. Few denticles in this region with lcrs not developed and more closer to ccp than denticles from other disc regions (Figs. 35G–H, 36E–F).

Rows of thorns in dorsal and laterals portions of tail in largest juvenile specimen (Fig. 37A). Three to five rows of developed thorns on tail of largest juvenile specimen in all pre caudal sting portion, with slightly high thorns in wide base. Single lateral

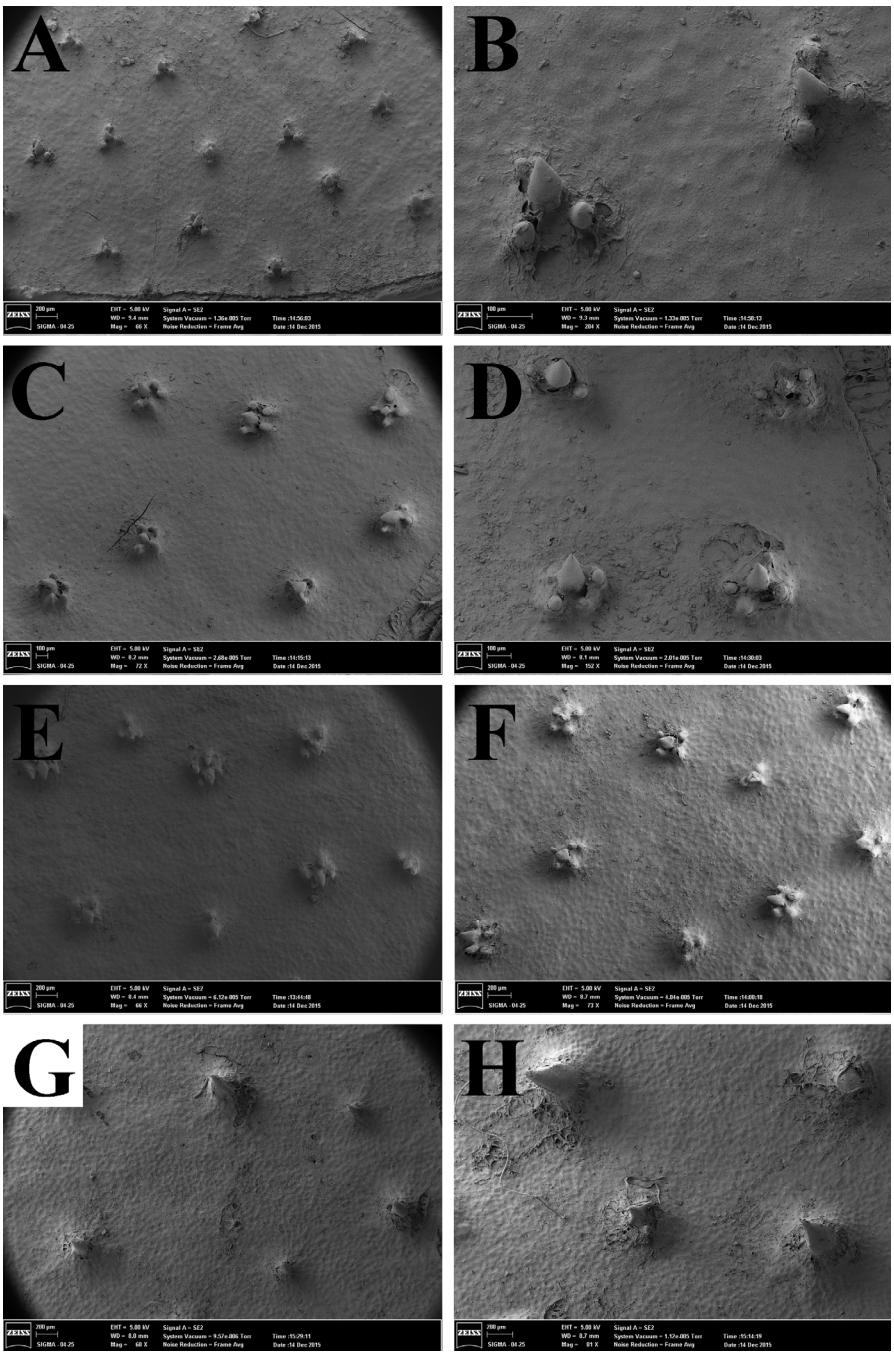

FIGURE 35 | Dorsal view of dermal denticles taken from SEM images of the following regions of the disc from *Paratrygon munduruku*, paratype MZUSP 103917, juvenile male. **A.** and **B.** Anterior margin; **C.** and **D.** Central; **E.** and **F.** Lateral; **G.** and **H.** Tail base.

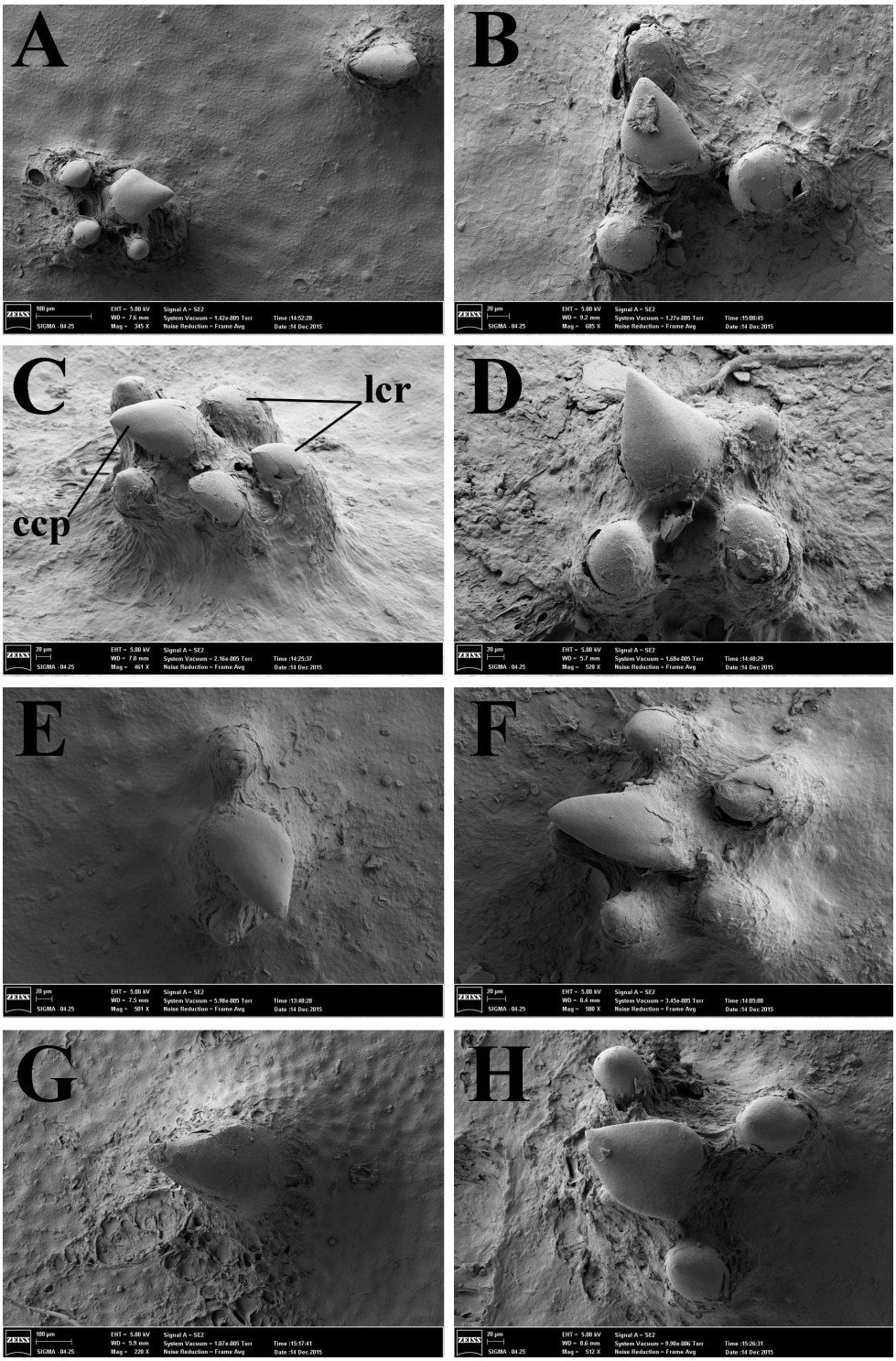

FIGURE 36 | Morphological details of dermal denticles taken from SEM images of the following regions of the disc from *Paratrygon munduruku*, paratype MZUSP 103917, juvenile male. **A.** and **B.** Anterior margin; **C.** and **D.** Central; **E.** and **F.** Lateral; **G.** and **H.** Tail base. Abbreviations see Fig. 8.

rows in this specimen in all pre caudal sting portion, and few after caudal sting region too. Thorns in lateral rows developed and more spaced than thorns of dorsal rows (Fig. 37A). Smaller juvenile specimens with just two to three dorsal rows. Lateral rows few developed, with just some thorns near insertion of caudal sting (Figs. 37B–C). Neonates with just initial portion of dorsal rows in base of tail (Fig. 37D). Small caudal sting with lenght mean 8.2% DW (7–10% DW) and width mean 0.9% DW (0.8–1.1% DW) (Tab. 5). Smaller juveniles and neonates with just one caudal sting, without medial dorsal groove, and lateral serrations in all caudal sting extension, with serrations more developed in final half of sting (Figs. 37E–F).

Ventral lateral line canals. JFC with posterior extremity formed by junction of HMD and IOC, and anterior by SPO and NAS (Fig. 38). Ang of HMD in wide external curvature to branchial basket. Jug with wide posterior curvature centrally to disc. Spl

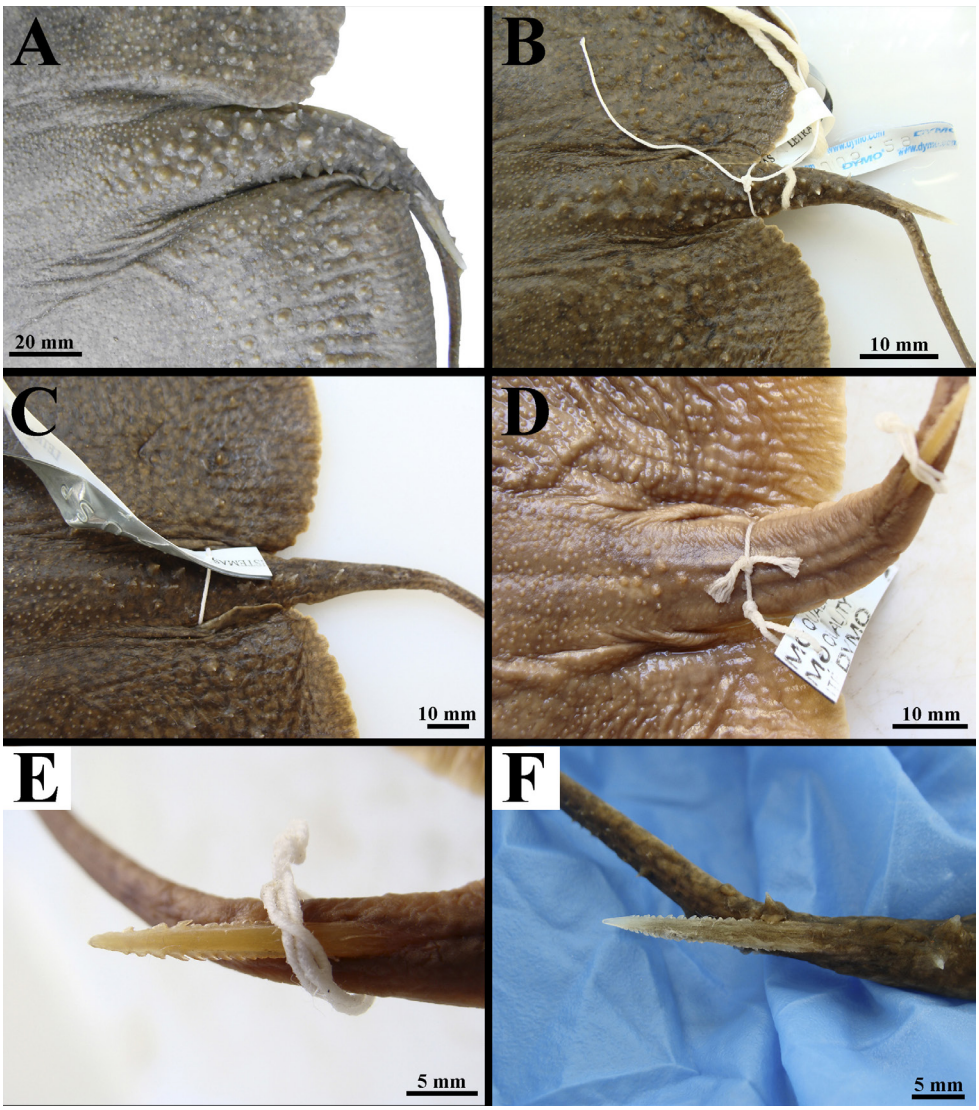

FIGURE 37 | Dorsal view of dorsal and lateral rows of thorns on tail **A-D**, and caudal stings **E-F** of *Paratrygon munduruku*. **A.** INPA 6884 (paratype), juvenile female; **B.** and **F.** MZUSP 103916, holotype, juvenile female; **C.** MZUSP 103917, paratype, juvenile male; **D.** and **E.** MZUSP 10288, paratype, juvenile male.

with four pst, one of them, more lateral, and little further away from other three. Spc straight. Spt in spc in level of posterior extremity of MNC. Anterior portion of spc close to anterior margin of disc, in posterior direction right after most anterior spt. Spc connects to pnc posteriorly. Sub of IOC with high number of ramifications and with just one point of connection with pnc. SPO with orb in slight median curvature and pnl narrow. Sbr of IOC with few vS, five. NAS anteriormedial from JFC and next to external margin of nostrils in 45° angle (Fig. 38).

Skeleton. Meristic counts of vertebrae, pectoral and pelvic fins radials in Tab. 6. Neurocranium with RPJ large and FCF narrow. FCF with posterior portion expanded (Fig. 39A). PRP laterally in same level of NC (Fig. 39A). PQ with lateral extremity expanded and in small "S" format. HYO straight and little robust (Fig. 39A). Synarcual cartilage with its floor slightly expanded laterally in anterior portion, and DS central to median line. LS not expanded anteriorly (Fig. 39B). Scapulocoraicoid with robust CB well curved in anterior surface, and straight in posterior (Fig. 40A). DMC laterally expanded and in same level of MSC. Final third of MSC laterally projected (Fig. 40B).

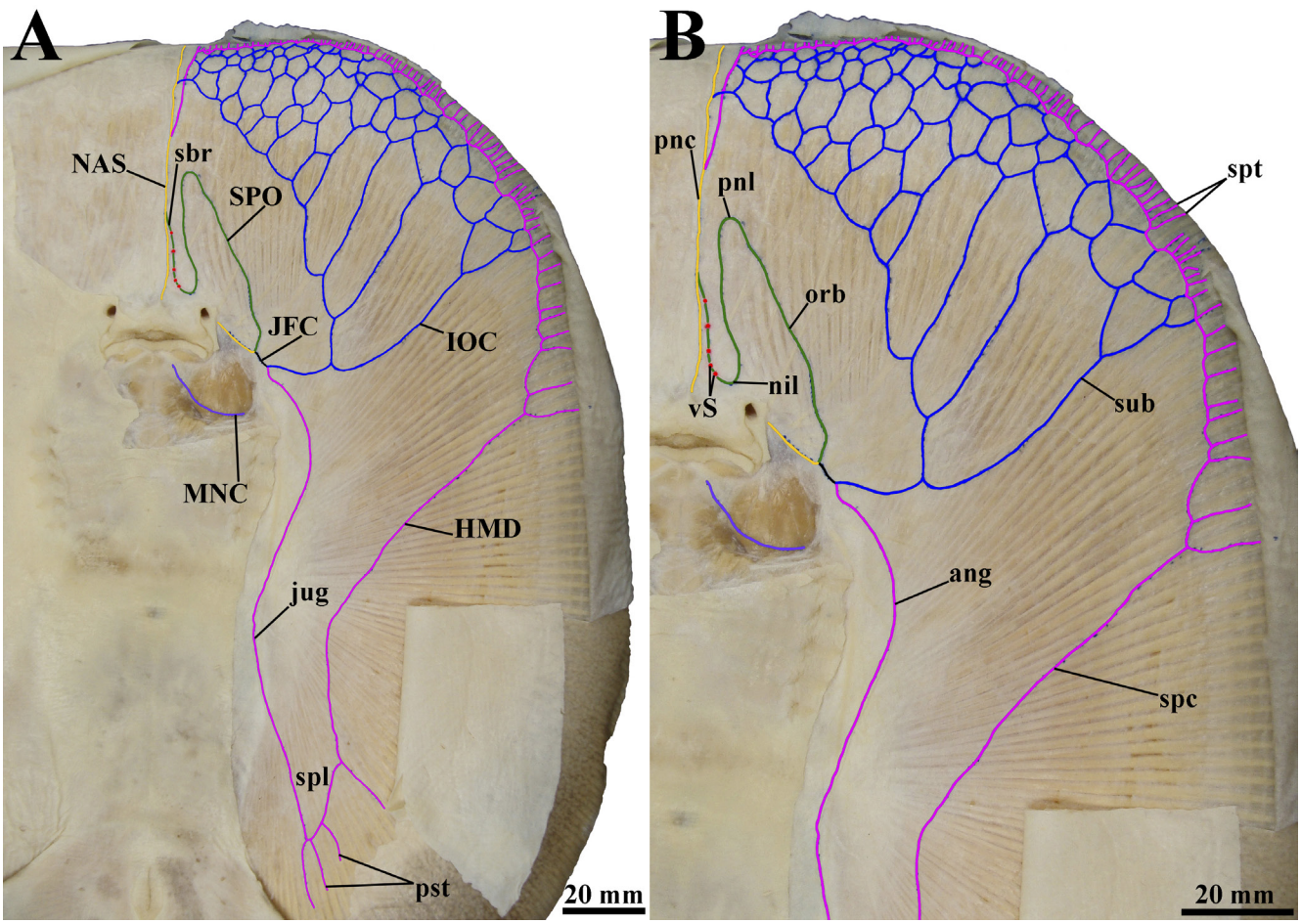

FIGURE 38 | Ventral canals of lateral line system in *Paratrygon munduruku*, MZUSP 103917, paratype, juvenile male. **A.** Distribution of all ventral canals; **B.** Detail of the anterior central disc ventral canals. Abbreviations see Fig. 11.

PPT arched and robust, with its posterior portion of articulation with scapulocoracoid robust, and anterior portion curved proximally. Noticeable width difference between anterior and posterior portions of PPT. Length of FSP between one-third and one-fourth of PPT length (Fig. 40A). MSP with its anterior portion much smaller in lenght than its posterior portion (Fig. 40B). MTP robust and arched, with four and more PSMs (Fig. 40C). PB slender and in inverted "V" format, with distance between anterior and posterior faces small (Fig. 39C). LPP triangular and well anterolaterally pronounced. IP small and thin, and ISP in triangular format, small and with distal extremity pointed (Fig. 39C).

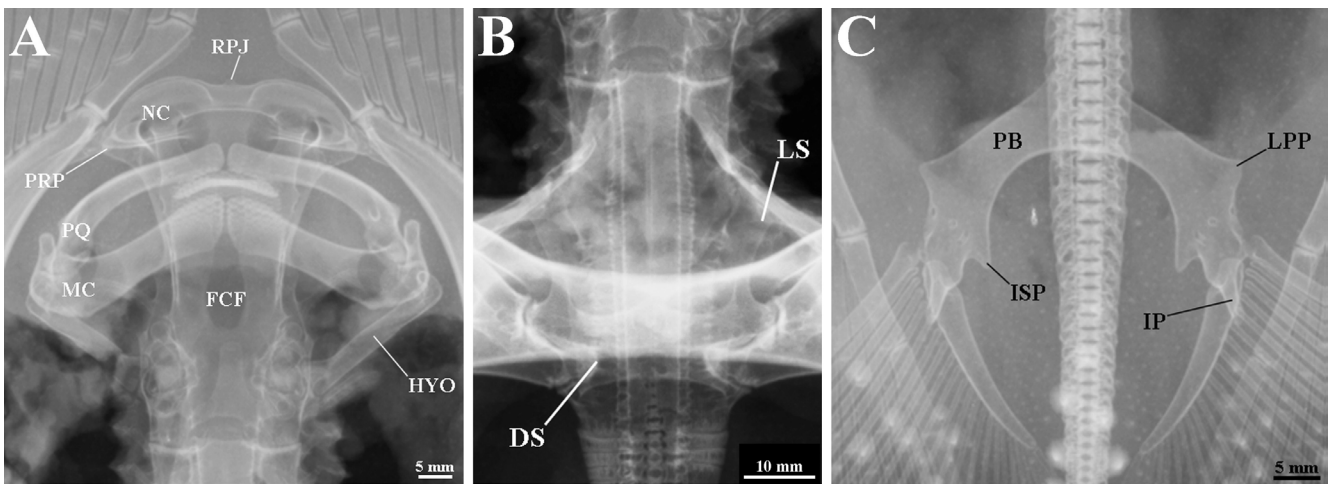

FIGURE 39 | Radiographys of pelvic girdle, *Paratrygon munduruku*, MZUSP 103916, holotype, juvenile female, upper view. **A.** Neurocranium and mandibular arch; **B.** Synarcual cartilage; **C.** Abbreviations: IP = iliac process; MC = Meckel's cartilage, FCF = frontoparietal component of fontanelle, HYO = hyomandibula, IS = internasal septum, NC = nasal capsule, PQ = palatoquadrate, RPJ = rostral projection. DS = dorsal socket, ISP = ischial process, LPP = lateral prepelvic process, LS = lateral stay, PB = puboischiadic bar.

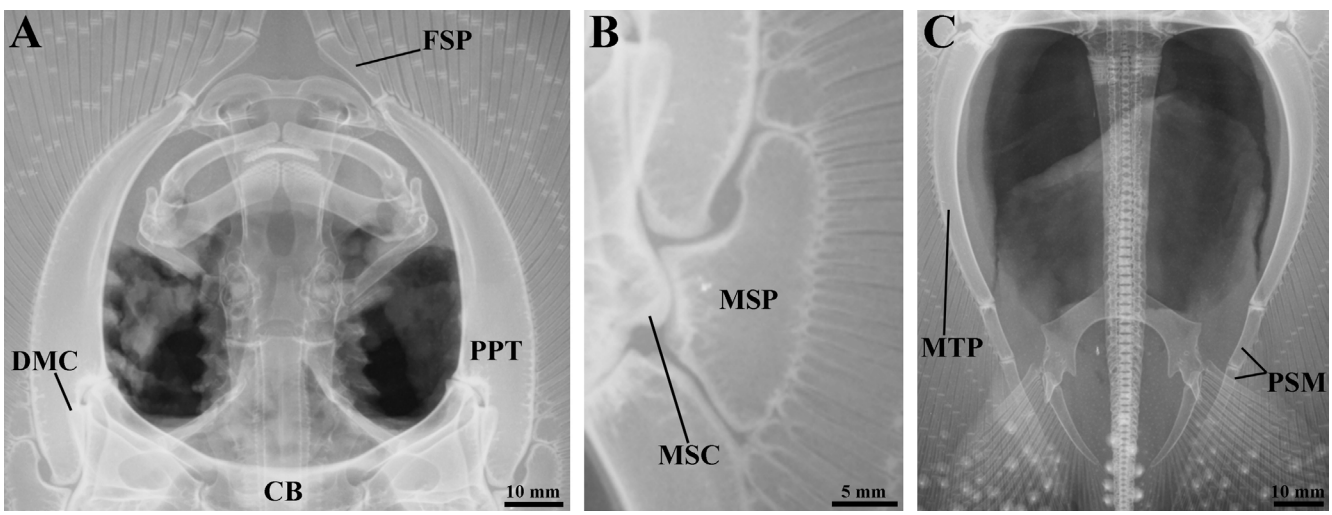

FIGURE 40 | Radiographys of scapulocoracoid and basal elements of pectoral fin of *Paratrygon munduruku*, MZUSP 103916, holotype, juvenile female, upper view. Abbreviations: ANT = antorbital cartilage, CB = coracoid bar, DLC = dorsolateral crest, FSP = first segment of propterygium, JMR = junction of medial radials, MSC = mesocondyle, MSP = mesopterygium, MTP = metapterygium, PPT = propterygium, PSM = posterior segments of metapterygium, SAS = small articulation surface.

Geographical distribution. *Paratrygon munduruku* has its distribution restricted to median portions of rio Tapajós (Fig. 15).

Etymology. The species epithet *munduruku* is in honor of the indigenous communities that live along various stretches of the Tapajós River, and who recognized themselves as Munduruku (Dopazo *et al*., 2023). Munduruku people are an ethnic group belonging to the Tupi family, distributed throughout different regions in the states of Amazonas, Pará, and Mato Grosso. A noun in apposition.

Conservation status. So far, *Paratrygon munduruku* has only been found in the middle portion of the Tapajós River. However, like the other clear water species of the genus, it probably also occurs in the middle part of the river and its main trbutaries. More data on its populations and the total area of occupancy are required to better understand the potential threats which now cannot be assessed without more distributional data. Therefore, the status of the species is Data Deficient (DD) based on the criteria established by the IUCN (IUCN, 2022).

Paratrygon raonii, new species

urn:lsid:zoobank.org:act:4B5C7DF1-94F3-4CF3-940D-24BD852654B5

(Figs. 41–53; Tabs. 7–8)

Paratrygon aiereba. —Rosa, 1985:487 (list of examined specimens). —Carvalho, Lovejoy, 2011:17 (list of examined specimens). —Frederico *et al*., 2012:73–79, figs. 1–3 (phylogeography, molecular analysis, conservation). —Fontenelle *et al*., 2021:6, 10, fig. 2, suppl. 3–4, 12, 25, figs. S2–S3 (list of specimens with genetic material analyzed, molecular phylogenys). —Sanches *et al*., 2021:1, 3, 5–9, 11, 13–15, figs. 1–3, tabs. 1–2 (molecular analysis of mitochondrial genes, molecular phylogenys).

Paratrygon sp. 8. —Loboda, 2016: vol. 1. vii, ix, 3, 7, 33, 60–61, 75–76, 87, 99–100, 113, 123, 126–127, 142, 154–168, 190–192, 254–259, vol. 2. xxi–xxii, 141–154, figs. 197–218 [citation of Frederico *et al*. (2012), specimens collected from rio Xingu, morphological comparisons with another *Paratrygon* species, citation from rio Xingu, synonymy, list of examined specimens, diagnosis, morphological description, distribution, endemicity for rio Xingu, morphometry, teeth count, meristics].

Holotype. MZUSP 104444, 557 mm DW, Brazil, Pará State, Municipality of São Félix do Xingu, rio Xingu, 06°39'23.33"S 51°59'56.72"W, 5 Jul 2005, F. Marques, M. V. Domingues & G. Mattox.

Paratypes. Specimens from rio Xingu, Brazil. Pará State: MZUSP 104445, 375 mm DW, Municipality of São Félix do Xingu, rio Xingu, 06°39'23.33"S 51°59'56.72"W, 6 Jul 2005, F. Marques, M. V. Domingues & G. Mattox. MZUSP 104436, 269 mm DW, Municipality of São Félix do Xingu, rio Xingu, 06°39'23.33"S 51°59'56.72"W, 1 Jul 2005, F. Marques, M. V. Domingues & G. Mattox. MZUSP 130350, 215 mm DW, Municipality of Senador José Porfírio, locality of Cotovelo, rio Xingu, Ilha Alta beach, 25 Apr 2013, Donato. MZUSP 130351, 214 mm DW, Municipality of Senador José Porfírio, locality of Cotovelo, rio Xingu, Ilha Alta beach, 25 Apr 2013, T. S. Loboda. Mato Grosso State: MZUSP 37216, 456 mm DW, Municipality of Peixoto de Azevedo, locality of Corredeira de Pedras, rio Xingu, 09°54'S 52°50'W, P. E. Vanzolini.

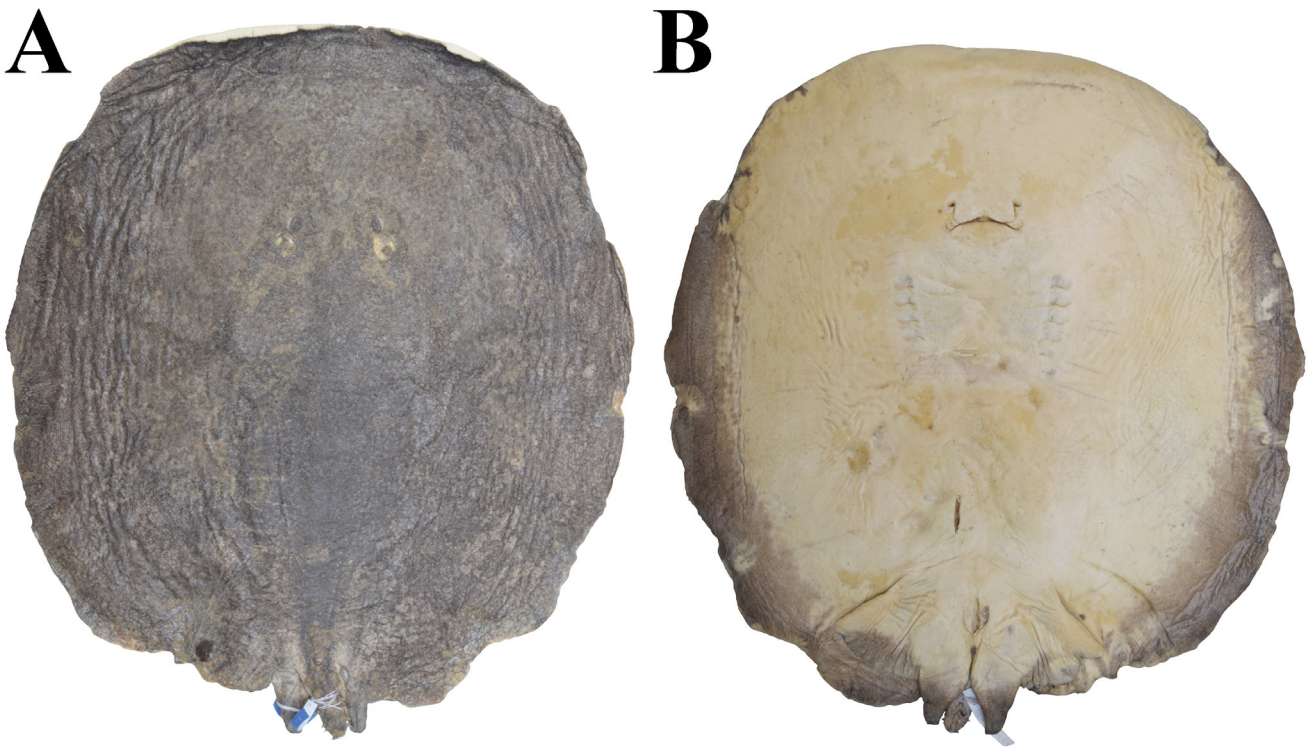

FIGURE 41 | Holotype of *Paratrygon raonii*, MZUSP 104444, adult male, 557 mm DW, from Xingu River. **A.** Dorsal; **B.** Ventral views.

Non-type. All specimens from rio Xingu, Brazil, Pará State: MZUSP 130352, 260 mm DW, Municipality of Senador José Porfírio, rio Xingu, Ilha da Fazenda, 24 Apr 2013, T. S. Loboda. MZUSP 130353, 236 mm DW, Municipality of Senador José Porfírio, rio Xingu, Ilha da Fazenda, 24 Apr 2013, T. S. Loboda. UFPA uncatalogued, 873 mm DW, Municipality of Altamira, Altamira port, Porto Seis, rio Xingu, 03°12'27.99"S 52°12'24.84"W, 17 Apr 2013, Maracajá. UFPA uncatalogued, 281 mm DW, Municipality of Altamira, rio Xingu. UFPA uncatalogued, 230 mm DW, Municipality of Altamira, locality of Itapuama, 03°33'18.6"S 52°21'24.5"W, 13 Apr 2013, Dinei. UFPA uncatalogued, 229 mm DW, Municipality of Altamira, rio Xingu. UFPA uncatalogued, 225 mm DW, Municipality of Altamira, locality of Itapuama, 03°33'18.6"S 52°21'24.5"W, 13 Apr 2013, R. S. da Silva. UFPA uncatalogued, 177 mm DW, Municipality of Senador José Porfírio, locality of Cotovelo, rio Xingu, Ilha Alta beach, 25 Apr 2013, R. S. da Silva.

Diagnosis. *Paratrygon raonii* can be distinguished from other *Paratrygon* species by the following combination of characters: the dorsal coloration of disc is gray, dark gray, light brown, brown, dark brown, or black with dark vermiculated, or axon-shaped spots that are evident and scattered throughout disc, with some specimens having light, rounded spots (*vs. P. aiereba*, *P. orinocensis*, *P. parvaspina* which have gray or light brown dorsal coloration and evident dark spots; *P. lucindai* with gray, dark gray, brown, and dark brown dorsal coloration that presents large, rounded, dark spots scattered throughout the disc; *P. araguaia* with a brown or dark brown dorsal disc that possesses

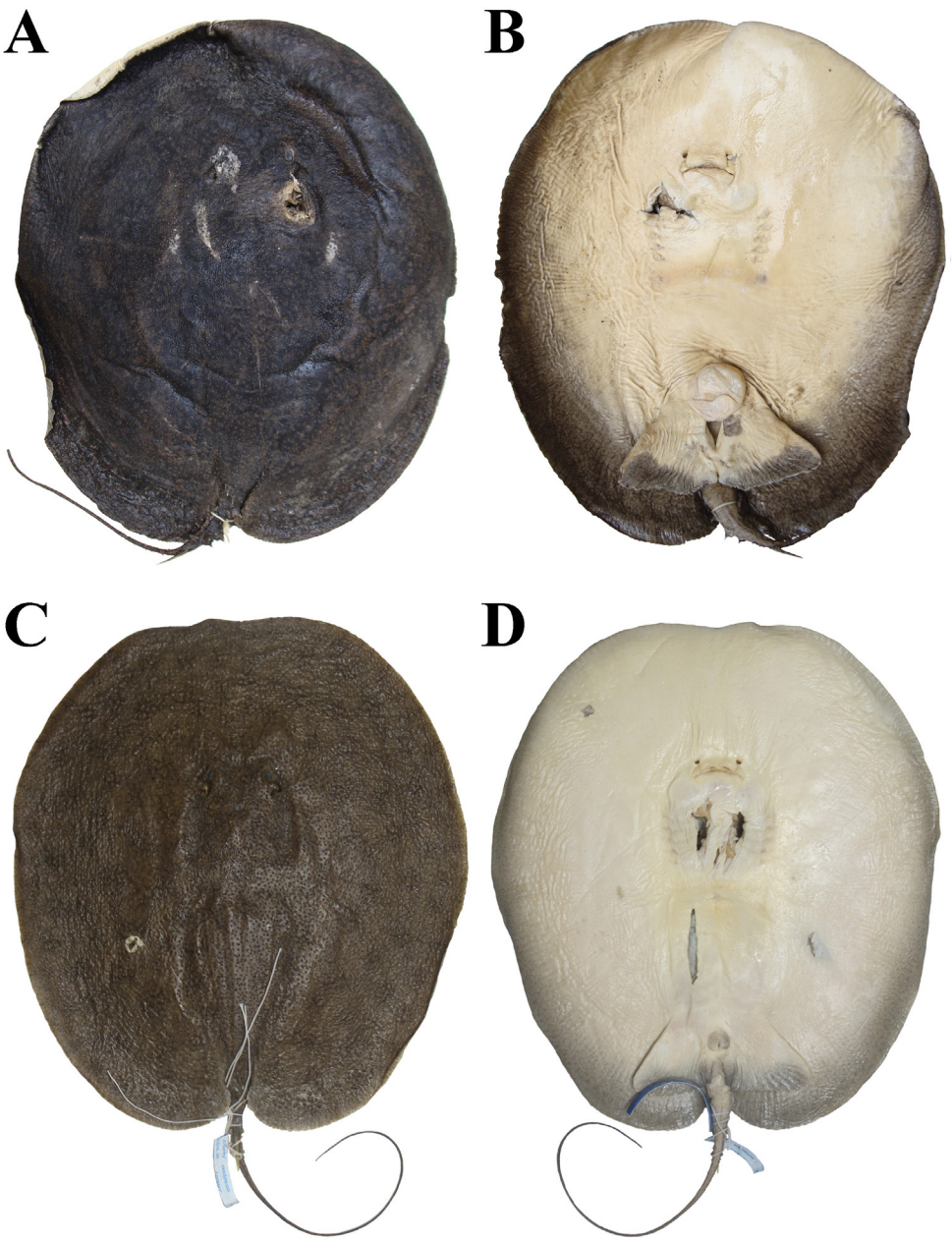

FIGURE 42 | Paratypes of *Paratrygon raonii*, MZUSP 37216, adult female, 456 mm DW, from Xingu River. **A.** Dorsal; **B.** Ventral views. MZUSP 104436, juvenile male, 269 mm DW, from Xingu River. **C.** Dorsal; **D.** Ventral views.

two types of spots scattered throughout the disc with one type light, big, and rounded, while the other is dark, small, and vermiculated, occurring between the light ones; *P. munduruku* has a brown dorsal coloration with numerous small, dark brown spots in an axon or vermiculated format spread throughout the disc, not evident, and without withish spots); very small spiracles that are generally proportional to the eyes or slightly larger, in a quadrangular format, with a mean length of 4% DW (3.4–5% DW), and with pronounced spiracle process (*vs. P. orinocensis* has a spiracle that is larger than the

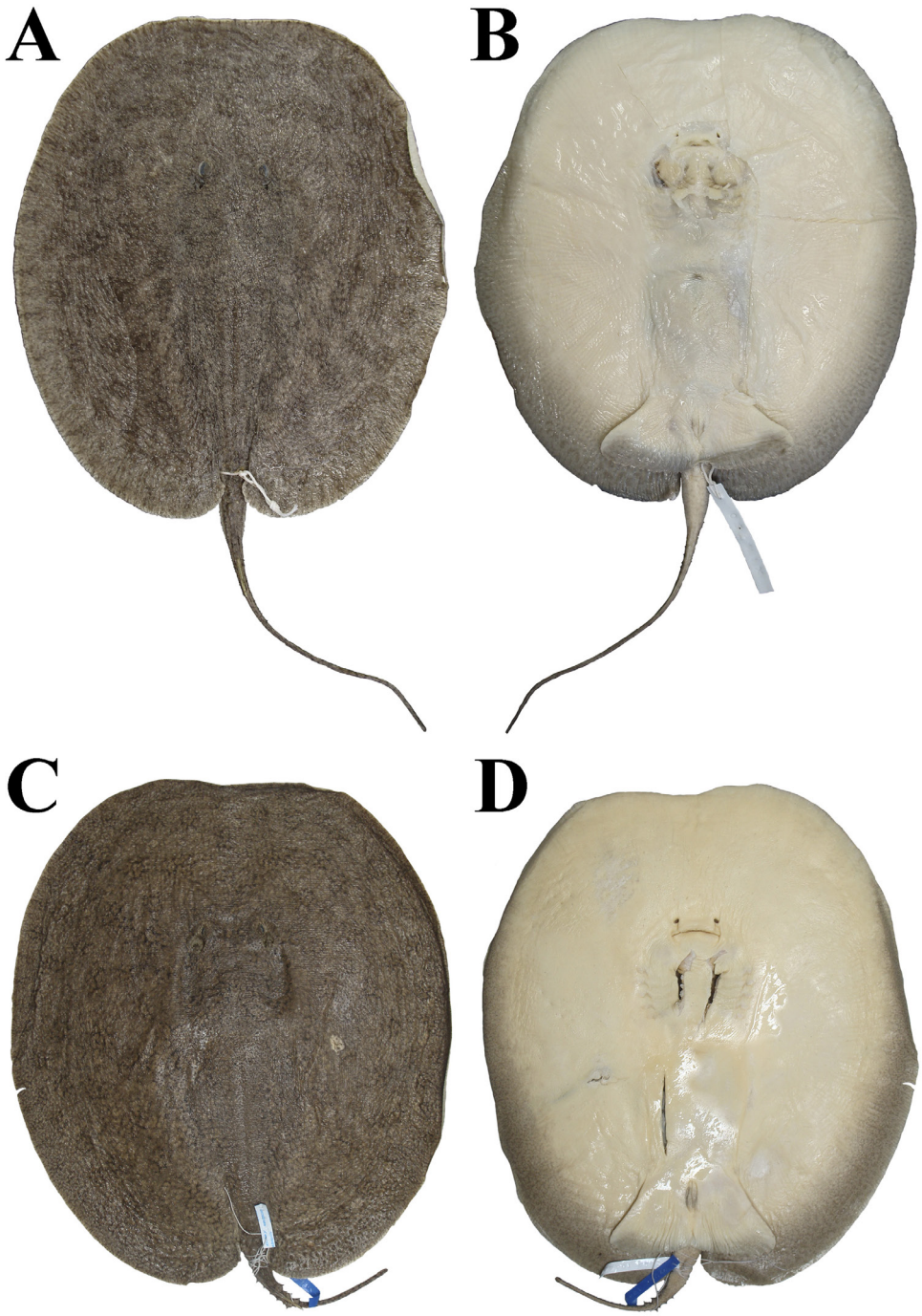

FIGURE 43 | Paratypes of *Paratrygon raonii*, MZUSP 130350, juvenile female, 215 mm DW, from Xingu River. **A.** Dorsal; **B.** Ventral views. MZUSP 104445, juvenile female, 375 mm DW, from Xingu River. **C.** Dorsal; **D.** Ventral views.

eye an in a triangular format, with a mean length of 5.6% DW; *P. aiereba*, *P. parvaspina*, *P. munduruku* have a quadrangular spiracle with a mean length greater than 5% DW and a very reduced spiracle process; *P. araguaia* with rounded spiracles and a length greater than 5% DW; *P. lucindai* with small and rounded spiracles); denticles on the central disc have a high crown and present a detached, well developed central coronal plate with a pointed shape, and also have well developed lateral coronal ridges in the range of six to eight, which are pointed and lower than the central coronal plate (*vs*. *P. aiereba* has a crown of central dermal denticles that present a pointed central coronal plate and pointed to slightly rounded lateral coronal ridges in the range of three to six, *P. orinocensis* has denticles that possess a well-developed and pointed central coronal plate and lateral coronal ridges, with more than twelve ridges; *P. parvaspina*, with central dermal denticles that present a pointed central coronal plate and pointed lateral coronal ridges that are much smaller than the central coronal plate and are few in number, between two to four; *P. lucindai*, with a crown of central dermal denticles that present a quadrangular central coronal plate and slightly rounded lateral coronal ridges; *P. araguaia* with central dermal denticles that present a pointed and reduced central coronal plate and rounded and well developed lateral coronal ridges; *P. munduruku* has dermal denticles on the central disc with a crown that has a central coronal plate and lateral coronal ridges that are the leaf-shaped and smaller than the central coronal plate); rostral projection of the neurocranium is very reduced and almost imperceptible (*vs*. *P. aiereba*, *P. orinocensis*, *P. lucindai*, *P. munduruku*, which have reduced but apparent projections; *P. parvaspina*, which has a robust projection that does not reach the anterior level of the nasal capsules; *P. araguaia*, which has a well expanded rostral projection that exceeds the anterior level of the nasal capsules).

Description. Measurements of *Paratrygon raonii* in Tabs. 7 and **S1**. Adult specimens with mean of total length 813.5 mm, with maximum value of 958 mm, mean of disc length in 670 mm, with maximum in 933 mm, and mean of disc width 628.7 mm, with maximum in 873 mm.

Disc subcircular with mean length in 109.6% DW. Adult specimens with minor disc length than juvenile and neonate specimens, mean in adults 106.6% DW, and in juveniles and neonates respectively 110.3% DW and 110.4% DW (Tab. **S6**). Anterior margin of disc with concavity very reduced in its medial portion (Figs. 41A, 42A, C, 43A, C). Mean distance between anterior margin of disc and cloaca 86% DW (75–91% DW) (Tab. 7), with adults 82% DW (75–86.9% DW), juveniles 87.3% DW (84.8–90.4% DW), and neonates 88.5% DW (86–91% DW) (Tab. **S6**). Head with small proportions, mean interorbital distance in 10.2% DW (9.6–11.2% DW), and mean interspiracular distance 14.5% DW (13.5–15.8% DW) (Tab. 7). Large eyes, not pedunculated (Fig. 44), with mean eye length 2.1% DW (0.9–3.4% DW) (Tab. 7), and with decrease of mean values at maturity: adults mean 1.4% DW (0.9–1.6% DW), juveniles 2.1% DW (1.6–2.7% DW), and neonates 3.1% DW (2.8–3.4% DW) (Tab. **S6**). Small spiracles, proportional with eyes or slightly larger, in quadrangular format (Fig. 45). Mean spiracle length 4% DW (3.4–5% DW) (Tab. 7). Spiracular process developed and stout, with simple format and extremity slightly globular (Fig. 45). Dermal denticles in spiracular process more apparent, numerous and sharp in adults. Spiracular process in neonates and juveniles covers much of posterior portion of spiracle, in adults covers entirely this

portion. Mean preorbital length in 32.5% DW (29.4–34% DW), mean prenasal length in 29.1% DW (26.7–31.1% DW), and mean preoral length 31.9% DW (29.7–33.5% DW). Small internasal distance with mean in 7.8% DW (7.2–8.8% DW), and mean mouth width 10.1% DW (9.3–10.9% DW) (Tab. 7).

Narrow branchial basket, with mean of distance between first gill slits in 20.1% DW (18.8–22.6% DW), mean of distance between fifth gill slits in 16.8% DW (15.7–17.5% DW), and mean of branchial basket length in 10.3% DW (9.2–11.3% DW) (Tab. 7). Pelvic fins triangular and dorsally covered by disc (Fig. **S7**). Mean of length of anterior

TABLE 7 | Measurements of specimens of *Paratrygon raonii* including the holotype, MZUSP 104444. Mean, Standard Deviation (SD) and Ranges are expressed in millimeters (mm) and proportions of disc width (%DW); (N) corresponds to the number of specimens analyzed.

Paratrygon raonii	Holotype		Average		SD		Range				N
	mm	%DW	mm	%DW	mm	%DW	mm		%DW		
Total length	–	–	473.2	162.5	173.5	31.3	266	958	109.7	203.5	13
Disc length	587	105.4	357.1	109.6	191.6	2.4	199	933	105.4	113.3	14
Disc width	557	100.0	328.4	100.0	182.3	0.0	177	873	100.0	100.0	14
Interorbital distance	59	10.6	34.0	10.2	18.9	0.4	18	90	9.6	11.2	14
Interespiracular distance	80	14.4	47.5	14.5	25.8	0.7	28	125	13.5	15.8	14
Eye length	9	1.6	5.9	2.1	1.4	0.6	4	9	0.9	3.4	14
Spiracle length	21	3.8	13.1	4.0	6.6	0.5	8	30	3.4	5.0	14
Preorbital length	165	29.6	105.2	32.5	58.1	1.4	60	288	29.4	34.0	14
Prenasal length	158	28.4	94.6	29.1	47.3	1.1	52	233	26.7	31.1	14
Preoral length	175	31.4	103.9	31.9	53.1	1.0	58	259	29.7	33.5	14
Internasal length	49	8.8	22.3	7.8	9.2	0.4	14	49	7.2	8.8	13
Mouth width	56	10.1	33.1	10.1	18.9	0.4	19	91	9.3	10.9	14
Distance between first gill slits	112	20.1	63.2	20.1	34.7	0.9	40	164	18.8	22.6	13
Distance between fifth gill slits	94	16.9	55.3	16.8	31.6	0.5	30	150	15.7	17.5	14
Branchial basket length	59	10.6	33.7	10.3	18.6	0.6	20	90	9.2	11.3	14
Length of anterior margin of pelvic fin	72	12.9	53.5	16.8	27.5	1.5	32	141	12.9	18.6	14
Pelvic fins width	228	40.9	133.5	40.3	70.5	2.8	75	336	36.0	45.8	13
External length of clasper	44	7.9	12.3	3.4	14.3	2.1	3	44	1.7	7.9	6
Internal length of clasper	92	16.5	31.8	9.6	27.2	3.2	14	92	7.4	16.5	6
Distance between cloaca and tail tip	–	–	189.3	70.6	62.5	29.9	75	276	19.5	112.2	13
Tail width	34	6.1	19.7	6.2	9.2	0.7	10	45	4.8	7.4	14
Distance between snout tip and cloaca	484	86.9	280.4	86.0	150.0	3.7	161	733	75.0	91.0	14
Distance between pectoral axil and posterior margin of pelvic fin	31	5.6	12.4	4.0	6.2	1.0	6	31	1.5	5.6	14
Distance between cloaca and caudal sting	–	–	53.3	20.6	14.6	2.3	38	90	17.4	24.7	12
Caudal sting length	–	–	26.8	11.0	5.3	2.1	20	35	7.7	15.8	11
Caudal sting width	–	–	2.3	0.9	0.4	0.2	2	3	0.7	1.4	12
Pseudosiphon length	11	2.0	11.0	2.0	0.0	0.0	11	11	2.0	2.0	1
Ventral pseudosiphon length	32	5.7	32.0	5.7	0.0	0.0	32	32	5.7	5.7	1

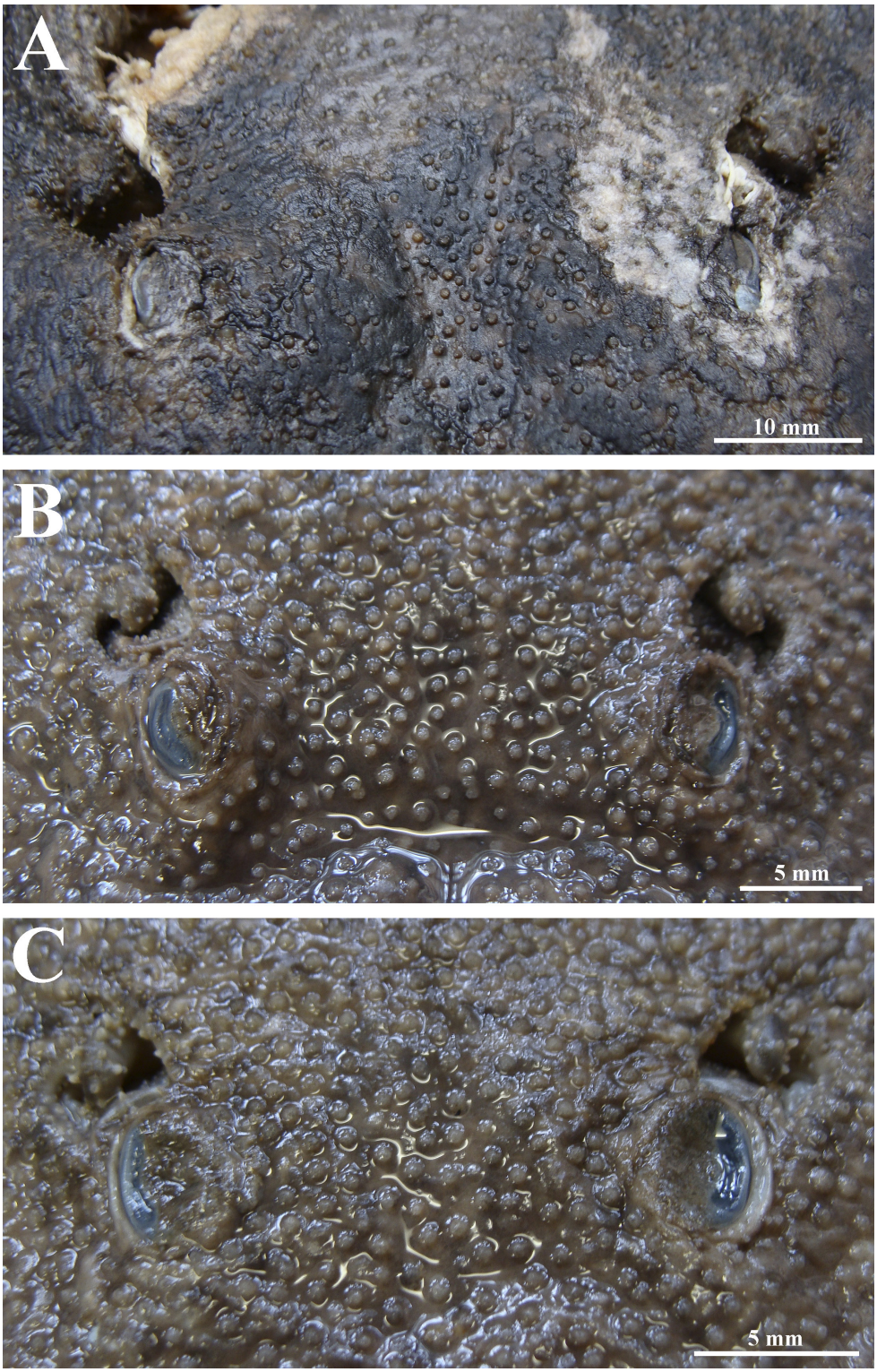

FIGURE 44 | Frontal view of eyes and spiracles of three specimens of *Paratrygon raonii*. **A.** MZUSP 37216, paratype, adult female, 456 mm DW; **B.** MZUSP 130352, juvenile male, 260 mm DW; **C.** MZUSP 130350, paratype, juvenile female, 215 mm DW.

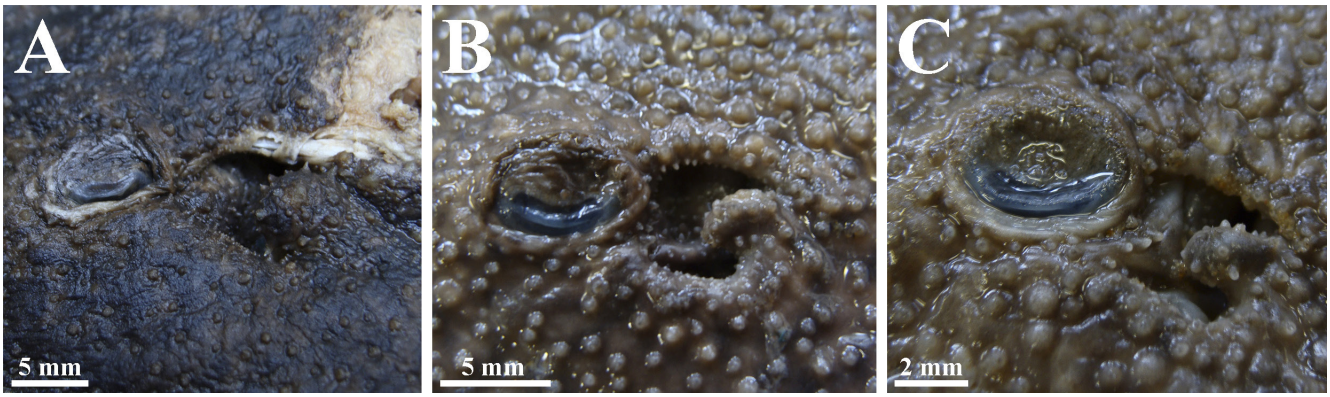

FIGURE 45 | Lateral view of spiracles and spiracles process of two specimens of *Paratrygon raonii*. **A.** MZUSP 37216, paratype, adult female, 456 mm DW; **B.** MZUSP 130352, juvenile male, 260 mm DW; **C.** MZUSP 130350, paratype, juvenile female, 215 mm DW.

margin of pelvic fin 16.8% DW (15.7–17.5% DW). Mean of pelvic fins width in 40.3% DW (36–45.8% DW), and mean of distance between pectoral axil and posterior margin of pelvic fin in 4% DW (1.5–5.6% DW) (Tab. 7). Clasper small, conical in shape, with base and medial portions robust, and extremity tapered (Fig. **S7**A). Means of external and internal lengths of clasper respectively 3.4% DW (1.7–7.9% DW) and 9.6% DW (7.4–16.5% DW) (Tab. 7). External length in adult male specimen 7.9% DW, in juvenile males mean of external length 2.6% DW (1.9–3.2% DW), and in neonates 2.2% DW (1.7–2.8% DW). Internal length in adult male specimen 16.5% DW, mean in juveniles males 8.4% DW (7.4–10% DW), and neonates 7.9% DW (Tab. **S6**). Pseudosiphon and ventral pseudosiphon lengths in male adult specimen respectively 2% and 5.7% DW (Tab. 7).

Tail with small pre-caudal sting portion, and post-caudal sting portion long and filiform. Means of pre-caudal sting portion (distance between cloaca and caudal sting) and tail width respectively 20.6% DW (17.4–24.7% DW), and 6.2% DW (4.8–7.4% DW) (Tab. 7). Lateral folds of tail in pre-caudal sting portion, and dorsal and ventral folds very discreet in post-caudal sting portion. Tail length with intermediate size, mean of tail length (distance between cloaca and tail tip) in 70.6% DW (19.5–122.2% DW) (Tab. 7). Tail length mean in adults 40% DW (19.5–60.5), in juveniles 87% DW (41.5–112.2% DW), and neonates 65.5% DW (35–96% DW) (Tab. **S6**).

Coloration in alcohol. Dorsal disc coloration gray, dark gray, light brown, brown, dark brown or black with vermiculated or axon format dark spots throughout disc, with rounded light spots in some specimens (Figs. 41A, 42A, C, 43A, C). Dark spots very evident in brown, dark brown or black colors with branched vermiculation or axon format, and moderated size slightly larger than spiracles. In some specimens more evident dark spots in rounded shape, and among these clear dark spots in vermiculated shape. Some evident dark spots in rounded shape with inside them small dark pontuations. Light spots in beige, light gray or light brown, with small size (smaller than spiracle length) or larger (diameter with two or three times spiracle length). Dorsal tail coloration as dorsal disc since its base until tip; majority of specimens with dark vermiculated spots in reduced size until tail tip. Ventral coloration of disc with two evident tonalities: light one in central disc and anterior margin of disc, and dark one in lateral and posterior margins. Dark tonality in some specimens until central posterior region of disc, and in

some cases with big spots near pelvic fins insertion (Figs. 41B, 42B, D, 43B, D). Light tonality in light beige and white. Dark tonality in gray, dark gray, brown and dark brown, with margins darker in specimens with this tonality in posterior central disc. All specimens with small and numerous dark spots throughout this tonality, in many shapes, as poligonal and vermiculated. Pelvic fins with same two tonalities of disc, with anterior margin, insertion and central portion in light tonality, and posterior margin in dark one. Majority of specimens with dark tonality around cloaca, and in some adult specimens big and evident. Claspers with light tonality in base, and rest of organ in dark tonality. Ventral tail coloration in pre-caudal sting portion from whitish or light beige to similar dark tonality of posterior disc. Post-caudal sting portion of tail with dark tonalities than tail base.

Squamation. Dermal denticles throughout all dorsal disc and tail. On disc, denticles in central region bigger and more visible than denticles of margins. Adult and larger juvenile specimens with numerous pointed tubercles on posterior margins of disc, and these tubercles with wide basal plate and high pointed crown. Tail with big denticles on pre-caudal sting portion, and on post-caudal sting portion denticles considerably minor (Fig. 46).

Small to medium dermal denticles of 1 mm in diameter on central disc, posterior margins and tail basis, whereas in anterior and lateral margins of disc denticles with 0.6 to 0.7 milimeters (Figs. 47–48). Denticles on central disc with high crown, detached, well developed, and pointed shape ccp. Ccp dislocated from central region of denticle, more close to crown margin. Lcrs between six and eight, well developed, also pointed shape, but lower than ccp. Lcrs generally surround ccp, and in opposite direction to marginal portion of ccp (Figs. 47C–D, 48B–D). Denticles in anterior, lateral margins of disc, and tail base with crown less developed than central denticles. Ccp of those denticles minors, and with lcrs reduced in size and number. Both ccp and lcrs from marginal denticles with more rounded tips than central disc denticles (Figs. 47A–B, G–H, 48A, G–H). Denticles of posterior margins of disc silghtly larger than centrals, with apparent star shaped bp in diameter bigger than one milimeter, and cr in pointed spine shape, well developed and high (Figs. 47E–F, 48E). Some denticles of disc posterior margins with pointed crowns without spine format, and some few lcrs closer and connected to crown (Fig. 48F).

Adult specimens with dorsal and laterals rows of pointed spines on tail (Figs. 49A–B). Dorsal rows from one to three in all pre-caudal sting portion, with developed, high and broad based spines, and in some specimens tubercled. One lateral rows on each side of tail, well developed in adult specimens, from almost entire pre-caudal sting portion to little part of post-caudal sting portion. Lateral pointed spines developed, higher than dorsals, with tubercled bases (Figs. 49A–B). In larger juvenile dorsal and lateral rows similar to adults, with their spines developed and base wide. Juvenile specimens with complete dorsal rows of small spines not totally completed in all pre-caudal sting portion. Lateral rows in juveniles well developed, with minor spines, and in some specimens, lateral spines tubercled (Figs. 49C–D).

Caudal sting long, with mean of caudal sting length 11% DW (7.7–15.8% DW) and mean of caudal sting width 0.9% DW (0.7–1.4% DW) (Tab. 7). Caudal sting length in adult specimen 7.7% DW, mean in juveniles 11.2% DW (8.7–15.8% DW), and mean in neonates 11.1% DW (10.3–11.9% DW). Caudal sting width values in adult and

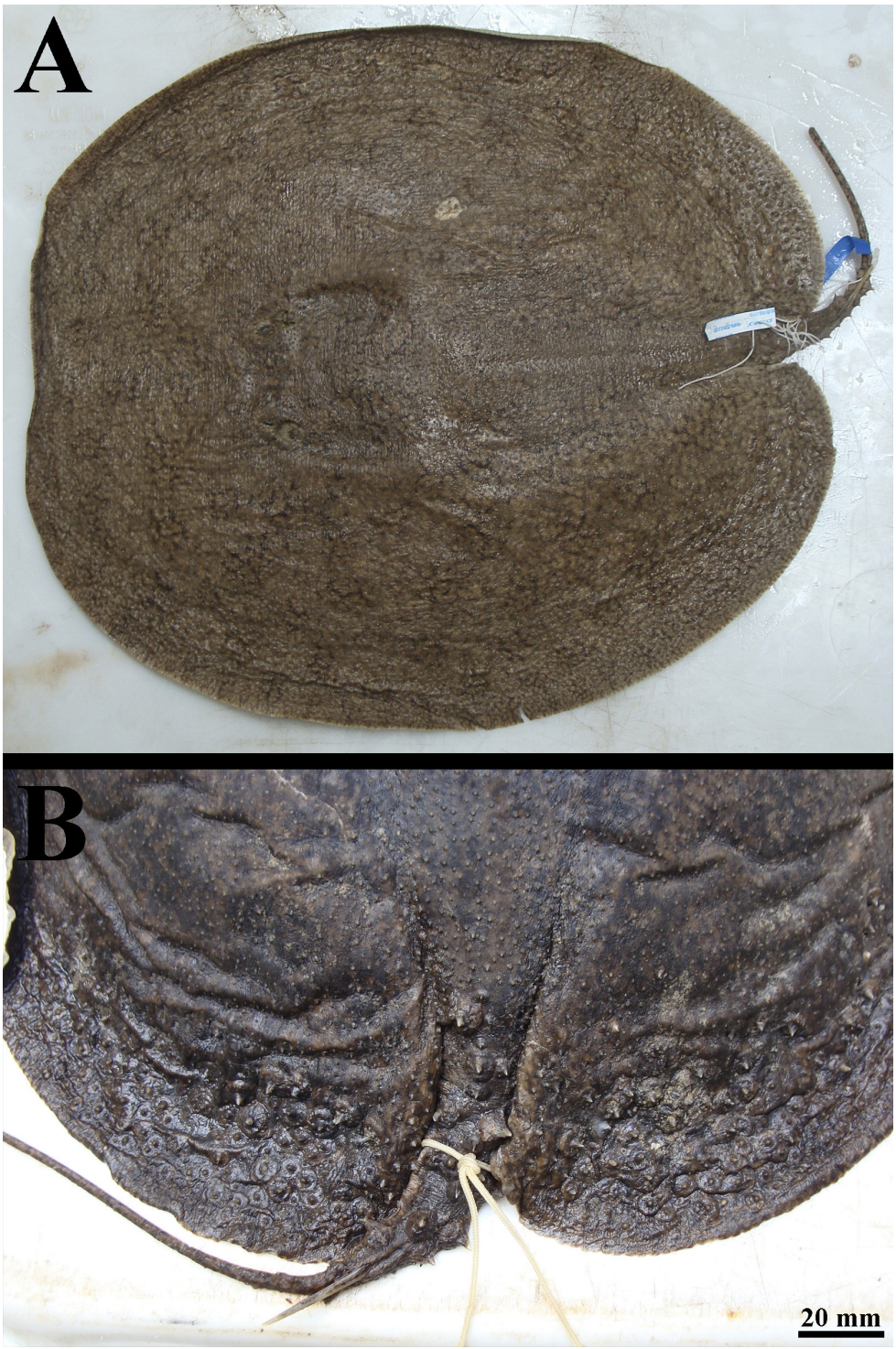

FIGURE 46 | Dermal denticles present on dorsal disc and tail in *Paratrygon raonii*. **A.** Distribution of dermal denticles in paratype MZUSP 104445, juvenile female; **B.** Denticles present on posterior margins of disc and tail in paratype MZUSP 37216, adult female.

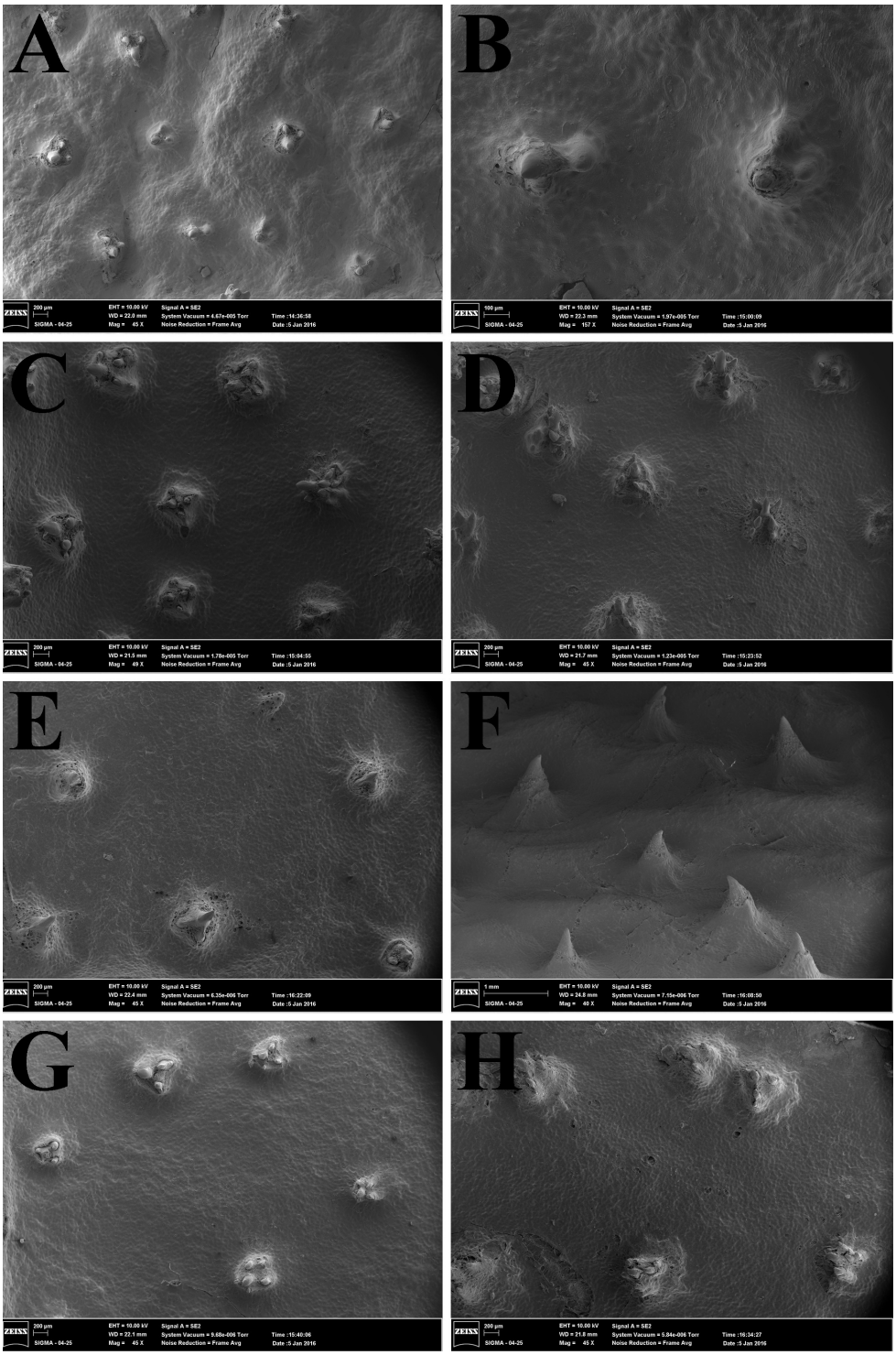

FIGURE 47 | Dorsal view of dermal denticles taken from SEM images of the following regions of the disc from *Paratrygon raonii*, paratype MZUSP 130351, juvenile male. **A.** and **B.** Anterior margin; **C.** and **D.** Central; **E.** and **F.** Posterior; **G.** Lateral; **H.** Tail base.

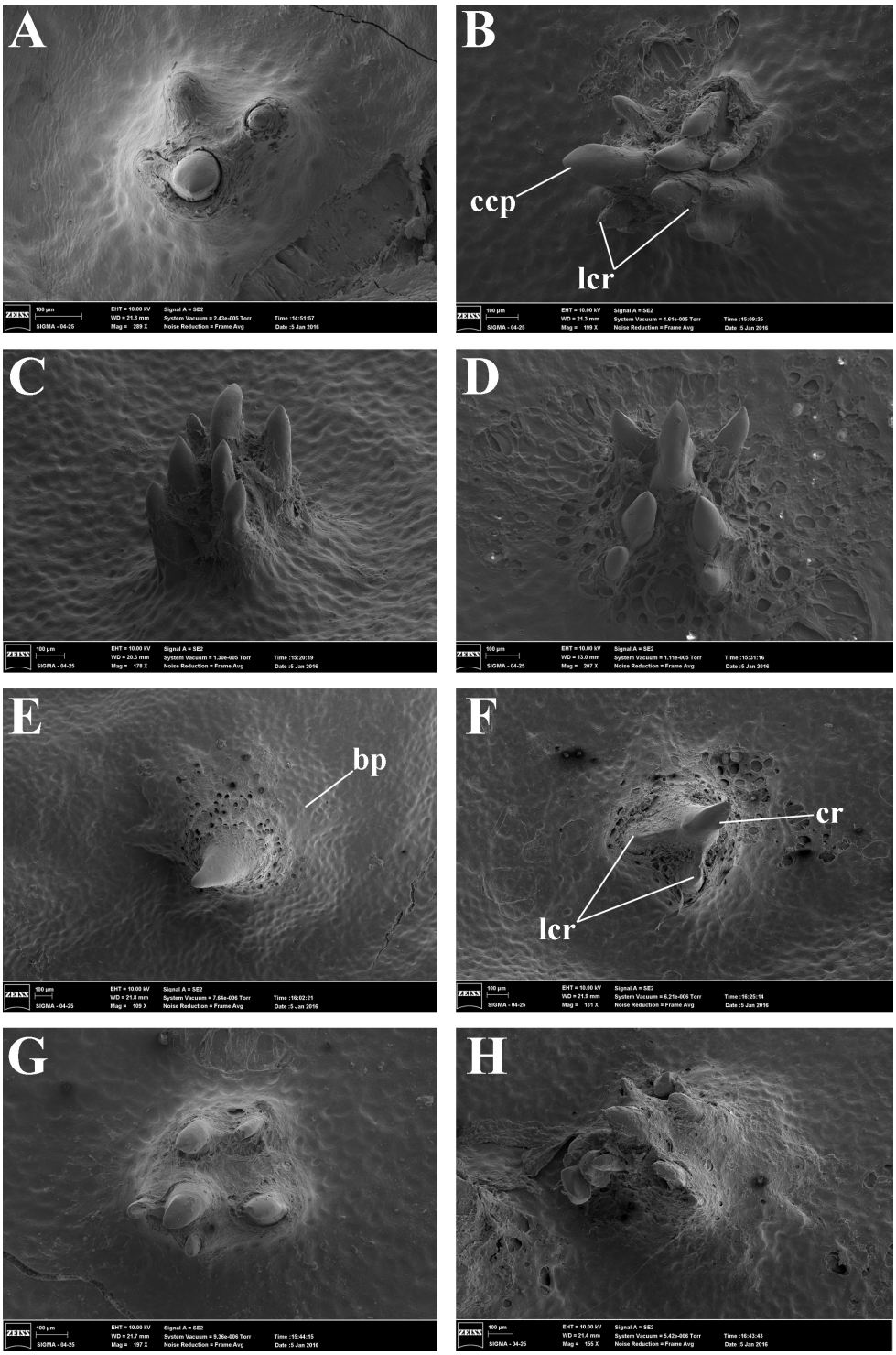

FIGURE 48 | Morphological details of dermal denticles taken from SEM images of the following regions of the disc from *Paratrygon raonii*, paratype MZUSP 130351, juvenile male, 214. **A.** Anterior margin; **B–D.** Central; **E.** and **F.** Posterior; **G.** Lateral; **H.** Tail base. Abbreviations see Fig. 8.

juveniles specimens mean respectively 0.7% DW and 0.8% DW (0.7–0.9% DW), and neonates with wider spines, mean in 1.3% DW (1.1–1.4% DW) (Tab. **S6**). Developed caudal sting in adult specimen, with lateral serrations in its final two thirds, with small and slightly bigger serrations in final third (Fig. 49E). Big caudal stings in larger juvenile specimens with small lateral serrations, more developed in final third of sting. Medial dorsal groove in proximal third of sting (Fig. 49F).

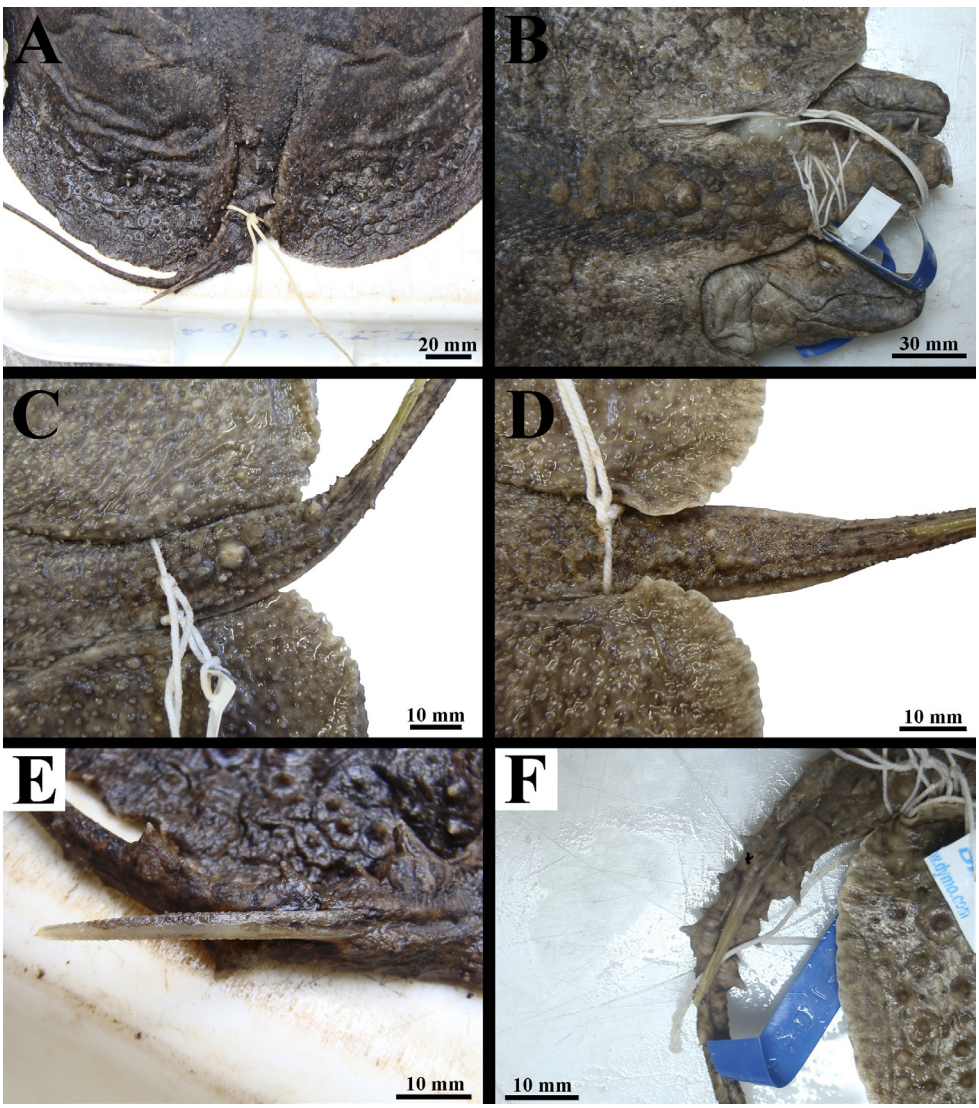

FIGURE 49 | Dorsal view of dorsal and lateral rows of thorns on tail **A–D** and caudal stings **E.** and **F.** of *Paratrygon raonii*. **A.** and **E.** MZUSP 37216, paratype, adult female; **B.** MZUSP 104444, holotype, adult male; **C.** MZUSP 130351, paratype, juvenile male; **D.** MZUSP 130350, paratype, juvenile female; **F.** MZUSP 104445, paratype, juvenile female.

Ventral lateral line canals. JFC long and HMD ang with curvature not so open. Jug of HMD with long central curvature. Spl with three pst, and most central one bifurcated. Spc of HMD paralel to jug, and in slighlty posterior level of pectoral girdle. Spt from spc at level of first gill slits. Final extremity of HMD after most anterior spt connecting to pnc of NAS below connection of this canal to IOC (Fig. 50). IOC with wide sub, well branched, and in large number of branches. Unique connection between sub and pnc. SPO with wide and more discrete curvature after JFC. Nil wide and open. Sbr of SPO with five to six vS throughout its extension. NAS straight and inclined to nostrils from JFC, and pnc closer to anterior margin of disc and medially located. MNC from Meckel's cartilage region circumventing internally and posteriorly *adductor mandibulae* muscle (Fig. 50).

Skeleton. Meristic counts of vertebrae and pectoral and pelvic fins radials in Tab. 8. Neurocranium with narrow IS. RPJ very reduced, and FCF in eight number format (Figs. 51A–B). Mandibular arch with PQ and MC robust, arched and slightly short, however PQ with sharp curvature in articulation portion with MC. HYO slender and slighlty shorth, with discreet curvature in medial portion (Figs. 51A–B). Synarcual cartilage with LS well developed and little expanded (Fig. 52A). Scapulocoracoid with CB little robust. Anterior face of CB curved, with slight convexity between central portion and extremity, and posterior face straight. DLC of scapular process pronounced

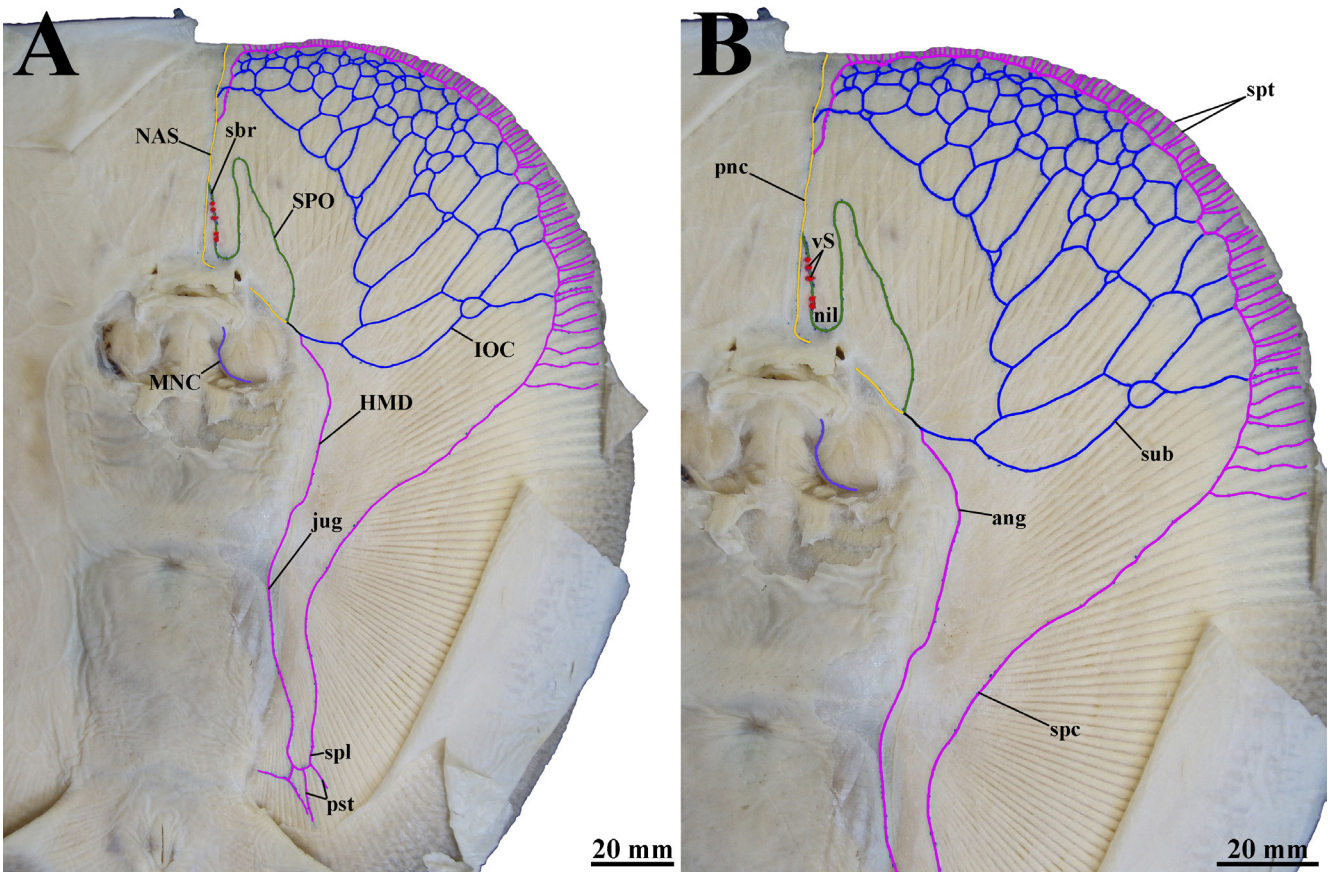

FIGURE 50 | Ventral canals of lateral line system in *Paratrygon raonii*, MZUSP 130350, paratype, juvenile female. **A.** Distribution of all ventral canals; **B.** Detail of the anterior central disc ventral canals. Abbreviations see Fig. 11.

TABLE 8 | Meristic data taken from specimens of *Paratrygon raonii* radiographed; "M" corresponds to mode, and "R" corresponds to range.

Paratrygon raonii	MZUSP 130353	MZUSP 130350 (paratype)	MZUSP 130352	M	R
Precaudal vertebrae	36	37	40	–	36–40
Caudal vertebrae	–	–	63	–	–
Total vertebrae	–	–	103	–	–
Diplospoldylic vertebrae	–	–	60	–	–
Propterygial radials	46	45	50	–	45–50
Mesopterygial radials	27	26	26	26	26–27
Metapterygial radials	41	41	38	41	38–41
Total radials	114	112	114	114	112–114
Pelvic radials	21	19	19	19	19–21

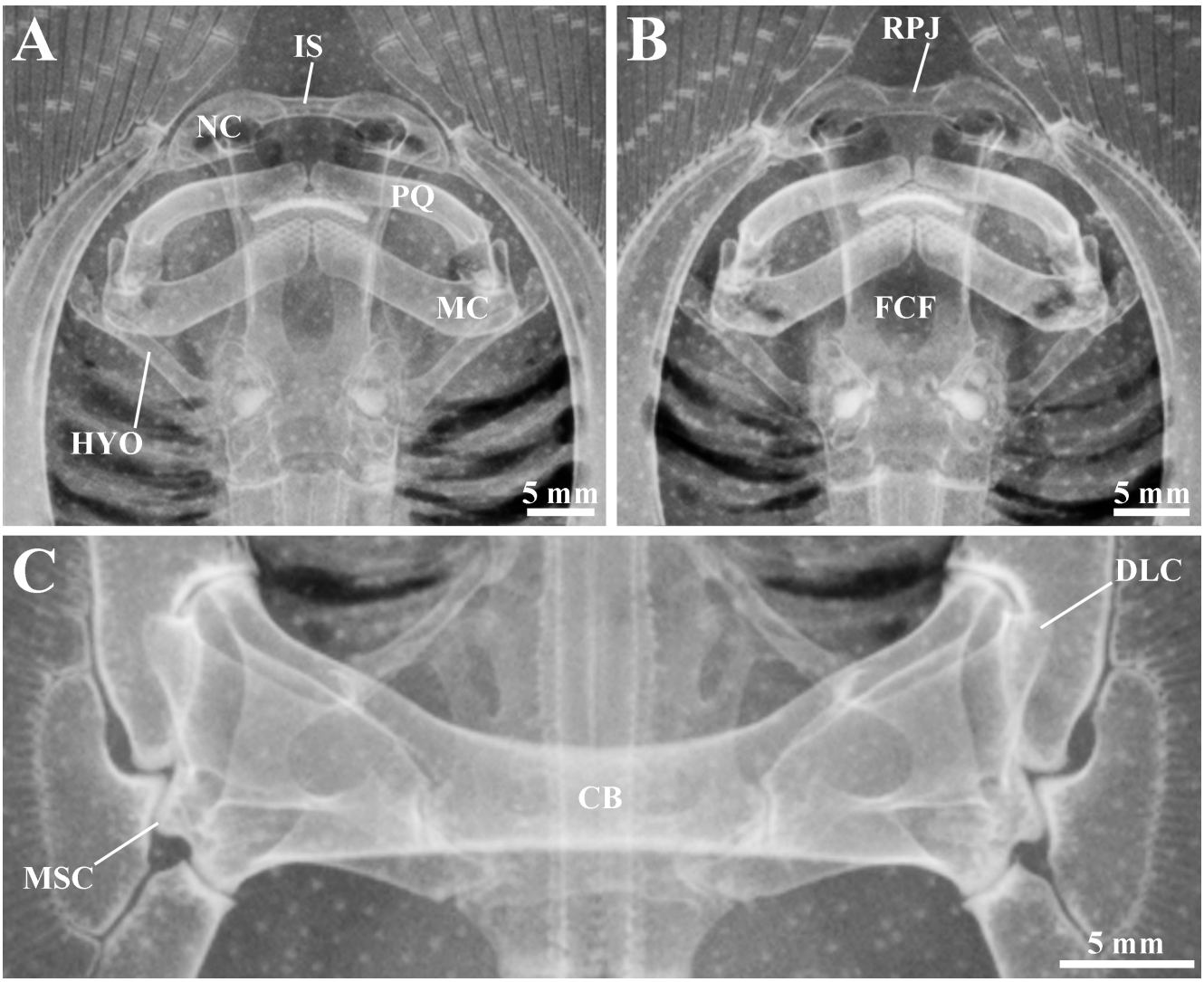

FIGURE 51 | Radiographys of *Paratrygon raonii*. **A.** and **B.** Neurocranium and mandibular arch; **C.** Scapulocoracoid. **A.** MZUSP 130351, paratype, juvenile male; **B.** and **C.** MZUSP 130350, paratype, juvenile female, upper views. Abbreviations see Figs. 12 and 14.

and surpassing laterally MSC final third. Final third of MSC few pronounced (Fig. 51C). PPT few robust and straight, without pronounced curvature in proximal anterior portion. FSP between one third and one fourth PPT length (Fig. 53A). MSP articulated with MSC and PPT very next to each other, with short portion of MSP articulation (Fig. 53B). MTP straight. PSM of MTP next to level of prepelvic process base of pelvic girdle (Fig. 53C). PB arched, slightly in inverted "V" format and slender, and also with shorter distance between anterior and posterior faces. Lateral extremities of PB without posterior prolongations. ISP few developed with its final extremity in pointed shape. LPP triangular and projected laterally (Fig. 52B).

Geographical distribution. *Paratrygon raonii* is restricted to median portion of rio Xingu, approximately between the municipalities of São Felix do Xingu and Senador José Porfírio (Fig. 15).

Etymology. The species epithet *raonii* is in honor to Raoni Metuktire, an indigenous Kayapo leader, environmentalist and activist who has fought for decades to preserve the rio Xingu and its indigenous people, as well as the Amazon rainforest. A noun in a genitive case.

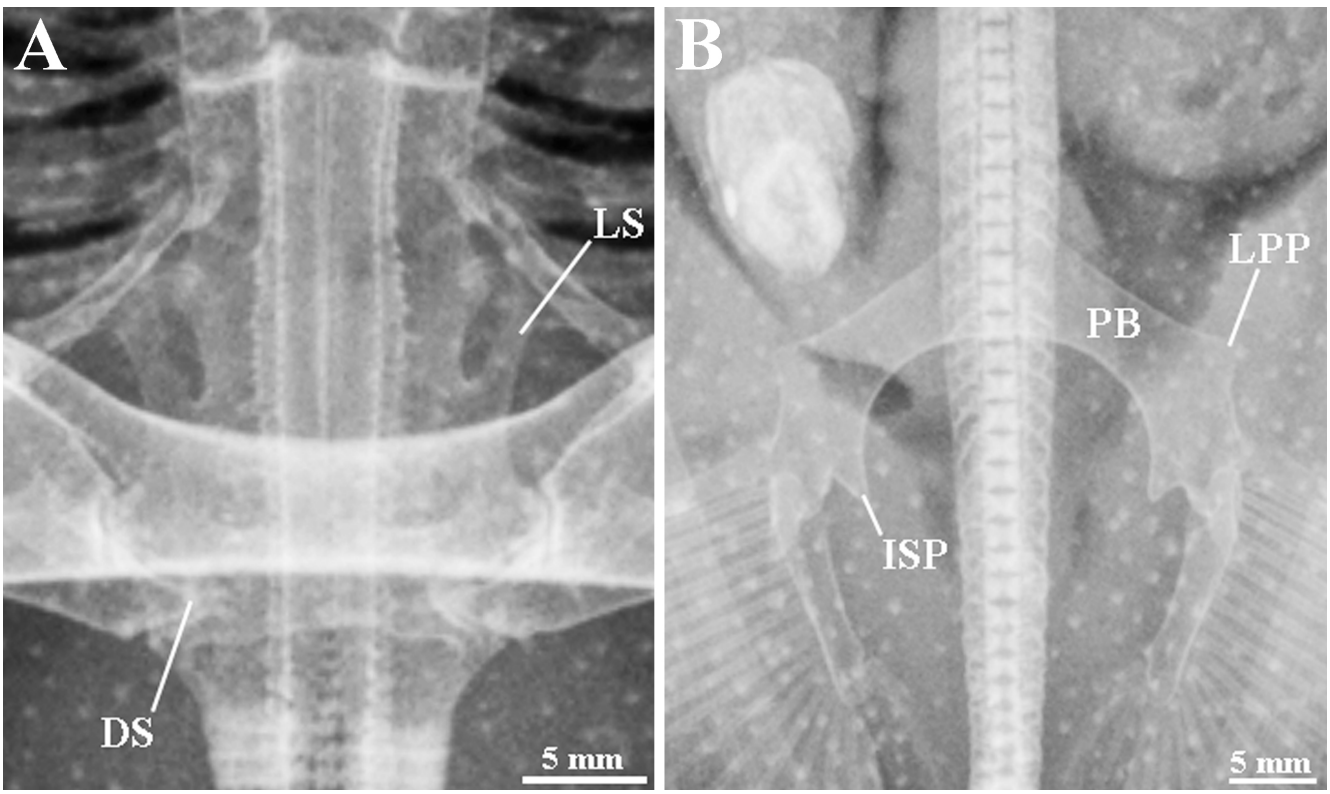

FIGURE 52 | Radiographys of *Paratrygon raonii*, MZUSP 130350, paratype, juvenile female, upper view. **A.** Synarcual cartilage; **B.** Pelvic girdle. Abbreviations see Fig. 13.

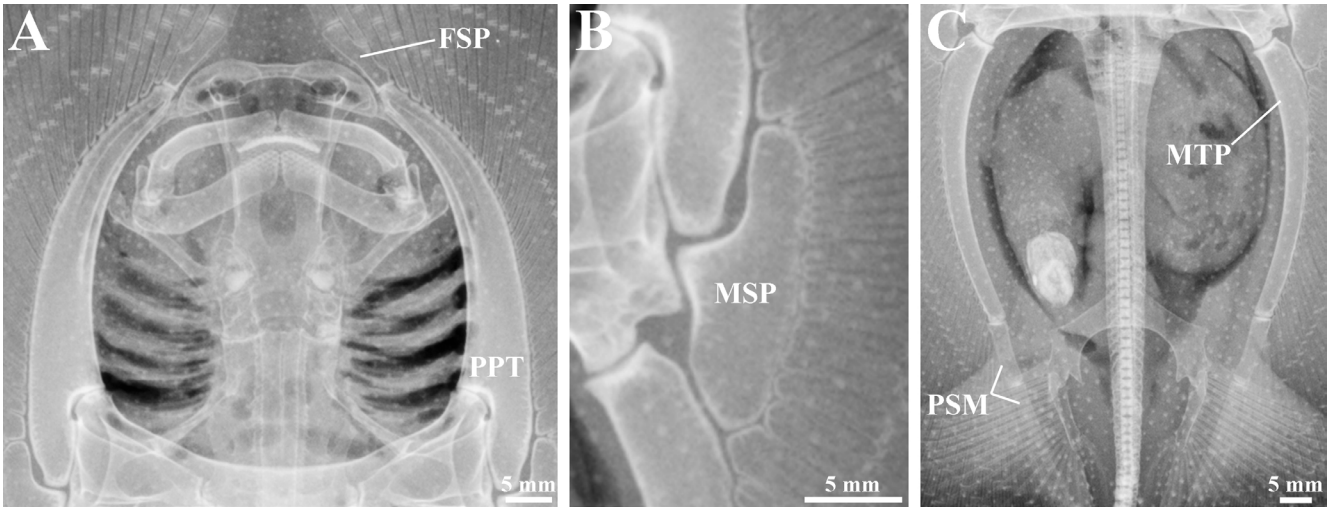

FIGURE 53 | Radiographys of basal elements of pectoral fin of *Paratrygon raonii*, MZUSP 130350, paratype, juvenile female, upper view. Abbreviations see Fig. 14.

Conservation status. *Paratrygon raonii* is widespread throughout the middle portion of the Xingu River and its tributaries, and it probably could occur in the upper part. While populations of this species currently face no imminent threats, more studies on their status are needed. According to the International Union for Conservation of Nature (IUCN) categories and criteria (IUCN, 2024) the species is classified as Data Deficient (DD).

Key to identification of species of *Paratrygon*

1a. Dorsal disc colors in beige, light gray and light brown 2
1b. Dorsal disc colors in dark brown, dark gray and black 3
2a. Tail with lateral rows of pointed spines 4
2b. Tail without lateral rows of pointed spines ..... *P. orinocensis*
3a. Dorsal disc with large round spots in beige, gray, brown, dark brown or reddish brown color, with two to three times spiracle's diameter ..... *P. lucindai*
3b. Dorsal disc with small dark spots minor than two times spiracle's diameter 5
4a. Presence of a pair of big dark spots in preorbital dorsal disc ..... *P. aiereba*
4b. Preorbital dorsal disc without a pair of big dark spots ..... *P. parvaspina*
5a. Dorsal disc with just presence (or predominance) of vermiculated dark spots 6
5b. Dorsal disc with two types of spots, with predominance of round spots in light beige ..... *P. araguaia*
6a. Dermal denticles on central disc with crown possessing central coronal plate and lateral coronal ridges in leaf shape, with lateral coronal ridges smaller and between two to five ..... *P. munduruku*
6b. Dermal denticles on central disc with high crown, presenting central coronal plate detached, well developed, with pointed shape, and lateral coronal ridges in six to eight, well developed, also with pointed shape ..... *P. raonii*

DISCUSSION

The four new species of *Paratrygon* described in detail here, *P. lucindai*, *P. araguaia*, *P. munduruku*, and *P. raonii*, are based on taxonomic studies and analyses of morphological characteristics by Loboda (2016). These results are also supported by morphological and, mostly, molecular data from the aforementioned previously published studies (Santos *et al*., 2004; Frederico *et al*., 2012; Fontenelle *et al*., 2021a; Sanches *et al*., 2021).

These four new species are strikingly different from the three previously described, *P. aiereba*, *P. orinocensis* and *P. parvaspina*, due to their darker dorsal coloration, which is especially prominent in *P. araguaia*, *P. munduruku*, and *P. raonii*. *Paratrygon raonii* and *P. munduruku* have the darkest dorsal disc coloration of all *Paratrygon* species, with *P. raonii* having the darkest. They all have differences in the tones and distribution of spots in their dorsal coloration, as highlighted in their respective diagnoses and descriptions (see Results), which makes it easy to identify each species. *Paratrygon munduruku* and *P. raonii* have the most similar coloration patterns, however as mentioned above, *P. raonii* has darker coloration and small light spots, which *P. munduruku* lacks (Figs. 29–30, 41–43).

Even juvenile specimens of these four new species differ greatly in characteristics mentioned in their diagnoses and descriptions, including coloration. As Carvalho (2016a:34–35) points out, neonates and juveniles of possibly closely related species, such as *Potamotrygon jabuti* and *P. motoro*, are very similar to each other. This is not the case with the four *Paratrygon* species described here. Even species that are visibly similar in terms of coloration, such as *P. munduruku* and *P. raonii*, have very distinct juveniles (Figs. 29–30, 42C–D, 43). These differences extend beyond coloration to include several morphological aspects, such as morphometrics, spiracle process, dermal denticles, pointed spines of tail rows, and elements of skeleton and ventral canals of lateral line.

Paratrygon lucindai was first recognized as morphologically distinct from *P. aiereba* by Santos *et al*. (2004). They published a brief morphological description of the species, focusing mainly on morphometrics, and named it "*Paratrygon* sp.". Fontenelle *et al*. (2021a) provided molecular data from the mitochondrial sequences ATPase 6, COI and Ctyb, as well as the nuclear sequence its1 for a specimen here identified as *P. lucindai* ("*P. aiereba* - Rio Tocantins"). In their resulting cladogram, the species appears in a polytomy as a sister group to *P. raonii* ("*P. aiereba* – rio Xingu") and a clade formed by *P. munduruku* ("*P. aiereba* – rio Tapajós") and populations of *P. aiereba* from the Branco, Negro and Solimões-Amazonas rivers. *Paratrygon lucindai* has one of the thinnest caudal spines among *Paratrygon* species, with a mean caudal sting length of 9.3% DW (4.3–14.7% DW), and a mean caudal sting width of 0.7% DW (0.4–1.2% DW) (Tab. 1). It has a small JFC, which is unique among *Paratrygon* species. The anterior end is positioned more externally than the posterior end and if formed by the connection between the IOC and the SPO. The posterior end is formed by the connection between the HMD and NAS canals, a similar pattern which is found in *Potamotrygon* species. The *IOC* also has an *ic* between JFC and the sub which has a unique condition among *Paratrygon* species. The suborbital component is the smallest component among *Paratrygon* species, with the fewest ramifications. Lastly, the posterior end of the MSP is more pronounced and larger than in other *Paratrygon* species.

Frederico *et al*. (2012) previously identified *P. araguaia* as a possible new species based on molecular characters, using ATPase 6 and COI sequences. Fontenelle *et al*. (2021a) confirmed this identification using ATPase 6, COI, Ctyb, and its1 sequences.

Using COI sequences, Frederico *et al*. (2012) identified *P. araguaia* ("*Paratrygon aiereba* Araguaia River – ARA") as a sister group to a clade comprising populations of *P. aiereba* from the Negro and Solimões-Amazonas rivers and *P. raonii* ("*Paratrygon aiereba* Xingu River – XIN"), and with ATPase 6 sequences, *P. araguaia* fell into a sister group with *P. munduruku* ("*Paratrygon aiereba* Tapajós River – TAP"). In Fontenelle *et al*. (2021a) analysis, *P. araguaia* ("*P. aiereba* – rio Araguaia") fell into a sister group with a clade formed by the *Paratrygon* species from Orinoco basin: *P. orinocensis* and *P. parvaspina*. *Paratrygon araguaianesis* also has the smallest mean interorbital distance of all *Paratrygon* species, at 10% DW (8.4–11.2% DW). Its pelvic fins have a long anterior margin and possess the largest mean of the genus *Paratrygon*: 18.5% DW (15.8–20.5% DW). However, the distance between the distal extremities of the pelvic fins has the smallest mean of the genus: 36.7% DW (31.4–41.3% DW). The caudal sting is long and one of the thickest among *Paratrygon* species, with a mean width of 0.8% DW (0.7–1.3% DW). The presence of a small tubule directed toward the central disc region posteriorly in the *jug* of HMD is found only in *P. araguaia* among *Paratrygon* species. The anterior portion of the MSP in *P. araguaia* is shorter than in other congeners, with a length between half and slightly less than half that of the posterior portion. In other species, both portions are similar in length, with the anterior portion slightly longer than the posterior (Fig. 28B).

Frederico *et al*. (2012) and Fontenelle *et al*. (2021a) were the first to publish works pointing out *Paratrygon munduruku* as a possible new taxon using the above-reported *P. araguaia* sequences. In Frederico *et al*. (2012), *P. munduruku* was a sister group to *P. araguaia* in the ATPase 6 analysis. In Fontenelle *et al*. (2021a), *P. munduruku* was in a polytomy with *P. aiereba* populations from the Solimões-Amazonas and Negro rivers. *Paratrygon munduruku* is one of the *Paratrygon* species with the smallest distance from the anterior margin of the disc to the cloaca, with a mean of 85.4% DW (78.7–89.5% DW). Its head is also one of the smallest among *Paratrygon* species, with mean interorbital and interespiracular distances of 10.6% DW (10.2–11.2% DW), and 14.2% DW (11.2–17.4% DW), respectively. *Paratrygon munduruku* has one of the widest mouths among *Paratrygon* species with a mean of 10.3% DW (10.1–10.5% DW) and the lowest for the distance between the first pair and the distance between the first and fifth pairs among *Paratrygon* species, with means of 19.9% DW (19.1–21.6% DW), and 10% DW (9–11.1% DW), respectively. This species has a small caudal sting compared to other *Paratrygon* species, with a mean length of 8.2% DW (7–10% DW) and a mean width of 0.9% DW (0.8–1.1% DW). *Paratrygon munduruku* exhibits significant differences in width between the anterior and posterior portions of the *PPT*.

Paratrygon raonii was previosuly identified as a probable new species by Frederico *et al*. (2012) and Fontenelle *et al*. (2021a), as was done for *P. araguaia* and *P. munduruku* with the same sequences mentioned above, and also by Sanches *et al*. (2021) with COI and Ctyb sequences. In COI sequence analysis of Frederico *et al*. (2012), *P. raonii* was identified as a sister group to *P. aiereba* populations from the Negro and Solimões-Amazonas rivers. In ATPase 6 analysis of these authors, *P. raonii* was identified as a sister group to *P. araguaia* + *P. munduruku* clade. In Fontenelle *et al*. (2021a), *P. raonii* formed a polytomy with *P. lucindai*, as well as with a clade consisting of *P. munduruku* and *P. aiereba* populations from the Branco, Negro and Solimões-Amazonas rivers. Sanches *et al*. (2021) analyzed only the potamotrygonid fauna of the Xingu River and demonstrated differentiation in COI and Ctyb sequences between *P. raonii* ("H7 AF110629 *Paratrygon aiereba*" for

Ctyb and "H18 *Paratrygon aiereba*7104" for COI) and *P. aiereba* from the lower part of the river. *Paratrygon raonii* adult specimens had a mean total length of 813.5 mm (the second highest in the genus), a maximum total length of 958 mm, a mean disc length of 670 mm (the highest in *Paratrygon* species), and a maximum disc length of 933 mm (the highest in *Paratrygon* species). The mean spiracle length of 4% DW (3.4–5% DW) is the lowest among *Paratrygon* species. *Paratrygon raonii* has the narrowest branchial basket among *Paratrygon* species. The mean distance between the first gill slits is 20.1% DW (18.8–22.6% DW). The mean of distance between the fifth gill slits is 16.8% DW (the lowest value in the *Paratrygon* genus) (15.7–17.5% DW). The mean branchial basket length is 10.3% DW (9.2–11.3% DW). The caudal sting is longer compared to other *Paratrygon* species. The mean caudal sting length is 11% DW (7.7–15.8% DW) and the mean caudal sting width is 0.9% DW (0.7–1.4% DW).

Geographical distribution of the four new species. The four species of *Paratrygon* described here, *P. lucindai*, *P. araguaia*, *P. munduruku*, and *P. raonii*, are endemic to the following four large, clear water rivers flowing out of the Cerrado and Brazilian Shield into the right margin of the lower, final part of the Solimões-Amazonas rivers in the Amazon biome: the Tocantins, Araguaia, Tapajós, and Xingu rivers. These rivers are known as permanent clear water rivers in the Amazon basin (Goulding *et al*., 2010). They are relatively transparent and oliver green in color, and characterized by minimal suspended sediment loads and considerable chemical variability. The clear water rivers of the eastern Amazon basin are slightly acidic with pH values ranging from about 6.0 to 6.8 and low conductivity. One example is the Tapajós River, which currently has conductivity values of 14.4 ± 13.1 µS/cm. These rivers typically drain weathered Precambrian Brazilian crystalline shield soils, which explains their low dissolved sediment loads (Duncan, Fernandes, 2010; Goulding *et al*., 2010).

Regarding the biodiversity of the ichthyofauna in these rivers in general, the data of Albert *et al*. (2011) are correlated with the ecoregions established by Abell *et al*. (2008), reveals that the Tocantins-Araguaia system boasts the highest total diversity, harboring 346 species, 153 of which are endemic. This is followed by the Tapajós-Juruena system, which supports 244 species, 58 of which are endemic. Lastly, the Xingu River is home to 142 species, 36 of which are endemic. Dagosta, de Pinna (2019) updated the total number of fish species in each system: 705 in the Tocantins-Araguaia, 529 in the Tapajós, and 509 in the Xingu. Various studies have confirmed that the ichthyofauna in these four rivers is more similar to that in other rivers draining shield areas than to the ichthyofauna in the western and central parts of the Amazon basin (Goulding *et al*., 2010; Lima, Ribeiro, 2011; Dagosta, de Pinna, 2017, 2019). Actinopterygii taxa suggest a potential biogeographical relationship among these three sub-basin systems (Lima, Ribeiro, 2011).

Dagosta, de Pinna (2019) defined the historical biogeographic relationship between the ichthyofauna of these three systems and some Madeira River tributaries as "Brazilian Shield". The authors emphasized lineages that occur exclusively in these systems. In their biogeographic analysis, Dagosta, de Pinna (2017, fig. 6) found that the ichthyofauna of the Xingu and Tocantins-Araguaia systems probably have a deeper historical and biogeographic relationship with each other than with the ichthyofauna of the Tapajós River. The ichthyofauna of the Tapajós appear to be more closely related to those found in the Madeira River tributaries of the Brazilian Shield (the Aripuanã, Ji-Paraná, and

Marmelos rivers). Additionally, the author's results showed that the ichthyofaunas of both the Tapajós and Xingu rivers are historically hybridized, especially in the Tapajós River (Dagosta, de Pinna, 2017, figs. 7–8).

Regarding Potamotrygoninae, Fontenelle *et al*. (2021b) addressed the diversification of the genus into other South American basins, which occurred at the end of the Pebas System (prior to 10 Ma). Of the three crystalline shield river systems discussed here, there is a possible ancestral relationship among them following Fontenelle *et al.* (2021b). However, the results are similar to those of Dagosta, de Pinna (2017): the Tocantins-Araguaia system is a sister group of the Xingu system; the Tapajós system is more closely related to other basins, including the central Solimões-Amazonas channel and the Branco and Negro river systems. According to Fontenelle *et al*. (2021b) biogeographic analysis, Potamotrygoninae lineages occurring in the Brazilian Shield drainages originated from the upper Amazon and Negro/Branco ranges between the late Miocene and Pliocene (10 to 5 Ma).

Among the potamotrygonines that occur in the clear water rivers of the Brazilian crystalline shield, there is a group of "black stingrays" (Carvalho, 2016b) of the genus *Potamotrygon* which are endemic to them, and are found mainly in the upper and middle parts of these drainages. Similar to the *Paratrygon* species described here, only one species of *Potamotrygon* black stingray exists in each of these rivers: *P. rex* (middle and upper Tocantins), *P. henlei* (Araguaia and lower Tocantins), *P. leopoldi* (middle and upper Xingu) and *P. albimaculata* (middle and upper Tapajós) (Fig. 54; Carvalho, 2016a,b). Several morphological characters are shared between *P. rex*, *P. henlei*, and *P. leopoldi*, as shown by Carvalho (2016b:553), which could indicate a possible relationship between these species. *Potamotrygon albimaculata* differs from the others because it has two angular cartilages of different sizes (whereas *P. henlei*, *P. leopoldi* and *P. rex* have two angular cartilages of similar size), smaller and more numerous teeth (whereas the other black stingrays have larger and fewer teeth, with only *P. rex* having a similar number of tooth rows to *P. albimaculata*), besides other characteristics mentioned by Carvalho (2016a:27). These characteristics may indicate an ichthyofaunal relationships between the potamotrygonids of the Tocantins-Araguaia, Xingu, and Tapajós, as well as a closer historical association between the Actinopterygii fauna of these rivers, as shown by Dagosta, de Pinna (2017, 2019).

Paratrygon aiereba is endemic to the Amazon basin and is typically found in muddy rivers that rise from the Andes. It occurs in the central channel of the Solimões-Amazonas rivers and its large tributaries in the upper part of the channel, including the Madeira, Purus, and Juruá rivers (Loboda *et al*., 2021). This species follows the "Amazon-only lowland" pattern coined by Dagosta, de Pinna (2019). The four Amazonian species of the genus *Paratrygon* described here are each endemic to one of the four major clear water rivers of the Brazilian Crystalline Shield: *P. araguaia* from the Araguaia River, *P. lucindai* from the Tocantins River, *P. raonii* from the Xingu River, and *P. munduruku* from the Tapajós River. Their distributions follow the "Brazilian Shield" pattern described by Dagosta, de Pinna (2019). The current distribution of these five *Paratrygon* species in the Amazon basin (Fig. 15) suggests that the chemical composition of these rivers may have influenced the evolution and speciation of the genus throughout the basin's evolutionary and geological history. This finding supports Duncan, Fernandes (2010) hypothesis that the chemistry of the different Amazonian rivers types acts as a biogeographic barrier, promoting allopatric speciation. Notably, the four new species

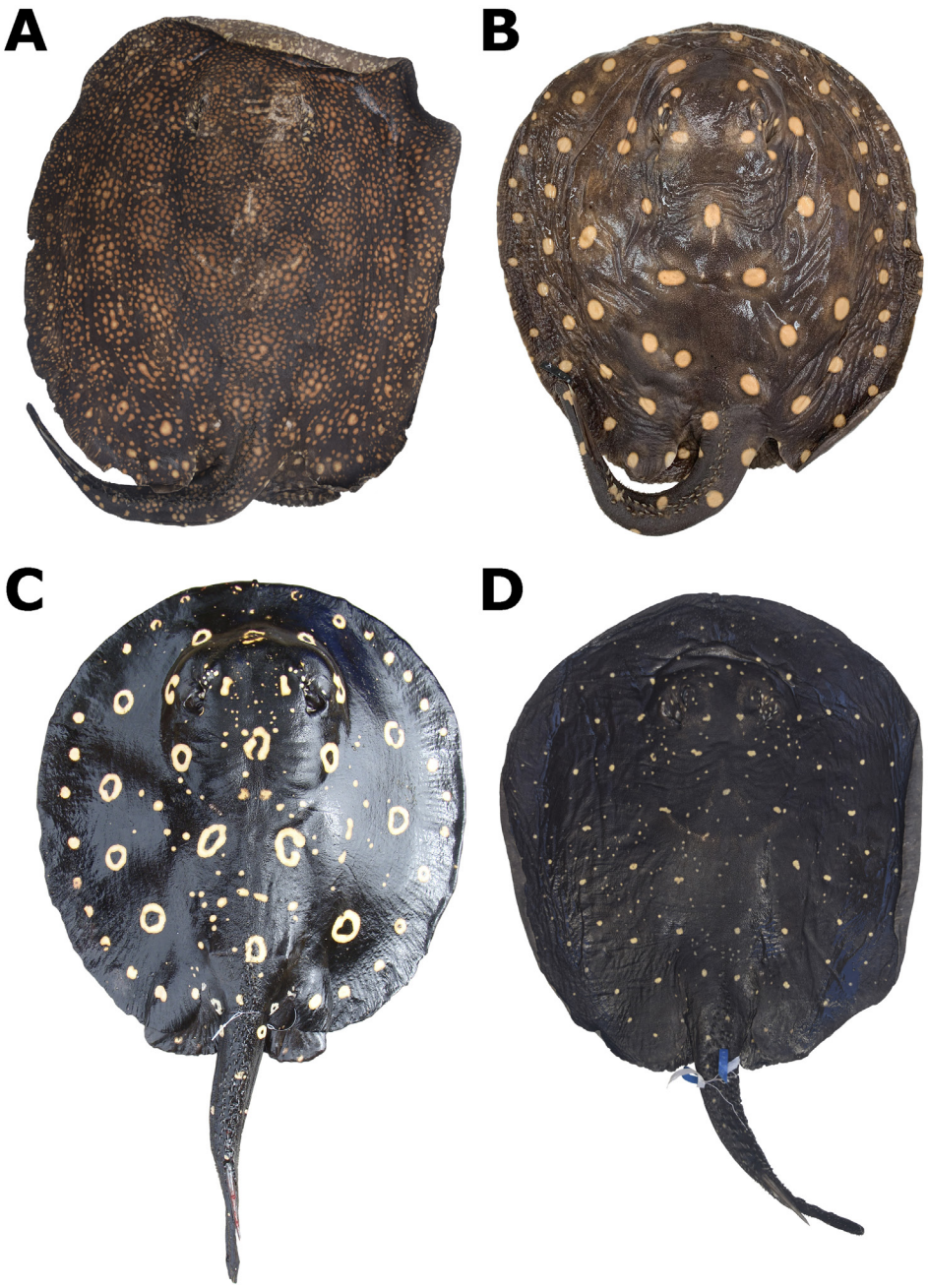

FIGURE 54 | Dorsal view of four black stingrays species of genus *Potamotrygon*. **A.** *P. rex*, holotype, MZUSP 120371; **B.** *P. henley*, specimen deposited at the Universidade de Brasília; **C.** *P. leopoldi*, fresh specimen photographed on Xingu River in 2013; **D.** *P. albimaculata*, holotype, MZUSP 105016. Images of **A**, **C** and **D** by TSL; **B** by Julia P. Azevedo.

are distributed in the middle and upper parts of these crystalline shield systems, while *P. aiereba* is found in the lower parts. In these regions, the physicochemical effects of the water from the central Solimões-Amazonas channel predominate. As Duncan, Fernandes (2010:457) have stated, these effects can influence the distribution limits of these potamotrygonines.

There are now seven described species of *Paratrygon*, two of which are found in the Orinoco basin and five in the Amazonas basin. *Paratrygon aiereba*, *P. orinocensis*, and *P. parvaspina* are species exclusive to the Amazon biome. *Paratrygon aiereba* has a typical lowland distribution in the Amazon, while *P. orinocensis* and *P. parvaspina* are endemic and sympatric to the Orinoco basin. The four species described here, *P. lucindai*, *P. araguaia*, *P. munduruku*, and *P. raonii*, occur in the Amazon biome as well as in the transition between the Cerrado and Amazon biomes. According to the criteria of Dagosta, de Pinna (2019), these species have a typical Brazilian Shield distribution. These four species are possibly the most endangered of the genus *Paratrygon* because they are endemic to the rivers where they occur, and their geographical areas are highly influenced by anthropogenic activities, especially in the Tocantins-Araguaia system.

According to Fontenelle *et al*. (2021b), species from the clear water rivers of the Crystalline Shield may be more recent than those in lowlands of the Amazon and Orinoco basins. However, morphological and molecular evidence suggests a possible ancestral relationship between most black stingray group of genus *Potamotrygon*, and for the four new species of *Paratrygon* described here, especially between species in the Tocantins-Araguaia and Xingu systems. To better evaluate these hypotheses of the and the relationships between these species and the others in the *Paratrygon* genus, phylogenetic and biogeographic analyses are being conducted (T. S. Loboda, A. Datovo, working in progress).

ACKNOWLEDGMENTS

I would like to thank my colleagues and friends at MZUSP, Aléssio Datovo, Mário de Pinna, Murilo Pastana, Naércio Menezes, Osvaldo Oyakawa and Michel Gianeti for their valuable discussions during the writing and final preparation of this work. From MZUSP, I would also like to thank Arthur de Lima, Laura Donin, Vinicius Reis, Jonatas Pereira, Vinicius Carvalho, Nonato Mendes Junior, Hanna Silva and Vinicius Oliveira. I am grateful to Paulo Lucinda (UFT), Wolmar Wosiacki (MPEG), Leandro Souza (UFPA) and Lucia Rapp Py-Daniel (INPA) for their support and help during my visits to their respective instituions, especially to Leandro Souza for the possibility of my field work in Xingu in May 2013. Thanks to Hugo Idalgo and Reginaldo B. Silva (FMVZ-USP) for their contributions with the digital radiographs, and to Enio Mattos and Phillip Lenktaitis (IBUSP) for the assistance with the SEM images of the dermal denticles. Thanks also to João Paulo C. B. da Silva (UFPB), Monica T. Piza (IBUSP) and George Mattox (UFSCar) for their suggestions at the beginning of this work, and to Julia P. Azevedo (UnB) for kindly providing the image of the *Potamotrygon henlei* specimen.

REFERENCES

- **Abell R, Thieme ML, Revenga C, Bryer M, Kottelat M, Bogutskaya N *et al*.** Freshwater ecoregions of the world: a new map of biogeographic units of freshwater biodiversity conservation. BioScience. 2008; 58(5):403–14. https://doi.org/10.1641/B580507
- **Albert JS, Petry P, Reis RE.** Major biogeographic and phylogenetic patterns. In: Albert JS, Reis RE, editors. Historical biogeography of Neotropical freshwater fishes. Berkeley: University of California Press; 2011. p.21–57.

- **Bailey RM.** Comment on the proposed suppression of *Elipesurus spinicauda* Schomburgk (Pisces) Z. N. (S.) 1825. Bull Zool Nomencl. 1969; 25:133–34.
- **Carvalho MR.** Description of two extraordinary new species of freshwater stingrays of the genus *Potamotrygon* endemic to the rio Tapajós basin, Brazil (Chondrichthyes: Potamotrygonidae), with notes on other Tapajós stingrays. Zootaxa. 2016a; 4167(1):1–63. https://doi.org/10.11646/zootaxa.4167.1
- **Carvalho MR.** *Potamotrygon rex*, a new species of Neotropical freshwater stingray (Chondrichthyes: Potamotrygonidae) from the middle and upper rio Tocantins, Brazil, closely allied to *Potamotrygon henlei* (Castelnau, 1855). Zootaxa. 2016b; 4150(5):537–65. https://doi.org/10.11646/zootaxa.4150.5.2
- **Carvalho MR, Loboda TS, Silva JPCB.** A new subfamily Styracuninae, a new genus, *Styracura*, for *Himantura schmardae* (Werner, 1904) and *Himantura pacifica* (Beebe & Tee-Van, 1941) (Chondrichthyes: Myliobatiformes). Zootaxa. 2016; 4175(3):201–21. https://doi.org/10.11646/zootaxa.4175.3.1
- **Carvalho MR, Lovejoy NR.** Morphology and phylogenetic relationships of a remarkable new genus and two new species of Neotropical freshwater stingrays from the Amazon basin (Chondrichthyes: Potamotrygonidae). Zootaxa. 2011; 2776(1):13–48. https://doi.org/10.11646/zootaxa.2776.1.2
- **Carvalho MR, Lovejoy NR, Rosa RS.** Family Potamotrygonidae (river stingrays). In: Reis RE, Kullander SO, Ferraris CJ Jr., editors. Checklist of the freshwater fishes of South and Central America. Porto Alegre: Edipucrs; 2003. p.22–29.
- **Carvalho MR, Maisey JG, Grande L.** Freshwater stingrays of the Green River Formation of Wyoming (Early Eocene), with the description of a new genus and species and an analysis of its phylogenetic relationships (Chondrichthyes: Myliobatiformes). Bull Am Mus Nat Hist. 2004; 2004(284):1–136. https://doi.org/10.1206/0003-0090(2004)284<0001:FSOTGR>2.0.CO;2
- **Carvalho MR, Ragno MP.** An unusual, dwarf new species of Neotropical freshwater stingray, *Plesiotrygon nana* sp. nov., from the upper and mid Amazon basin: the second species of *Plesiotrygon* (Chondrichthyes: Potamotrygonidae). Pap Avulsos Zool. 2011; 51(7):101–38. https://doi.org/10.1590/S0031-10492011000700001
- **Castex MN.** Estado actual de los estudios sobre la raya fluvial neotropical. Cicuentenario del Museo Provincial de Ciencias Naturales “Florentino Ameghino”. 1964.
- **Compagno LJV.** Phyletic relationships of living sharks and rays. Am Zool. 1977; 17(2):303–22.
- **Compagno LJV.** Endoskeleton. In: Hamlett WC, editor. Sharks, skates, and rays. The biology of elasmobranch fishes. Baltimore: The John Hopkins University Press; 1999. p.69–92.
- **Dagosta FCP, de Pinna M.** Biogeography of Amazonian fishes: deconstructing river basins as biogeographic units. Neotrop Ichthyol. 2017; 15(3):e170034. https://doi.org/10.1590/1982-0224-20170034
- **Dagosta FCP, de Pinna M.** The fishes of the Amazon: distribution and biogeographic patterns, with a comprehensive list of species. Bull Am Mus Nat Hist. 2019; 2019(431):1–163. https://doi.org/10.1206/0003-0090.431.1.1
- **Deynat P, Séret B.** Le revêntement cutané des raies (Chondrichthyes, Elasmobranchii, Batoidea). I - Morphologie et arrangement des denticules cutanés. Ann Sci Nat Zool Bio Anim. 1996; 17(2):65–83.
- **Dingerkus G, Uhler LD.** Enzyme clearing of alcian blue stained whole smaller vertebrates for demonstrating of cartilage. Stain Technol. 1977; 52(4):229–32. https://doi.org/10.3109/10520297709116780
- **Dopazo M, Wosiacki WB, Britto MR.** New species of *Farlowella* (Siluriformes: Loricariidae) from the rio Tapajós basin, Pará, Brazil. Neotrop Ichthyol. 2023; 21(1):e220097. https://doi.org/10.1590/1982-0224-2022-0097
- **Duméril AHA.** Historie naturelle des poissons ou ichthyologie générale. Tome Premier. I. Elasmobranches. Plagiostomes et Holocéphales ou Chimères. Paris: Librarie encyclopédique de Roret; 1865.
- **Duncan WP, Fernandes MN.** Physicochemical characterization of the white, black and clearwater rivers of the Amazon Basin and its implications on the distribution of freshwater stingrays (Chondrichthyes, Potamotrygonidae). Pan-Am J Aquat Sci. 2010; 5(3):454–64.

- **Fontenelle JP, Carvalho MR.** Systematic revision of the *Potamotrygon scobina* Garman, 1913 species-complex (Chondrichthyes: Myliobatiformes: Potamotrygonidae), with the description of three new freshwater stingrays species from Brazil and comments on their distribution and biogeography. Zootaxa. 2017; 4310(1):1–63. https://doi.org/10.11646/zootaxa.4310.1.1
- **Fontenelle JP, Loboda TS, Kolmann MA, Carvalho MR.** Angular cartilage structure and variation in Neotropical freshwater stingrays (Chondrichthyes: Myliobatiformes: Potamotrygonidae), with comments on their function and evolution. Zool J Linn Soc. 2018; 183(1):121–42. https://doi.org/10.1093/zoolinnean/zlx054
- **Fontenelle JP, Lovejoy NR, Kolmann MA, Marques FPL.** Molecular phylogeny for the Neotropical freshwater stingrays (Myliobatiformes: Potamotrygoninae) reveals limitations of tradicional taxonomy. Biol J Linn Soc. 2021a; 134(2):381–401. https://doi.org/10.1093/biolinnean/blab090
- **Fontenelle JP, Marques FPL, Kolmann MA, Lovejoy NR.** Biogeography of the neotropical freshwater stingrays (Myliobatiformes: Potamotrygoninae) reveals effects of continent-scale paleogeographic change and drainage evolution. J Biogeogr. 2021b; 48:1406–19. https://doi.org/10.1111/jbi.14086
- **Fontenelle JP, Silva JPCB, Carvalho MR.** *Potamotrygon limai*, sp. nov., a new species of freshwater stingray from the upper Madeira Rio system, Amazon basin (Chondrichthyes: Potamotrygonidae). Zootaxa. 2014; 3765(3):249–68. https://doi.org/10.11646/zootaxa.3765.3.2
- **Fowler HW.** Os peixes de água doce do Brasil. Arq Zool. 1948; 6:1–204.
- **Frederico RG, Farias IP, Araújo MLG, Charvet-Almeida P, Alves-Gomes JA.** Phylogeography and conservation genetics of the Amazonian freshwater stingray *Paratrygon aiereba* Müller & Henle, 1841 (Chondrichthyes: Potamotrygonidae). Neotrop Ichthyol. 2012; 10(1):71–80. https://doi.org/10.1590/S1679-62252012000100007
- **Fricke R, Eschmeyer WN, Fong JD.** Eschmeyer's catalog of fishes: genera/species by family/subfamily [Internet]. San Francisco: California Academy of Science; 2025. Available from: http://researcharchive.calacademy.org/research/ichthyology/catalog/SpeciesByFamily.asp
- **Garcia DA, Lasso CA, Morales M, Caballero SJ.** Molecular systematics of the freshwater (Myliobatiformes: Potamotrygonidae) of the Amazon, Orinoco, Magdalena, Esequibo, Caribbean, and Maracaibo basins (Colombia-Venezuela): evidence of three mitochondrial genes. Mitochondrial DNA Part A. 2016; 27(6):4479–91. http://dx.doi.org/10.3109/19401736.2015.1101536
- **Garman S.** On the pelvis and external sexual organs of selachians, with special references to the new genera *Potamotrygon* and *Disceus* (with descriptions). Proc Boston Soc Nat Hist. 1877; 19:197–215.
- **Garman S.** On the lateral canal system of the Selachia and Holocephala. Bull Mus Comp Zool. 1888; 17:57–119.
- **Garman S.** The Plagiostomia. Cambridge: Memoirs of the Museum of Comparative Zoology, Harvard College; 1913.
- **Goulding M, Barthem R, Ferreira E.** The Smithsonian Atlas of the Amazon. Washington: Smithsonian Books; 2010.
- **Günther A.** Catalogue of the fishes in the British Museum. Vol. 8. London: British Museum (Natural History); 1870.
- **International Union for Conservation of Nature (IUCN). Standards and petitions committee.** Guidelines for using the IUCN Red List categories and criteria. Version 16 [Internet]. Gland; 2024. Available from: http://www.iucnredlist.org/documents/RedListGuidelines.pdf
- **Jardine W.** The natural history of fishes of Guiana. Part II. The Naturalist's Library. Vol. 5. Edinburgh: W. H. Lizars; 1843.
- **Lasso CA, Rosa RS, Sanchéz-Duarte P, Morales-Betancourt M, Agudelo-Córdoba E.** IX Rayas de agua dulce (Potamotrygonidae) de Suramérica. Parte I. Colombia, Venezuela, Ecuador, Perú, Brasil, Guyana, Surinam y Guayana Francesa: diversidade, bioecología, uso y conservación. Bogotá: Serie Editorial Recursos Hidrobiológicos y Pesqueros Continentales de Colombia; 2013.
- **Lima FCT, Ribeiro AC.** Continental-scale tectonic controls of biogeography and ecology. In: Albert JS, Reis RE, editors. Historical biogeography of Neotropical freshwater fishes. Berkeley: University of California Press; 2011. p.145–64.

- **Loboda TS.** Revisão taxonômica e morfológica do gênero *Paratrygon* Duméril, 1865 (Chondrichthyes: Myliobatiformes: Potamotrygonidae). [PhD Thesis]. São Paulo: Universidade de São Paulo; 2016.
- **Loboda TS, Carvalho MR.** Systematic revision of the *Potamotrygon motoro* (Müller & Henle, 1841) species complex in the Paraná-Paraguay basin, with description of two new ocellated species (Chondrichthyes: Myliobatiformes: Potamotrygonidae). Neotrop Ichthyol. 2013; 11(4):696–737. https://doi.org/10.1590/S1679-62252013000400001
- **Loboda TS, Lasso CA, Rosa RS, Carvalho MR.** Two new species of freshwater stingrays of the genus *Paratrygon* (Chondrichthyes: Potamotrygonidae) from the Orinoco basin, with comments on the taxonomy of *Paratrygon aiereba*. Neotrop Ichthyol. 2021; 19(2):e200083. https://doi.org./10.1590//1982-0224-2020-0083
- **Lovejoy NR.** Systematics of myliobatoid elasmobranchs: with emphasis on the phylogeny and historical biogeography of neotropical freshwater stingrays (Potamotrygonidae: Rajiformes). Zool J Linn Soc. 1996; 117(3):207–57. https://doi.org/10.1111/j.1096-3642.1996.tb02189.x
- **Miranda Ribeiro A.** Fauna brasiliense. Peixes II (Desmobranchios). Arq Mus Nac Rio de Janeiro. 1907; 14:129–217.
- **Moreira RA, Loboda TS, Carvalho MR.** Comparative anatomy of the clasper of the subfamily Potamotrygoninae (Chondrichthyes: Myliobatiformes). J Morphol. 2018; 279(5):598–608. https://doi.org/10.1002/jmor.20795
- **Müller J, Henle FGJ.** Systematiche Beschreibung der Plagiostomen. Berlin: Verlag von Veit und Comp; 1841.
- **Nishida K.** Phylogeny of the suborder Myliobatidoidei. Mem Fac Fish Hokkaido Univ. 1990; 37:1–108.
- **Rizo-Fuentes MA, Correa-Cárdenas CA, Lasso CA, Morales-Betancourt MA, Barragán-Barrera DC, Caballero S.** Phylogeography, genetic diversity and population structure of the freshwater stingray, *Paratrygon aiereba* (Müller & Henle, 1841) (Myliobatiformes: Potamotrygonidae) in the Colombian Amazon and Orinoco basins. Mitochondrial DNA A. 2021; 32(1):20–33. https://doi.org/10.1080/24701394.2020.1844679
- **Rosa RS.** A systematic revision of the South American freshwater stingrays (Chondrichthyes: Potamotrygonidae). [PhD Thesis]. Williamsburg: The College of William and Mary; 1985a.
- **Rosa RS.** Further comment on the nomenclature of the freshwater stingray *Elipesurus spinicauda* Schomburgk, 1843 (Chondrichthyes: Potamotrygonidae). Rev Bras Zool. 1985b; 3(1):27–31. https://doi.org/10.1590/S0101-81751985000100003
- **Rosa RS.** *Paratrygon aiereba* (Müller & Henle, 1841): the senior synonym of the freshwater stingray *Disceus thayeri* Garman, 1913 (Chondrichthyes: Potamotrygonidae). Rev Bras Zool. 1991; 7(4):425–37. https://doi.org/10.1590/S0101-81751990000400001
- **Rosa RS, Charvet-Almeida P, Quijada CCD.** Biology of the South American potamotrygonid stingrays. In: Carrier JC, Musick JA, Heithaus MR, editors. Sharks and their relatives II: biodiversity, adaptative physiology and conservation. New York: CRC Press; 2010. p.241–81.
- **Sanches D, Martins T, Lutz I, Veneza I, Silva R, Araújo F *et al*.** Mitochondrial DNA suggests hybridization in freshwater stingrays *Potamotrygon* (Potamotrygonidae: Myliobatiformes) from the Xingu river, Amazonia and reveals speciation in *Paratrygon aiereba*. An Acad Bras Ciên. 2021; 93(3):e20191325. https://doi.org/10.1590/0001-3765202120191325
- **Santos GM, Mérona B, Juras AA, Jégu M.** Peixes do baixo rio Tocantins: 20 anos depois da usina hidrelétrica Tucuruí. Brasilia: Eletronorte; 2004.
- **Silva JPCB, Carvalho MR.** Systematic and morphology of *Potamotrygon orbignyi* (Castelnau, 1855) and allied forms (Chondrichthyes: Myliobatiformes: Potamotrygonidae). Zootaxa. 2015; 3982(1):1–82. https://doi.org/10.11646/zootaxa.3982.1
- **Silva JPCB, Loboda TS.** *Potamotrygon marquesi*, a new species of neotropical freshwater stingray (Potamotrygonidae) from the Brazilian Amazon Basin. J Fish Biol. 2019; 95(2):584–612. https://doi.org/10.1111/jfb.14050
- **Stehmann MFW.** Batoid Fishes. In: Fisher W, editor. FAO species Identification Sheets for Fisheries Purposes, Western Central Atlantic, fishing area. Rome: FAO United Nations; 1978.

- **Taniuchi T, Ishihara H.** Anatomical comparison of claspers of freshwater stingrays (Dasyatidae and Potamotrygonidae). Jpn J Ichthyol. 1990; 37(1):10–16. https://doi.org/10.11369/jji1950.37.10
- **Thorson TB, Brooks DR, Mayes MA.** The evolution of freshwater adaptation in stingrays. Natl Geogr Res. 1983; 15:663–94.
- **Thorson TB, Woorton RM, Georgi TA.** Rectal gland of freshwater stingrays, *Potamotrygon* spp. (Chondrichthyes: Potamotrygonidae). Biol Bull. 1978; 154(3):508–16. https://doi.org/10.2307/1541076
- **Venticinque E, Forsberg B, Barthem R, Petry P, Hess L, Mercado A *et al*.** An explicity GIS-based river basin framework for aquatic ecosystem conservation in the Amazon. Earth Syst Sci Data. 2016; 8(2):651–61. https://doi.org/10.5194/essd-8-651-2016

AUTHORS' CONTRIBUTION

Thiago Silva Loboda: Conceptualization, Data curation, Formal analysis, Funding acquisition, Investigation, Methodology, Project administration, Resources, Software, Supervision, Validation, Visualization, Writing-original draft, Writing-review and editing.

FUNDING INFORMATION

This work was made possible by the financial support of FAPESP (Fundação de Amparo à Pesquisa do Estado de São Paulo) through TSL grants 2011/23420–0 and 2022/12849–0.

ETHICAL STATEMENT

Not applicable.

DATA AVAILABILITY STATEMENT

The author confirms that the data supporting the findings of this study are available within the article.

AI STATEMENT

Not applicable.

COMPETING INTERESTS

The author declares no competing interests.

SUPPLEMENTARY MATERIAL

Supplementary material **S1**
Supplementary material **S2**
Supplementary material **S3**
Supplementary material **S4**
Supplementary material **S5**
Supplementary material **S6**
Supplementary material **S7**

HOW TO CITE THIS ARTICLE

- **Loboda TS.** Four new species of neotropical freshwater stingrays of the genus *Paratrygon* (Myliobatiformes: Potamotrygonidae) from clear water rivers of the Amazon basin. Neotrop Ichthyol. 2026; 24(1):e250087. https://doi.org/10.1590/1982-0224-2025-0087

Neotropical Ichthyology

OPEN ACCESS

Official Journal of the
Sociedade Brasileira de Ictiologia
SBI